

**UNCLASSIFIED**

**AD 4 2 2 8 8 2**

**DEFENSE DOCUMENTATION CENTER**

**FOR**

**SCIENTIFIC AND TECHNICAL INFORMATION**

**CAMERON STATION, ALEXANDRIA, VIRGINIA**



**UNCLASSIFIED**

NOTICE: When government or other drawings, specifications or other data are used for any purpose other than in connection with a definitely related government procurement operation, the U. S. Government thereby incurs no responsibility, nor any obligation whatsoever; and the fact that the Government may have formulated, furnished, or in any way supplied the said drawings, specifications, or other data is not to be regarded by implication or otherwise as in any manner licensing the holder or any other person or corporation, or conveying any rights or permission to manufacture, use or sell any patented invention that may in any way be related thereto.

422882

Report No. RF-TR-63-4

Copy 19

**THE REFLECTION OF ELECTROMAGNETIC RADIATION**

(Based on Classical Electrodynamics)

15 March 1963

VOLUME I



**U S ARMY MISSILE COMMAND**  
**REDSTONE ARSENAL, ALABAMA**

DDC Availability Notice

Qualified requesters may obtain copies of this report from the Defense Documentation Center for Scientific and Technical Information, Arlington Hall Station, Arlington 12, Virginia.

Destroy; do not return.

THE REFLECTION OF ELECTROMAGNETIC RADIATION

(Based on Classical Electrodynamics)

by

Herbert B. Holl

15 March 1963

VOLUME I

Advanced Systems Laboratory  
Future Missile Systems Division  
Directorate of Research and Development  
U. S. Army Missile Command  
Redstone Arsenal, Alabama

## • ABSTRACT

These studies, based on classical electrodynamics, present numerical values of the Fresnel intensity reflection coefficients in tables and graphs. The reflection coefficients are given for normal and oblique incidence for approximately 2500 indices of refraction  $N = n - ki$ , i.e.,  $n = 0.1 (0.1) 4.0$ ,  $k = 0 (0.1) 6.0$ , for angles of incidence  $\theta_0 = 0^\circ (5^\circ) 85^\circ$ . A set of graphs illustrate the solutions of the Fresnel equations. The supplementary remarks describe in detail the occurrence of reflection characteristics such as the angle of incidence  $\theta_0$  for which a) the amplitude of the wave oscillating parallel to the plane of incidence is a minimum, b) the degree of polarization is a maximum, and c) the two amplitudes of the reflected wave have a difference in phase of  $\delta = 90^\circ$ . Tables and graphs illustrating these three special circumstances are provided. Some examples of the determination of the index of refraction from reflection measurements are also given.

## PREFACE

Several new areas of research are reviving interest in the classical physical principles of electromagnetic wave propagation and wave interaction on materials. It is now certain that laser light will become an important tool in target determination and discrimination. The determination of reflection parameters is being used to investigate and predict the behavior of reflecting materials and surrounding media. A general tabulation of the numerical values of wave reflections would be useful in such studies and would greatly reduce duplication of research effort. To the writer's knowledge, these data are not available in reference form. Nearly all elementary physics textbooks contain graphs to demonstrate the variations in the reflectivity of glass, plotted against the angle of incidence; other examples of electromagnetic radiation reflections appear elsewhere in the literature but are not compiled in useable form; a great majority of the handbooks give the reflectivity for normal incidence only.

The tables which comprise Volume II are designed to partially fill this need, and the accompanying explanatory material provides a very simple method for extending the tables as required. The compilation of these data began during a study of the effects of solar radiation pressure on satellites (Ref. 1); the numerous reflection coefficient values required were tabulated for internal use. For this report, the tables have been completed and expanded to present the numerical values for the index of refraction  $N = n - ki$  for all combinations of  $n = 0.1 (0.1) 4.0$ ,  $k = 0.0 (0.1) 6.0$ , and the angle of incidence  $\theta_0 = 0^\circ (5^\circ) 85^\circ$ . The selected ranges of indices of refraction and angles of incidence cover a whole region in sufficient density to permit interpolation.

Chapter 1 briefly discusses the basic principles of electromagnetic wave propagation and reflection, and contains the reflection formulas which were applied in preparing the tables.

For the purposes of this paper, the relative index of refraction is considered as a fundamental constant defined by the complex number  $N = n - ki$ . This notation is commonly used in optics and,

in the case of reflection, the constant  $k$  is a positive number and  $N$  is independent of the angle of incidence of radiation. The macroscopic approach to the electromagnetic theory defines the index of refraction as dependent on the material constants  $\sigma$ ,  $\epsilon$ , and  $\mu$  (specific conductivity, dielectric constant or permittivity, and magnetic permeability, respectively), as well as the wavelength  $\lambda$ . In the visible and infrared region of the spectrum the material constants  $n$  and  $\kappa$ , which appear in the refraction index  $N = n - ki = n(1 - \kappa i)$ , are restricted to a phenomenological description of the material qualities. The quantum theory and the dispersion theory have to be employed in order to derive equations for  $n$  and  $k$  which take into account the atomic structure.

Chapter 1 provides some details about the derivation of the index of refraction by physical constants. By virtue of the definition of the complex index of refraction  $N = n - ki$ , the set of complex numbers for  $N$  is located in the fourth quadrant of the plot of the complex numbers as long as the index of refraction of matter is considered with respect to vacuum or air. The case of thin layers will be excluded; therefore, the index of refraction is a parameter for the bulk material considered and does not depend on its thickness. For the plot of complex numbers, the names "Gaussian plane of complex numbers" and "Argand diagram" are both in usage.

Given the definition  $N = n - ki$ , the conjugate complex values of  $N$  ( $N = n + ki$ ), which are located in the first quadrant of the complex plane of numbers, possess a distinct physical meaning. If an electromagnetic wave passes through the interface between two materials with conducting or absorbing qualities, defined by the relative indices of refraction with respect to vacuum or air [i. e.,  $N_1 = n_1 - k_1 i$  and  $N_2 = n_2 - k_2 i$  ( $k_1 \geq 0$ ,  $k_2 \geq 0$ )], the relative index of refraction  $N_{12} = N_2/N_1$  can take on one of the two forms  $N_{12} = n_{12} + k_{12} i$  or  $N_{12} = n_{12} - k_{12} i$ , where the coefficient  $k_{12}$  is required to be non-negative. Which of the two forms of  $N_{12}$  we get depends on the numerical values of the coordinates of the two refraction indices. As long as we consider only isotropic dielectric and absorbing materials, the relative index of refraction will be represented only in the first or fourth quadrant of the Argand diagram and the reflectivity  $R_v$  will be in the interval  $0 \leq R_v \leq 1$ . Since the numerical values obtained by the Fresnel formula are the same for each pair of conjugate complex values of  $N$ , the illustrations in the complex plane are given only for one quadrant of the plane. The physical interpretation of the second and third quadrants, where the real refraction index  $n$  becomes negative, is beyond the scope of this study. For one pair

of the terms  $N = -n - ki$  ( $n \geq 0, k \leq 0$ ), the numerical values for the reflectance obtained from Fresnel equations are the reciprocal of the reflectance we receive for the same pair of the form  $N = n - ki$  ( $n \geq 0, k \leq 0$ ). The numerical results of  $R$  are then in the interval  $1 \leq R_V \leq \infty$ .

The tables of numerical values, which accomplish the main objective of this report, comprise the appendix which is published separately as Volume II for convenience in use. Table A, the principal exhibit, contains the reflection intensity coefficients of electromagnetic waves oscillating perpendicular and parallel to the plane of incidence for all combinations of  $n = 0.1$  (0.1) 4.0,  $k = 0.0$  (0.1) 6.0, and angles of incidence  $\theta_0 = 5^\circ$  (5°)  $85^\circ$ . Tables B, C, and D are for special cases, such as normal incidence ( $\theta_0 = 0^\circ$ ) or real indices of refraction, and are added to provide complete coverage. Numerical values for those cases in which  $R_2$  and  $R_2/R_1$  are a minimum are presented in Tables E and F; Table G contains numerical values with respect to the "principal angle of incidence," which is the angle of incidence at which the difference in phase between the two amplitudes of the reflected wave becomes  $90^\circ$ . The corresponding values of the reflectance are also given. The reflection coefficients and the other numerical values for the second decimal of the index of refraction can easily be interpolated from the tables. For many of the cases occurring outside the above-mentioned intervals, simplified equations of the reflection coefficients may suffice. An extension of the graphs (Chapter 2) will be helpful in arriving at a preliminary estimate.

Chapter 2 is composed entirely of graphic illustrations of the numerical reflectance values. Some of the graphs illustrate reflectances  $R_1$  and  $R_2$  as a function of the angle of incidence for selected indices of refraction. Other plots do the same for the unpolarized radiation  $R$ . In certain cases the Argand diagram was chosen for the complex index of refraction. One set of graphs illustrates the reflectances  $R_1$ ,  $R_2$ , and  $R = 1/2 (R_1 + R_2)$ , and another deals with the degree of polarization  $P = (R_1 - R_2)/(R_1 + R_2)$ . There is a separate diagram for each constant value of the angle of incidence  $\theta_0 = 0^\circ$  ( $10^\circ$ )  $70^\circ$  ( $5^\circ$ )  $85^\circ$ .

The remarks in Chapter 3, together with the graphs in Chapter 2, will aid in understanding the numerical solution of the very complicated Fresnel formulas in the whole plane of the index of refraction. One of the more interesting aspects covered in Chapter 3 is the occurrence of the characteristic reflection angles.

Chapter 4 suggests possible applications of the material presented in this report, and describes various methods of determining the index of refraction from reflection measurements.

It has recently come to the author's attention that a part of his findings, which were based on the numerical data obtained for this paper, had been published earlier by other authors. These publications are cited as Ref. 12 and 15 - 22.

All the numerical computations were performed on standard IBM machines and were sponsored by the George C. Marshall Space Flight Center (MSFC), Huntsville, Alabama. The author is very grateful to Dr. Hans J. Sperling of the MSFC Aeroballistics Division, for his assistance in the preparation of a major portion of the tables.

# TABLE OF CONTENTS

## VOLUME I

Chapter		Page
	PREFACE .....	iii
	LIST OF ILLUSTRATIONS .....	x
	GLOSSARY OF SYMBOLS .....	xii
1	BASIC PRINCIPLES AND MATHEMATICAL SOLUTION OF THE PROBLEM .....	1
2	NUMERICAL VALUES FOR REFLECTION FORMULAS IN GRAPHS (See detailed index at beginning of chapter.) .....	15
	Reflectivity Versus $\theta_0$ .....	21
	Reflectivity and N .....	37
	Degree of Polarization and N .....	68
	Characteristic Angles and N .....	78
3	SUPPLEMENTARY REMARKS AND REVIEW OF THE NUMERICAL VALUES .....	83
	3.1. Reflectivities $R_1$ and $R_2$ at Air-Dielectric Interface Versus $\theta_0$ .....	84
	3.2. Reflectivities $R_1$ and $R_2$ at Air-Conductor Interface Versus $\theta_0$ .....	84
	3.3. Reflectivity R of Unpolarized Radiation Versus $\theta_0$ .....	89
	3.4. Reflectivity R at Normal Incidence, and N .....	89
	3.5. Reflectivity $R_1$ and N .....	90
	3.6. Reflectivity $R_2$ and N .....	90
	3.7. Reflectivity R and N .....	91
	3.8. Degree of Polarization P and N .....	91

## TABLE OF CONTENTS (Continued)

Chapter	Page
3.9. Occurrence of the Characteristic Angles of Incidence .....	93
3.9.1. First Brewster Angle and N .....	93
3.9.2. Second Brewster Angle and N ....	94
3.9.3. Third Brewster Angle and N .....	94
3.9.4. Angle of Incidence $\theta_0$ for Unpolarized Radiation $R_{min}$ and N .....	97
3.9.5. Angle of Incidence $\theta_0 = 45^\circ$ .....	97
3.9.6. Linear Eccentricity of the Polarization Ellipse .....	98
3.10. Summary .....	102
4 PROPOSED APPLICATIONS .....	103
4.1. Use of the Data .....	103
4.2. Determination of N from Reflection Measurements .....	104
4.2.1. Specular Reflection Under Ideal Test Conditions .....	105
4.2.2. Adulterated Experimental Data .....	114
4.2.3. Nonspecular Reflection .....	122
REFERENCES .....	127

# TABLE OF CONTENTS (Concluded)

## VOLUME II

	Page
Appendix TABLES OF RADIATION REFLECTION FUNCTIONS (See detailed index, p. iii of Vol. II.)	
Table A - Reflection Coefficients $R_1$ and $R_2$ for N at Oblique Incidence .....	1
Table B - Reflection Coefficient $R = R_1 = R_2$ for N at Normal Incidence .....	173
Table C - Reflection Coefficients $R_1$ and $R_2$ for n at Oblique Incidence .....	179
Table D - Reflection Coefficient $R = R_1 = R_2$ for n at Normal Incidence .....	183
Table E - Reflection Coefficient $R_2 = \text{Minimum}$ and the First Brewster Angle of Incidence for N .....	185
Table F - Reflectance Ratio $\frac{R_2}{R_1} = \text{Minimum}$ and the Second Brewster Angle of Incidence for N .....	197
Table G - Reflectance Coefficients $R_1$ and $R_2$ and the Third Brewster Angle of Incidence for N .....	209

## LIST OF ILLUSTRATIONS

Figure	Title	Page
1	The Variation of the Index of Refraction with Wavelength for a Number of Conducting Materials .....	4
2	The Index of Refraction of Conducting Materials for Yellow and Red Light .....	5
3 thru 64	Numerical Values for Reflection Formulas in Graphs (see detailed index at beginning of Chapter 2) .....	15
65	Illustration of the Definition of the First, Second, and Third Brewster Angle of Incidence, for $N = 0.6 - 0.6i$ .....	88
66	Vibration Ellipse of a Harmonic Wave ( $\delta = 60^\circ$ ) .....	99
67	Reflectance Curves $R_1$ , $R_2$ , and $R_1 - R_2$ , and the Square of the Linear Eccentricity of the Polarization Ellipse $e^2$ for $N = 0.6 - 0.6i$ .....	101
68	The Determination of $N$ from Reflection Measurements (Example of Group 1) .....	107
69	Reflectance Curves $R_1$ and $R_2$ ( $\theta_0 = 40^\circ$ ) .....	109
70	Relation among the First Brewster Angle of Incidence (where $R_2$ is a Minimum), the Reflectance $(R_2)_{\min}$ , and the Complex Index of Refraction $N = n - ki$ .....	111
71	Relation among the Second Brewster Angle of Incidence (where $P$ is a Maximum), the Degree of Polarization $P_{\max}$ , and the Complex Index of Refraction $N = n - ki$ .....	112

# LIST OF ILLUSTRATIONS (Concluded)

Figure		Page
72	Relation among the Third Brewster Angle of Incidence = Principal Angle of Incidence (where the Phase Difference $\delta$ is $90^\circ$ ), the Reflectance $R_2$ , and the Complex Index of Refraction $N = n - ki$ .....	113
73	Determination of $N$ from Reflection Values Obtained at Characteristic Angles of Incidence (Example of Group 2) .....	114
74	Particular Example of the Determination of $N$ from Experimental Data for $R_1$ and $R_2$ ( $\theta_0 = 70^\circ$ ) .....	116
75	Particular Example of the Determination of $N$ from Experimental Data for $R_1$ and $R_2$ ( $\theta_0 = 80^\circ$ ) .....	117
76	Particular Example of the Determination of $N$ from Experimental Data for $P$ .....	118
77	Particular Example of the Determination of $N$ from Adulterated Experimental Data .....	120
78	Reflectance and Degree of Polarization for Indices of Refraction $N_1 = 2.00 - 4.40i$ , $N_2 = 0.80 - 1.70i$ , and $N_3 = 1.40 - 1.80i$ .....	121
79	Reflection from a Nonregular Surface (Description in Text) .....	123
80	Reflection Curves for Nickel ( $\lambda \sim 2.5\mu$ ) ( $R_1$ and $R_2$ , Smooth Surface; $R_{1,n}$ and $R_{2,n}$ , Rough Surface) (Description in Text) .....	124

## GLOSSARY OF SYMBOLS

The symbols used in this paper are those in general use in physics, and each symbol is fully explained when it first appears in the text. For convenience, the most frequently used abbreviations and symbols are defined below:

$N = n - ki$	complex index of refraction
$\theta_0$	angle of incidence
$r_v$	amplitude reflection coefficient
$R_v$	intensity reflection coefficient
$R_1 = R_{\perp}$	reflection coefficient - electric vector perpendicular to the plane of incidence
$R_2 = R_{\parallel}$	reflection coefficient - electric vector parallel to the plane of incidence
$R = \frac{1}{2} (R_1 + R_2)$	reflection coefficient of unpolarized radiation (natural light)
$P = (R_1 - R_2)/(R_1 + R_2)$	degree of polarization

## Chapter 1

### BASIC PRINCIPLES AND MATHEMATICAL SOLUTION OF THE PROBLEM

In an isotropic homogeneous medium, which contains no electrical charges, Maxwell's equations are valid to describe the electric field vector  $\mathbf{E}$  and the magnetic field vector  $\mathbf{H}$  for all kinds of electric and magnetic events (Refs. 2, 3, and 4). After the application of certain vector operations, Maxwell's fundamental equations lead to the wave equation which, by use of the m. k. s. system of units, becomes

$$\nabla^2 \mathbf{E} - \mu \epsilon \ddot{\mathbf{E}} - \mu \sigma \dot{\mathbf{E}} = 0, \quad (1)$$

where

$\nabla^2$  = Laplacian vector operator

$\epsilon, \mu$  = inductive capacities -- dielectric constant and permeability, respectively

$\sigma$  = conductivity.

If the field is monochromatic and of angular frequency  $\omega$ , we have  $\partial/\partial t \equiv -i\omega$ , and Eq. (1) can be written

$$\nabla^2 \mathbf{E} + k_v^2 \mathbf{E} = 0, \quad (2)$$

which is satisfied if

$$k_v^2 = \mu_v \epsilon_v \omega^2 - \mu_v \sigma_v \omega i. \quad (3)$$

The last equation is fundamental for all our considerations. The term  $k_v$ , which represents the intrinsic propagation coefficient for the medium (also called propagation constant, complex wave number, or separation constant), is of the dimension  $[\text{cm}^{-1}]$  and is determined by the material parameters of the medium through which the wave is propagating. The same wave equation is valid for the magnetic field vector  $\mathbf{H}$ , and the solutions of Eq. (1) have the general form

$$F_v = F_0 e^{i(k_v \bar{\sigma}_v \cdot \bar{r} - \omega t)} \quad (4)$$

where  $F_v$  denotes any field component of the wave traveling in the medium denoted by the subscript  $v$ ,  $\bar{\sigma}_v$  is the unit vector in the direction of propagation, and  $\bar{r}$  denotes the position vector drawn from a chosen origin. As long as  $k_v$  is constant, propagation will be undisturbed and the energy flow will suffer loss only by absorption. These transverse oscillations, described by Eq. (4), may be assumed to consist of two equal components which are plane-polarized in mutually perpendicular directions and are in phase with each other.

The case in which  $k_v$  varies indicates that the wave enters a second medium with material parameters different from the first. The field motion of charges in the second medium and the reaction which occurs in the first medium create the reflected wave. In the mathematical treatment of the boundary value problems, we assume a very thin interface located in the common boundary between the two media. The boundary conditions have to be fulfilled, which means that for the first derivative the field vectors have to be continuous across the interface.

We consider the first medium always as vacuum or air. As explained above, if the second medium is a dielectric there will be a reflected wave and a diffracted wave. The direction of propagation of the diffracted wave is given by Snell's law

$$\frac{\sin \theta_0}{\sin \theta_1} = \frac{k_1}{k_0} = \sqrt{\frac{\epsilon_1 \mu_1}{\epsilon_0 \mu_0}} = n_{01} \quad (5)$$

where the subscript  $0$  stands for the first medium and the subscript  $1$  for the diffracting medium. The angle  $\theta_0$  is called the incident angle, the angle  $\theta_1$  is the refraction angle, and the ratio of the propagation constants is the index of refraction.

If the second medium is an electrical conductor, the refracted wave penetrates only thin boundary layers and we have the effect of absorption in addition to the reflection. The propagation constant for the refracting medium becomes complex and the refraction angle  $\theta_1$  has to be replaced by a pair of complex angles since the incident angle is always real. In order to distinguish between the incident and refracted waves, which are both traveling in the same medium, the parameters of

the reflected wave are denoted by the subscript 2. Using Eq. (3), we write the propagation constant for the two media

$$\begin{aligned} k_1^2 &= \mu_1 \epsilon_1 \omega^2 - \mu_1 \sigma_1 \omega i & k_2^2 &= \mu_2 \epsilon_2 \omega^2 \\ k_1 &= \alpha_1 - \beta_1 i & k_2 &= \alpha_2 = \omega \sqrt{\mu_2 \epsilon_2} \end{aligned} \quad (6)$$

Snell's law has only a formal meaning but is still effective, and Eq. (5) for an electrical conductor becomes

$$\frac{\sin \theta_0}{\sin(\varphi + \chi i)} = \frac{\alpha_1}{\alpha_2} - \frac{\beta_1}{\alpha_2} i \quad (7)$$

or

$$\frac{\sin \theta_0}{\sin(\varphi + \chi i)} = N = n - ki = n(1 - \kappa i) \quad (8)$$

where  $n$  and  $k$  are the real and imaginary parts, respectively, of the index of refraction.

While the real indices of refraction of the dielectrics (transparent) vary only slightly with the wavelength, the complex indices for the conductors show marked dependence on wavelength. Two graphs are provided to depict this variation of the complex index of refraction with wavelength using values taken from Refs. 5 and 6. Figure 1 employs the Argand diagram to show the index of refraction  $N = n - ki$  for a number of metallic elements.

The axis of abscissa demonstrates the real part of the refractive index, and the axis of ordinate depicts the imaginary part. Each curve represents a different metal and shows how its index  $N$  changes with the wavelength. The three-place values at the beginning and end of the curves give the wavelength in  $m\mu$  ( $= 10^{-5}$  cm). In order to not overcrowd the graph, examples of only a few elements are shown. The curves were not smoothed because the values plotted are from various authors and therefore were not obtained under the same test conditions, such as surface treatments of the material considered. The surface structure is very important and has an effect on the numerical values of  $N$  for the bulk material. The second graph (Fig. 2) presents  $N$  for the wavelength of the sodium line D,  $\lambda = 5893 \text{ \AA}$ , and that of a ruby laser beam.



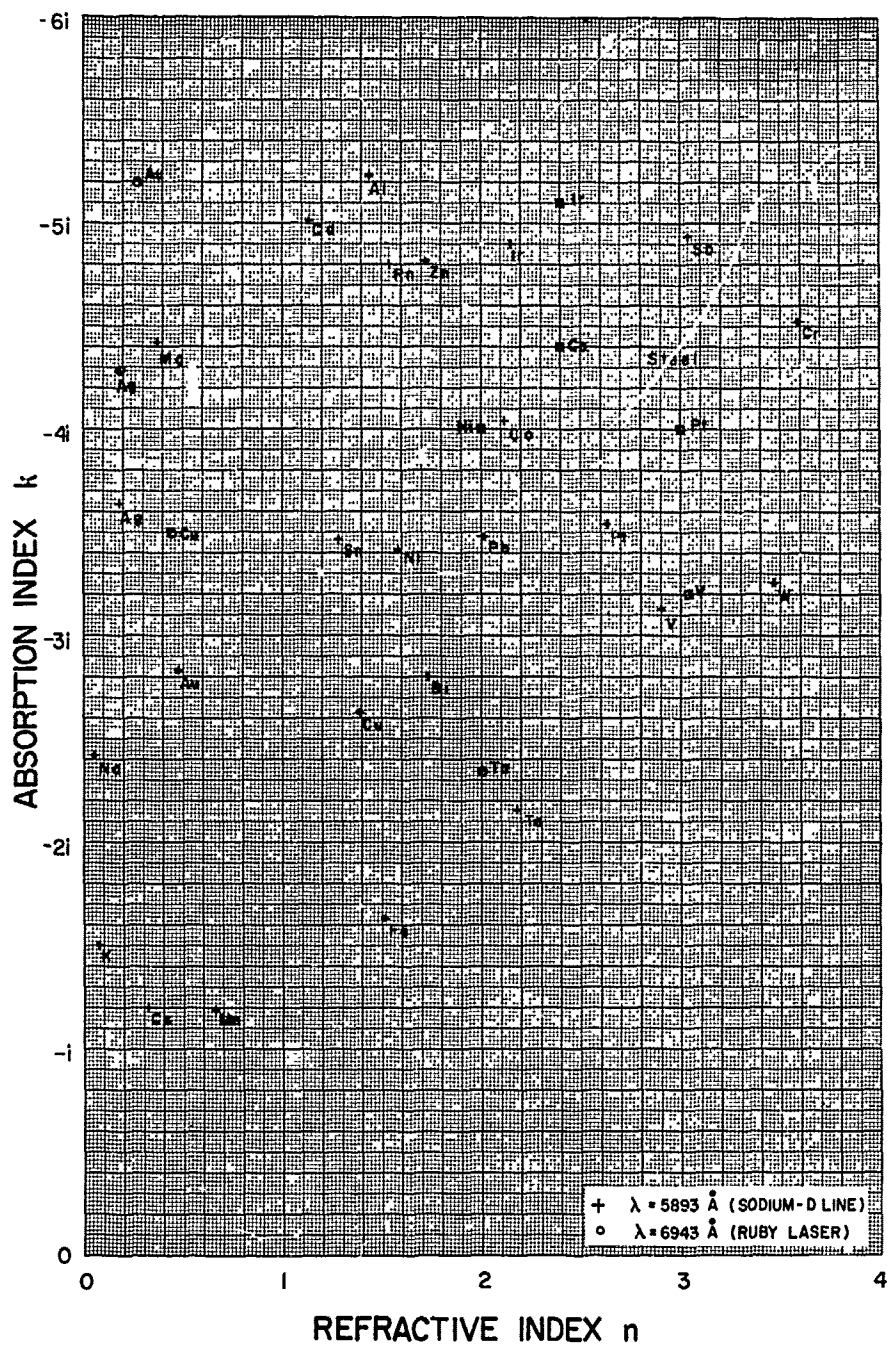


Fig. 2. THE INDEX OF REFRACTION OF CONDUCTING MATERIALS FOR YELLOW AND RED LIGHT

Maxwell's theory cannot describe the shortwave (optical) region because it assumes that the media are homogeneous, that is, that the dielectric constant  $\epsilon$  and the electrical charge density  $\rho$ , are parameters which do not change with space and time. It was necessary to apply the dispersion theory, an extension of Maxwell's theory, in order to take into account the atomic structure of the media. The dispersion theory leads to expressions for the constants  $n$  and  $\kappa$  which are in good agreement with the experimental results. The relationship between the optical and electrical constants (Maxwell's relation  $\sqrt{\epsilon} = n$ ) is of limited validity, and for the shortwave region there exists no direct connection between the index of refraction at optical frequencies and the static or quasi-static values of the electrical material constants ( $\epsilon$ ,  $\mu$ , and  $\sigma$ ). (This relationship is more fully described in relevant textbooks.) It follows that

$$\begin{aligned} n &\approx \frac{\alpha_1}{\alpha_2} \\ \kappa &\approx \frac{\beta_1}{\beta_2} \end{aligned} \quad (9)$$

However, the methods for determining the index of refraction in the optical region and that in the microwave and longwave region are very different. In optics, the index of refraction for dielectrics can be measured by means of Snell's law [Eq. (5)], whereas the definition for the conductors  $k$  or  $\kappa$  can be determined by measuring experimentally the light intensity  $I$  which is transmitted through thin films of opaque materials. The following formulas, known as Lambert's law, are found to hold true (Gaussian unit system):

$$\begin{aligned} I &= I_0 e^{-4\pi\kappa d/\lambda_1} \\ &= I_0 e^{-4\pi\kappa d/\lambda_0} \end{aligned} \quad (10)$$

with

$$\frac{\lambda_0}{\lambda_1} = n = \frac{k}{\kappa}$$

where

$I_0$  = incident intensity

$I$  = transmitted intensity

$\kappa$  = extinction or absorption index

$k$  = extinction or absorption coefficient

$\lambda_0$  = wavelength in vacuum

$\lambda_1$  = wavelength inside the medium

$d$  = thickness of the medium

These equations follow from Eq. (4) for  $t = 0$ , and will have the factor 2 instead of 4 in the exponent if the amplitudes are considered.

In the longwave region, the static measurements of material parameters lead to the determination of the propagation constants, and if the matter has conducting properties the equations for the propagation constants are

$$\alpha_1^2 = \frac{\omega^2 \mu_1 \epsilon_1}{2} \left[ \sqrt{1 + \frac{\sigma_1^2}{\epsilon_1^2 \omega^2}} + 1 \right] \quad (11)$$

$$\beta_1^2 = \frac{\omega^2 \mu_1 \epsilon_1}{2} \left[ \sqrt{1 + \frac{\sigma_1^2}{\epsilon_1^2 \omega^2}} - 1 \right] \quad (12)$$

where  $\nu$  is the frequency of the wave considered and

$$\omega = 2\pi\nu.$$

The index of refraction thus becomes

$$N = n - ki = \frac{k_1}{k_2} = \frac{\alpha_1}{\alpha_2} - \frac{\beta_1}{\alpha_2} i \quad (13)$$

$$n^2 = \left( \frac{\alpha_1}{\alpha_2} \right)^2 = 1/2 \cdot \frac{\mu_1 \epsilon_1}{\mu_2 \epsilon_2} \left[ \sqrt{1 + \frac{\sigma_1^2}{\epsilon_1^2 \omega^2}} + 1 \right] \quad (14)$$

$$k^2 = \left( \frac{\beta_1}{\alpha_2} \right)^2 = 1/2 \cdot \frac{\mu_1 \epsilon_1}{\mu_2 \epsilon_2} \left[ \sqrt{1 + \frac{\sigma_1^2}{\epsilon_1^2 \omega^2}} - 1 \right] \quad (15)$$

If the magnetic permeability and the specific inductive capacity are unity, written

$$\mu_m = \frac{\mu_1}{\mu_2} = 1$$

$$\epsilon_c = \frac{\epsilon_1}{\epsilon_2} = 1,$$

then Eq. (14) and (15) become

$$n^2 = 1/2 \left[ \sqrt{1 + \frac{\sigma_1^2}{\epsilon_1^2 \omega^2}} + 1 \right] \quad (16)$$

$$k^2 = 1/2 \left[ \sqrt{1 + \frac{\sigma_1^2}{\epsilon_1^2 \omega^2}} - 1 \right] \quad (17)$$

If the refracting medium is a plasma (ionized gas), the specific inductive capacity of the matter will not be unity, and Eqs. (14) and (15) become (Ref. 7)

$$n^2 = 1/2 \left[ \sqrt{\epsilon_r^2 + \frac{\sigma_{ac}^2}{\epsilon_1^2 \omega^2}} + \epsilon_r \right] \quad (18)$$

$$k^2 = 1/2 \left[ \sqrt{\epsilon_r^2 + \frac{\sigma_{ac}^2}{\epsilon_1^2 \omega^2}} - \epsilon_r \right] \quad (19)$$

The constants of the medium,  $\epsilon_r$  and  $\sigma_{ac}$ , can be calculated by

$$\sigma_{dc} = \frac{Ne^2}{m\nu} \quad (20)$$

$$\sigma_{ac} = \frac{Ne^2}{m} \cdot \frac{\nu}{\omega^2 + \nu^2} = \sigma_{dc} \left( 1 + \frac{\omega^2}{\nu^2} \right)^{-1} \quad (21)$$

$$\nu = n S_e \left( \frac{8kT}{\pi m} \right)^{1/2} \quad (22)$$

$$\sigma_{dc} = \sqrt{\frac{\pi}{8}} \cdot \frac{e^2}{\sqrt{mk}} \cdot \frac{1}{S_e} \cdot \frac{1}{\sqrt{T}} \cdot \frac{N}{n} \quad (23)$$

$$\epsilon_r = 1 - \frac{\sigma_{ac}}{\nu \epsilon_0} = 1 - \frac{N}{\epsilon_0} \cdot \frac{e^2}{m} \cdot \frac{1}{\omega^2 + \nu^2} = 1 - \frac{\omega_c^2}{\omega^2 + \nu^2} \quad (24)$$

$$\omega_c = \sqrt{\frac{Ne^2}{m \epsilon_0}} \quad (25)$$

where

$\sigma_{dc}$  = direct current conductivity

$\sigma_{ac}$  = alternating current conductivity

$N$  = electron number density

$e$  = electron charge

$m$  = electron mass

$\nu$  = electron collision frequency

$\omega$  = angular frequency of the electric field applied

$n$  = number density of molecules or atoms

$S_e$  = collision cross-section area

$k$  = Boltzmann constant

$T$  = temperature

$\omega_c$  = plasma frequency

Using Eqs. (20) to (25), the Eqs. (14) and (15) become

$$n^2 = 1/2 \left[ \sqrt{\left(1 - \frac{\omega_c^2}{\omega^2 + \nu^2}\right)^2 + \left(\frac{\nu \omega_c^2}{\omega(\omega^2 + \nu^2)}\right)^2} + \left(1 - \frac{\omega_c^2}{\omega^2 + \nu^2}\right) \right] \quad (26)$$

$$k^2 = 1/2 \left[ \sqrt{\left(1 - \frac{\omega_c^2}{\omega^2 + \nu^2}\right)^2 + \left(\frac{\nu \omega_c^2}{\omega(\omega^2 + \nu^2)}\right)^2} - \left(1 - \frac{\omega_c^2}{\omega^2 + \nu^2}\right) \right] \quad (27)$$

The relation among the incident, refracted, and reflected amplitudes of the wave can be determined from the boundary conditions. In the case of reflection, the amplitudes of the electromagnetic field vectors  $E$  become

$$\begin{aligned} E_{\perp}^r &= E_{\perp}^i r_{\perp} e^{-i\delta_{\perp}} \\ E_{\parallel}^r &= E_{\parallel}^i r_{\parallel} e^{-i\delta_{\parallel}} \end{aligned} \quad (28)$$

where  $r_{\perp}$  and  $r_{\parallel}$  are the Fresnel reflection coefficients. The exponents  $\delta_{\perp}$  and  $\delta_{\parallel}$  account for the phase difference between the incoming and reflected waves and will be discussed later. Here we are considering only reflection, and have to distinguish between the ratios of the amplitudes and of the intensities, which are given in terms of the numerical value of the incident wave. Note that the Fresnel amplitude reflection coefficients are

$$\begin{aligned} r_{\perp} &= \frac{E_{\perp}^r}{E_{\perp}^i} = - \frac{\sin(\theta_0 - \theta_1)}{\sin(\theta_0 + \theta_1)} \\ r_{\parallel} &= \frac{E_{\parallel}^r}{E_{\parallel}^i} = \frac{\tan(\theta_0 - \theta_1)}{\tan(\theta_0 + \theta_1)} \end{aligned} \quad (29)$$

Using Snell's law, the Fresnel intensity reflection formulas can then be derived as (Ref. 4)

$$R_{\perp} = \frac{\left( \frac{\mu_2}{\mu_1} \frac{q}{\alpha_2} - \cos \theta_0 \right)^2 + \left( \frac{\mu_2}{\mu_1} \right)^2 \left( \frac{p}{\alpha_2} \right)^2}{\left( \frac{\mu_2}{\mu_1} \frac{q}{\alpha_2} + \cos \theta_0 \right)^2 + \left( \frac{\mu_2}{\mu_1} \right)^2 \left( \frac{p}{\alpha_2} \right)^2} \quad (30)$$

$$R_{\parallel} = \frac{\left[ \left[ \left( \frac{\alpha_1}{\alpha_2} \right)^2 - \left( \frac{\beta_1}{\alpha_2} \right)^2 \right] \cos \theta_0 - \frac{\mu_1}{\mu_2} \frac{q}{\alpha_2} \right]^2 + \left[ 2 \frac{\alpha_1}{\alpha_2} \cdot \frac{\beta_1}{\alpha_2} \cos \theta_0 - \frac{\mu_1}{\mu_2} \frac{p}{\alpha_2} \right]^2}{\left[ \left[ \left( \frac{\alpha_1}{\alpha_2} \right)^2 - \left( \frac{\beta_1}{\alpha_2} \right)^2 \right] \cos \theta_0 + \frac{\mu_1}{\mu_2} \frac{q}{\alpha_2} \right]^2 + \left[ 2 \frac{\alpha_1}{\alpha_2} \cdot \frac{\beta_1}{\alpha_2} \cos \theta_0 + \frac{\mu_1}{\mu_2} \frac{p}{\alpha_2} \right]^2} \quad (31)$$

where  $p$  and  $q$  are functions of  $\theta_0$ ,  $\frac{\alpha_1}{\alpha_2}$ , and  $\frac{\beta_1}{\alpha_2}$ . In this report, only the case where  $n_m = \frac{\mu_1}{\mu_2} \approx 1$  will be considered; included will be all types of materials with the exception of the ferromagnetics among the electrical conductors. For the sake of convenience, we will generally use the following abbreviations in the remainder of this report:

$$R_1 = R_{\perp}$$

$$R_2 = R_{\parallel}$$

$$R = 1/2 (R_1 + R_2),$$

and corresponding expressions for  $E$ ,  $r$ , and  $\delta$ . The term  $R$  also represents the intensity reflection coefficient of unpolarized radiation such as natural light.

Based on the assumption that  $\mu_2 = \mu_1$ , Eq. (31) was reduced to a more proper form by Pfeiffer (see Ref. 2, pp. 241 and 242). Following his equation, the Fresnel intensity reflection formula can be rendered as

$$R_1 = \frac{\left(\frac{q}{\alpha_2} - \cos \theta_0\right)^2 + \left(\frac{p}{\alpha_2}\right)^2}{\left(\frac{q}{\alpha_2} + \cos \theta_0\right)^2 + \left(\frac{p}{\alpha_2}\right)^2} \quad (32)$$

$$R_2 = \frac{\left(\frac{q}{\alpha_2} - \cos \theta_0\right)^2 + \left(\frac{p}{\alpha_2}\right)^2}{\left(\frac{q}{\alpha_2} + \cos \theta_0\right)^2 + \left(\frac{p}{\alpha_2}\right)^2} \cdot \frac{\left(\frac{q}{\alpha_2} - \sin \theta_0 \tan \theta_0\right)^2 + \left(\frac{p}{\alpha_2}\right)^2}{\left(\frac{q}{\alpha_2} + \sin \theta_0 \tan \theta_0\right)^2 + \left(\frac{p}{\alpha_2}\right)^2} \quad (33)$$

For the calculation of the quantities  $q$  and  $p$  the following two equations can be used:

$$\begin{aligned} \left(\frac{p(\theta_0)}{\alpha_2}\right)^2 = 1/2 \left[ -\left(\frac{\alpha_1}{\alpha_2}\right)^2 + \left(\frac{\beta_1}{\alpha_2}\right)^2 + \sin^2 \theta_0 \right. \\ \left. + \sqrt{4\left(\frac{\alpha_1}{\alpha_2}\right)^2 \left(\frac{\beta_1}{\alpha_2}\right)^2 + \left[\left(\frac{\alpha_1}{\alpha_2}\right)^2 - \left(\frac{\beta_1}{\alpha_2}\right)^2 - \sin^2 \theta_0\right]^2} \right] \quad (34) \end{aligned}$$

$$\left(\frac{q(\theta_0)}{\alpha_2}\right)^2 = 1/2 \left[ \left(\frac{\alpha_1}{\alpha_2}\right)^2 - \left(\frac{\beta_1}{\alpha_2}\right)^2 - \sin^2 \theta_0 + \sqrt{4 \left(\frac{\alpha_1}{\alpha_2}\right)^2 \left(\frac{\beta_1}{\alpha_2}\right)^2 + \left[ \left(\frac{\alpha_1}{\alpha_2}\right)^2 - \left(\frac{\beta_1}{\alpha_2}\right)^2 - \sin^2 \theta_0 \right]^2} \right] \quad (35)$$

A corresponding set of reflection formulas occasionally used (Ref. 3, p. 1594) are

$$R_1 = \frac{\sin^2 (\theta_0 - \phi) + \sinh^2 \chi}{\sin^2 (\theta_0 + \phi) + \sinh^2 \chi} \quad (36)$$

$$R_2 = \frac{\sin^2 (\theta_0 - \phi) + \sinh^2 \chi}{\sin^2 (\theta_0 + \phi) + \sinh^2 \chi} \cdot \frac{\cos^2 (\theta_0 + \phi) + \sinh^2 \chi}{\cos^2 (\theta_0 - \phi) + \sinh^2 \chi} \quad (37)$$

Equations (38) to (41) given below will be used to determine the angles  $\phi$  and  $\chi$ , which were previously introduced by Eqs. (7) and (8):

$$\sinh^2 \chi = -\frac{c}{2} + \sqrt{\frac{c^2}{4} + b^2} \quad (38)$$

$$\cos \phi = \frac{b}{\sinh \chi} \quad (39)$$

$$b = \pm \frac{\kappa \sin \theta_0}{n(1 + \kappa^2)} = \pm \frac{k \sin \theta_0}{n^2 + k^2}$$

$$= \pm \frac{\frac{\beta_1}{\alpha_2} \sin \theta_0}{\frac{\alpha_1}{\alpha_2} \left(1 + \frac{\beta_1^2}{\alpha_1^2}\right)} = \pm \frac{\frac{\beta_1}{\alpha_2} \sin \theta_0}{\frac{\alpha_1^2}{\alpha_2^2} + \frac{\beta_1^2}{\alpha_2^2}} \quad (40)^*$$

$$c = 1 - \frac{\sin^2 \theta_0}{(\kappa^2 + 1) n^2} = 1 - \frac{\sin^2 \theta_0}{n^2 + k^2} \\ = 1 - \frac{\sin^2 \theta_0}{\left(\frac{\beta_1^2}{\alpha_1^2} + 1\right) \frac{\alpha_1^2}{\alpha_2^2}} = 1 - \frac{\sin^2 \theta_0}{\frac{\alpha_1^2}{\alpha_2^2} + \frac{\beta_1^2}{\alpha_2^2}} \quad (41)$$

\* The plus sign should be used in Eq. (40) if  $N = n - ki$  is used, and the minus sign if  $N = n + ki$  ( $n \geq 0$ ,  $k \geq 0$ ) is used.

It naturally follows that the rigorous Eqs. (32), (33), (36), and (37) can be converted into the familiar Fresnel equations for dielectrics if the index of refraction is real. They then become

$$R_1 = \frac{\sin^2 (\theta_0 - \theta_1)}{\sin^2 (\theta_0 + \theta_1)} \quad (42)$$

$$R_2 = \frac{\tan^2 (\theta_0 - \theta_1)}{\tan^2 (\theta_0 + \theta_1)} \quad (43)$$

At normal incidence ( $\theta = 0^\circ$ ), the intensity reflection formulas are

#### Index of Refraction - Complex

$$R = R_1 = R_2 = \frac{(n - 1)^2 + k^2}{(n + 1)^2 + k^2} \quad (44)$$

#### Index of Refraction - Real

$$R = R_1 = R_2 = \left( \frac{n - 1}{n + 1} \right)^2 \quad (45)$$

Using Eq. (28), the phase difference  $\delta$  between the two reflected waves is expressed by

$$\frac{r_{\parallel}}{r_{\perp}} e^{-i(\delta_{\parallel} - \delta_{\perp})} = \sqrt{\frac{R_2}{R_1}} e^{-i\delta} \quad (46)$$

The relation of the phase difference to the difference between the optical paths traversed by the two waves is expressed by

phase difference =  $\left( \frac{2\pi}{\lambda} \right)$  (optical path difference).

Since  $n_m \equiv 1$ , the phase shift  $\delta$  is determined by

$$\tan \delta = \frac{2 \frac{p(\theta_0)}{\alpha_2} \sin \theta_0 \tan \theta_0}{\sin^2 \theta_0 \tan^2 \theta_0 - \left( \frac{q(\theta_0)^2}{\alpha_2^2} + \frac{p(\theta_0)^2}{\alpha_2^2} \right)} \quad (47)$$

If  $\delta = 90^\circ$ , then Eq. (47) becomes

$$\sin^2 \theta_0 \tan^2 \theta_0 = \frac{q(\theta_0)^2}{\alpha_2^2} + \frac{q(\theta_0)^2}{\alpha_2^2}, \quad (48)$$

and if we substitute  $n$  and  $k$ , this reduces to

$$\begin{aligned} (n^2 - \sin^2 \theta_0)^2 + (k^2 + \sin^2 \theta_0)^2 + 2n^2 k^2 \\ = \sin^4 \theta_0 (\tan^4 \theta_0 + 1). \end{aligned} \quad (49)$$

The incidence angle  $\theta_0$  at which the phase delay  $\delta = 90^\circ$  occurs, called "the principal angle of incidence," is of great importance in optics and will be discussed more fully in Chapter 3.

The ratio  $\frac{r_{\parallel}}{r_{\perp}}$  defines the polarization of the wave, and the degree

of polarization  $P$  is expressed by the ratio of the excess to the sum of the two reflected intensities, which is

$$P = \frac{R_1 - R_2}{R_1 + R_2} = \frac{1 - \frac{R_2}{R_1}}{1 + \frac{R_2}{R_1}} \quad (50)$$

As long as we consider specular reflection only, the degree of polarization will always be positive and will fall between zero and unity. As was mentioned earlier, the direction of the refracted radiation in absorbing media cannot be calculated by Snell's law. The refracted wave will have only a very small penetration depth and will travel in a direction given by an angle  $\theta_1$  measured from the internal normal of the surface. For this angle, the equation

$$\frac{\sin \theta_0}{\sin \theta_1} = n(\theta_0) \quad (51)$$

is valid and gives a real index of refraction which is a function of the angle of incidence. By application of Kettler's equations (Refs. 2, 3, and 4), this index becomes

$$n(\theta_0) = \left( \frac{q(\theta_0)}{\alpha_2} \right)^2 + \sin^2 \theta_0. \quad (52)$$

## Chapter 2

### NUMERICAL VALUES FOR REFLECTION FORMULAS IN GRAPHS

#### INDEX TO GRAPHS

		Figure No.	Page
<u>Reflectivity Versus <math>\theta_0</math></u>			
Reflectance Curves $R_1$ and $R_2$			
(n = )	(k = )		
0.5	0, 0.2, 0.4, 0.5, 0.8, 1.0 (1.0) 6.0 .....	3 .....	21
1.0	.....	4 .....	22
1.5	.....	5 .....	23
2.0	.....	6 .....	24
2.5	0 (1.0) 6.0 .....	7 .....	25
3.0	.....	8 .....	26
3.5	.....	9 .....	27
4.0	.....	10 .....	28
Reflectance Curves R			
(n = )	(k = )		
0.5	0, 0.2, 0.4, 0.5, 0.8, 1.0 (1.0) 6.0 .....	11 .....	29
1.0	.....	12 .....	30
1.5	0 (1.0) 6.0 .....	13 .....	31
2.0	.....	14 .....	32

# INDEX TO GRAPHS (Continued)

Figure No.

Page

## Reflectance Curves R (Continued)

(n = )	(k = )			
2.5	0 (1.0) 6.0	{	.....	15 ..... 33
3.0			.....	16 ..... 34
3.5			.....	17 ..... 35
4.0			.....	18 ..... 36

## Relation Between the Reflectance and the Index of Refraction

Isoreflectance Curves R for Normal Incidence	..... 19	..... 37
---	----------	----------

## Isoreflectance Curves $R_1$ for Oblique Incidence

( $\theta_0 =$ )		
10°	..... 20	..... 38
20°	..... 21	..... 39
30°	..... 22	..... 40
40°	..... 23	..... 41
50°	..... 24	..... 42
60°	..... 25	..... 43
70°	..... 26	..... 44
75°	..... 27	..... 45
80°	..... 28	..... 46
85°	..... 29	..... 47

# INDEX TO GRAPHS (Continued)

	Figure No.	Page
Isoreflectance Curves $R_2$ for Oblique Incidence		
( $\theta_0 =$ )		
10° .....	30 .....	48
20° .....	31 .....	49
30° .....	32 .....	50
40° .....	33 .....	51
50° .....	34 .....	52
60° .....	35 .....	53
70° .....	36 .....	54
75° .....	37 .....	55
80° .....	38 .....	56
85° .....	39 .....	57

## Isoreflectance Curves R for Oblique Incidence

( $\theta_0 =$ )		
10° .....	40 .....	58
20° .....	41 .....	59
30° .....	42 .....	60
40° .....	43 .....	61
50° .....	44 .....	62
60° .....	45 .....	63
70° .....	46 .....	64
75° .....	47 .....	65
80° .....	48 .....	66
85° .....	49 .....	67

# INDEX TO GRAPHS (Continued)

	Figure No.	Page
<u>Relation Between the Degree of Polarization P and the Index of Refraction N for Oblique Incidence</u>		

( $\theta_0 =$  )

10° .....	50 .....	68
20° .....	51 .....	69
30° .....	52 .....	70
40° .....	53 .....	71
50° .....	54 .....	72
60° .....	55 .....	73
70° .....	56 .....	74
75° .....	57 .....	75
80° .....	58 .....	76
85° .....	59 .....	77

## Relation Between the Characteristic Angles and N

Relation Between the First Brewster Angle (Where  $R_2$  is a Minimum) and the Complex Index of Refraction

$N = n - ki$ .....	60 .....	78
--------------------	----------	----

Relation Between the Second Brewster Angle (Where P is a Maximum) and the Complex Index of Refraction

$N = n - ki$ .....	61 .....	79
--------------------	----------	----

# INDEX TO GRAPHS (Concluded)

	Figure No.	Page
Relation Between the Third Brewster Angle = Principal Angle of Incidence (Where the Phase Difference $\delta$ is $90^\circ$ ) and the Complex Index of Refraction $N = n - ki$ .....	62	80
The Third Brewster Angle of Incidence = Principal Angle of Incidence, for Small Values of the Index of Refraction $N = n - ki$ .....	63	81
Relation among the Angle of Incidence $\theta_0$ where the Reflectance $R = \frac{1}{2} (R_1 + R_2)$ is a Minimum, the Reflectance $R_{min}$ , and the Complex Index of Refraction $N = n - ki$ .....	64	82

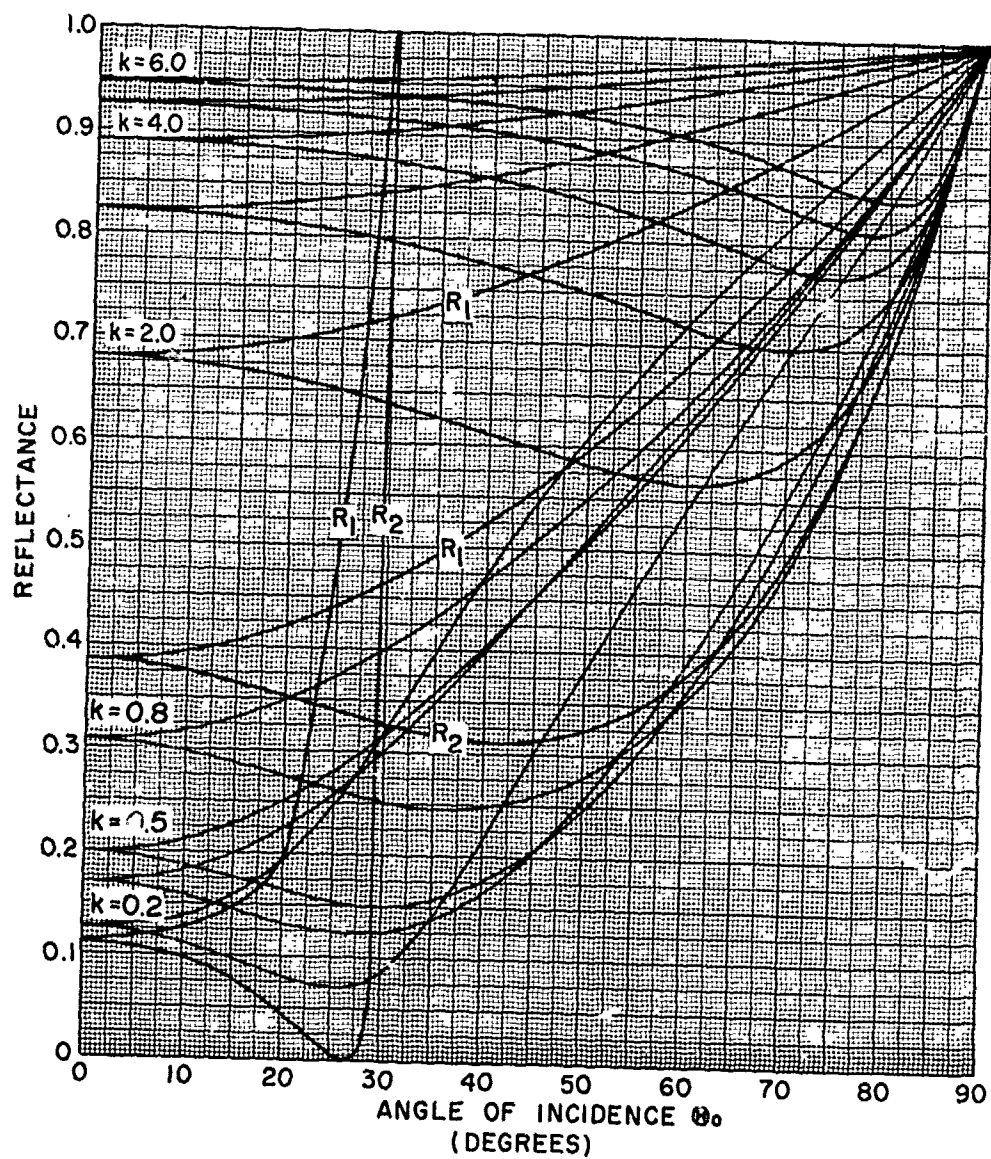


Fig. 3. REFLECTANCE CURVES  $R_1$  AND  $R_2$  FOR  $N = 0.5 - ki$ ;  
 $k = 0, 0.2, 0.4, 0.5, 0.8, 1.0 (1.0) 6.0$

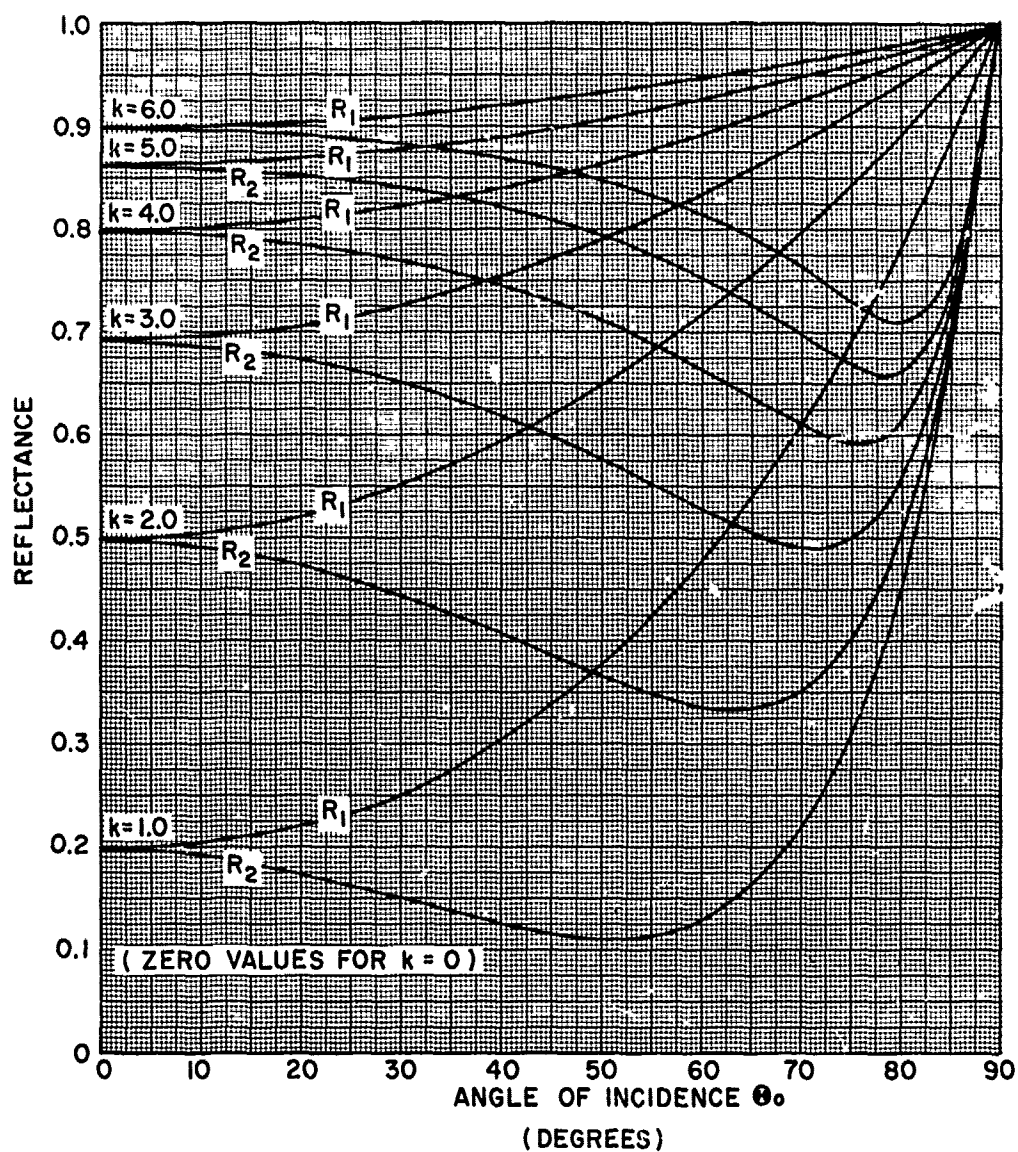


Fig. 4. REFLECTANCE CURVES  $R_1$  AND  $R_2$  FOR  $N = 1.0 - ki$ ;  
 $k = 0$  (1.0) 6.0

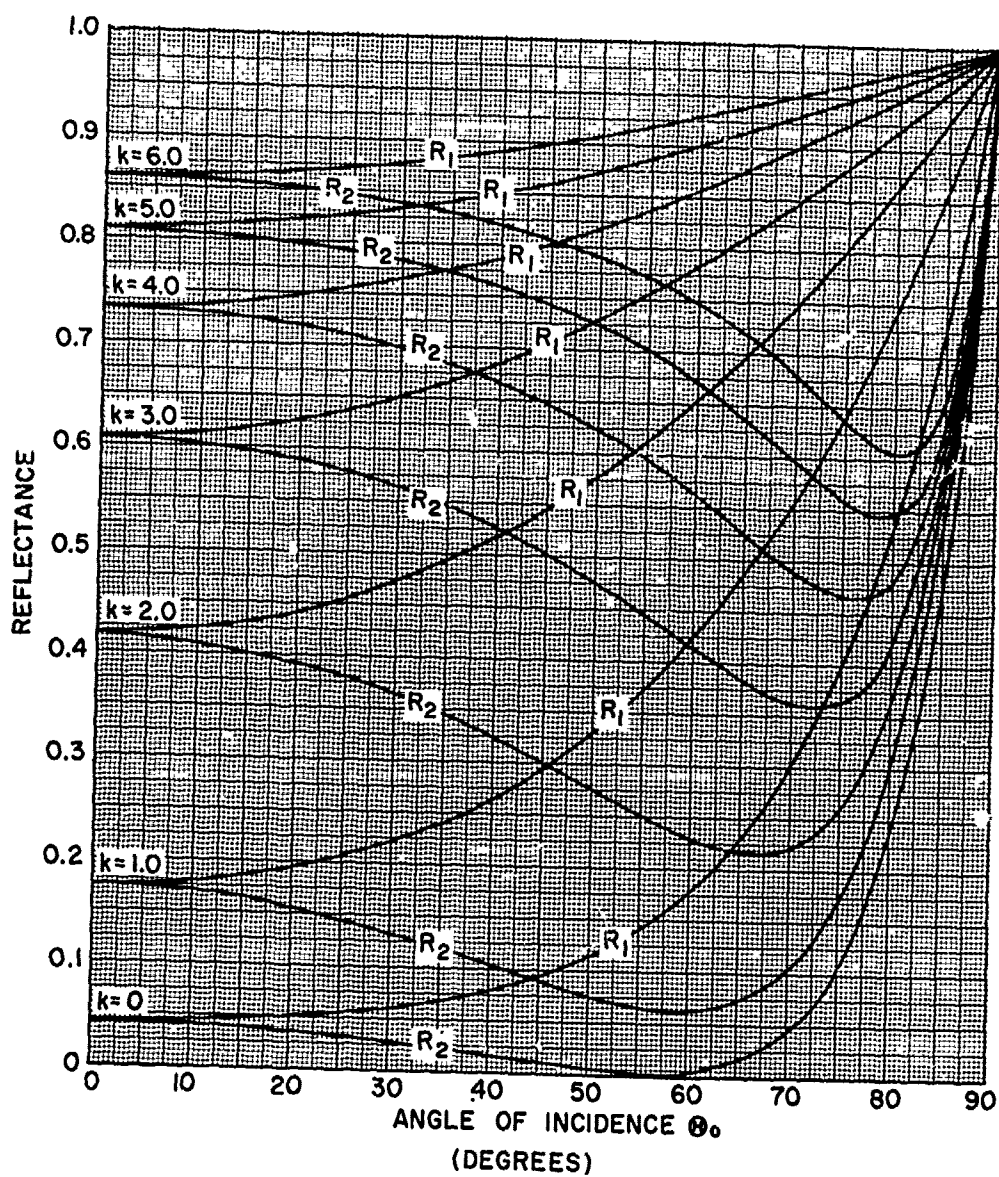


Fig. 5. REFLECTANCE CURVES  $R_1$  AND  $R_2$  FOR  $N = 1.5 - ki$ ;  
 $k = 0$  (1.0) 6.0

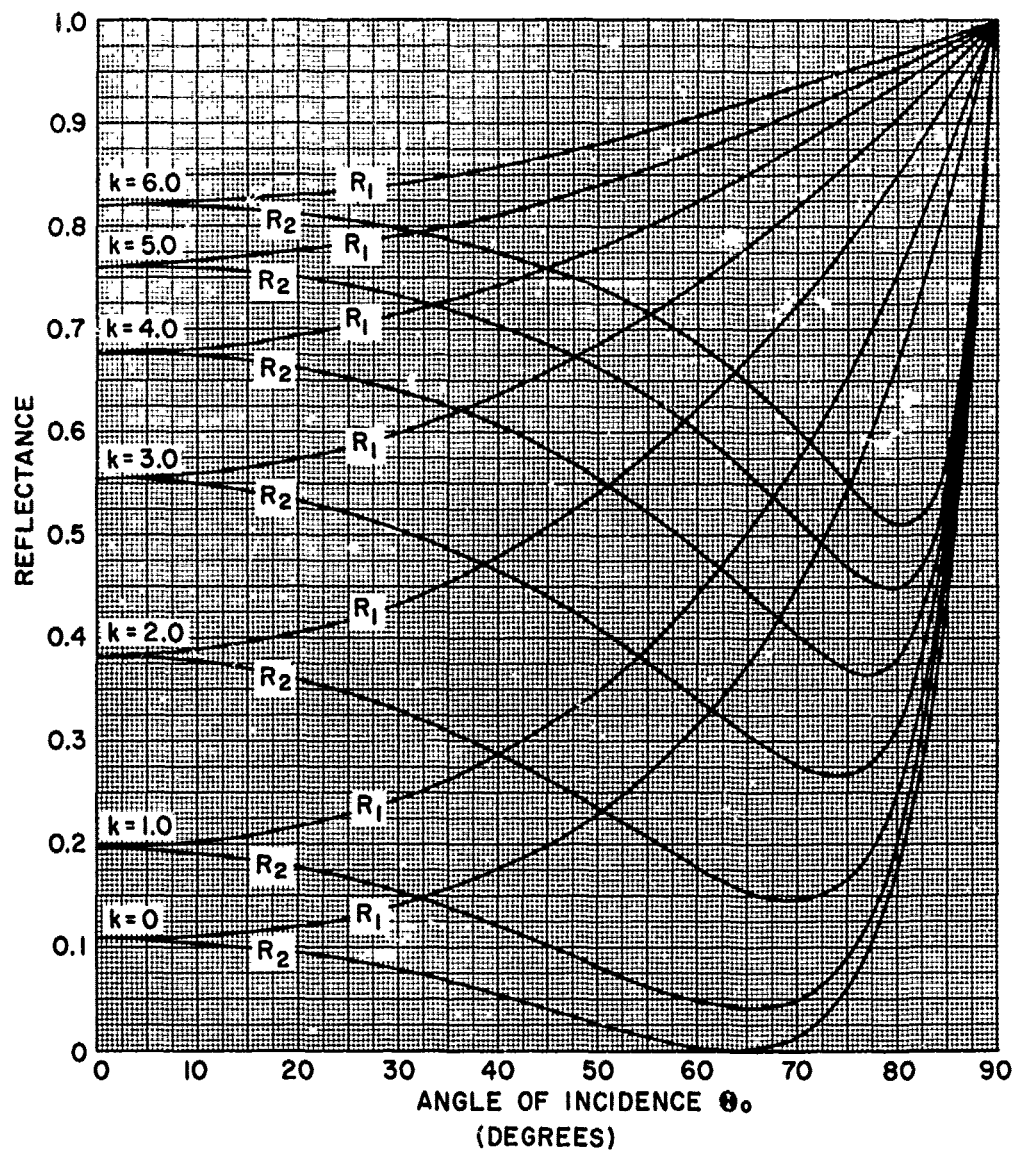


Fig. 6. REFLECTANCE CURVES  $R_1$  AND  $R_2$  FOR  $N = 2.0 - ki$ ;  
 $k = 0$  (1.0) 6.0

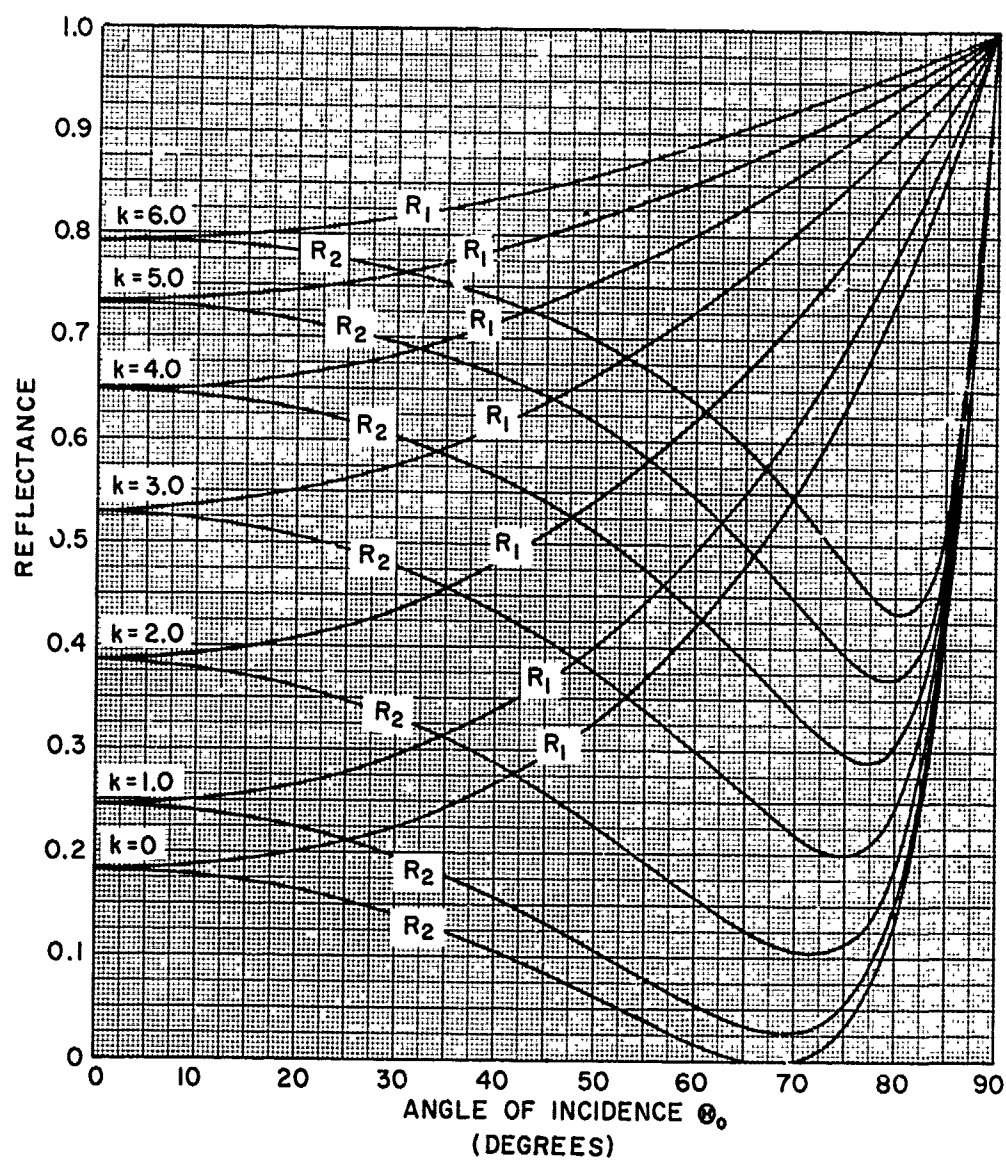


Fig. 7. REFLECTANCE CURVES  $R_1$  AND  $R_2$  FOR  $N = 2.5 - ki$ ;  
 $k = 0$  (1.0) 6.0

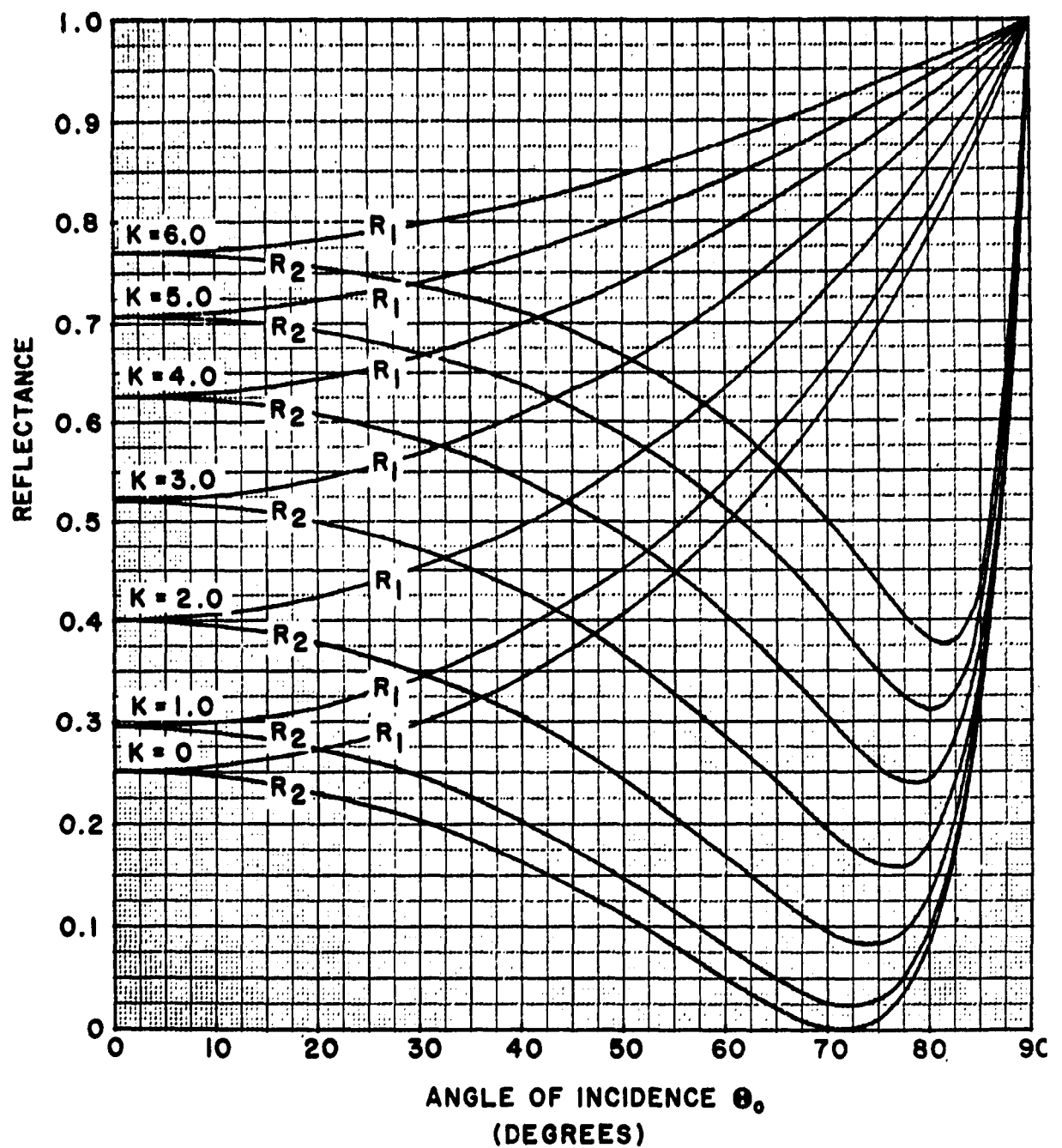


Fig. 8. REFLECTANCE CURVES  $R_1$  AND  $R_2$  FOR  $N = 3.0 - ki$ ;  
 $k = 0 (1.0) 6.0$

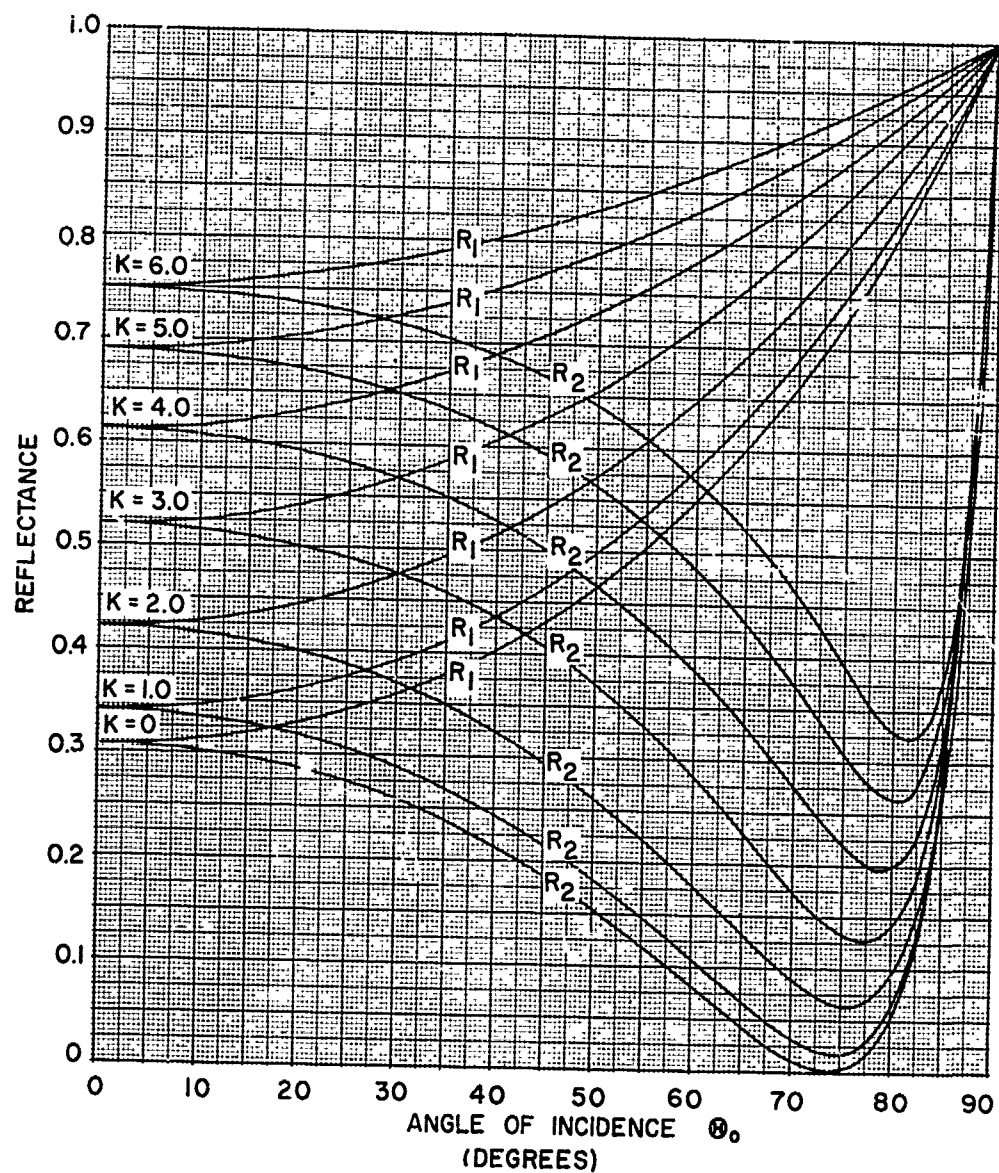


Fig. 9. REFLECTANCE CURVES  $R_1$  AND  $R_2$  FOR  $N = 3.5 - ki$ ;  
 $k = 0$  (1.0) 6.0

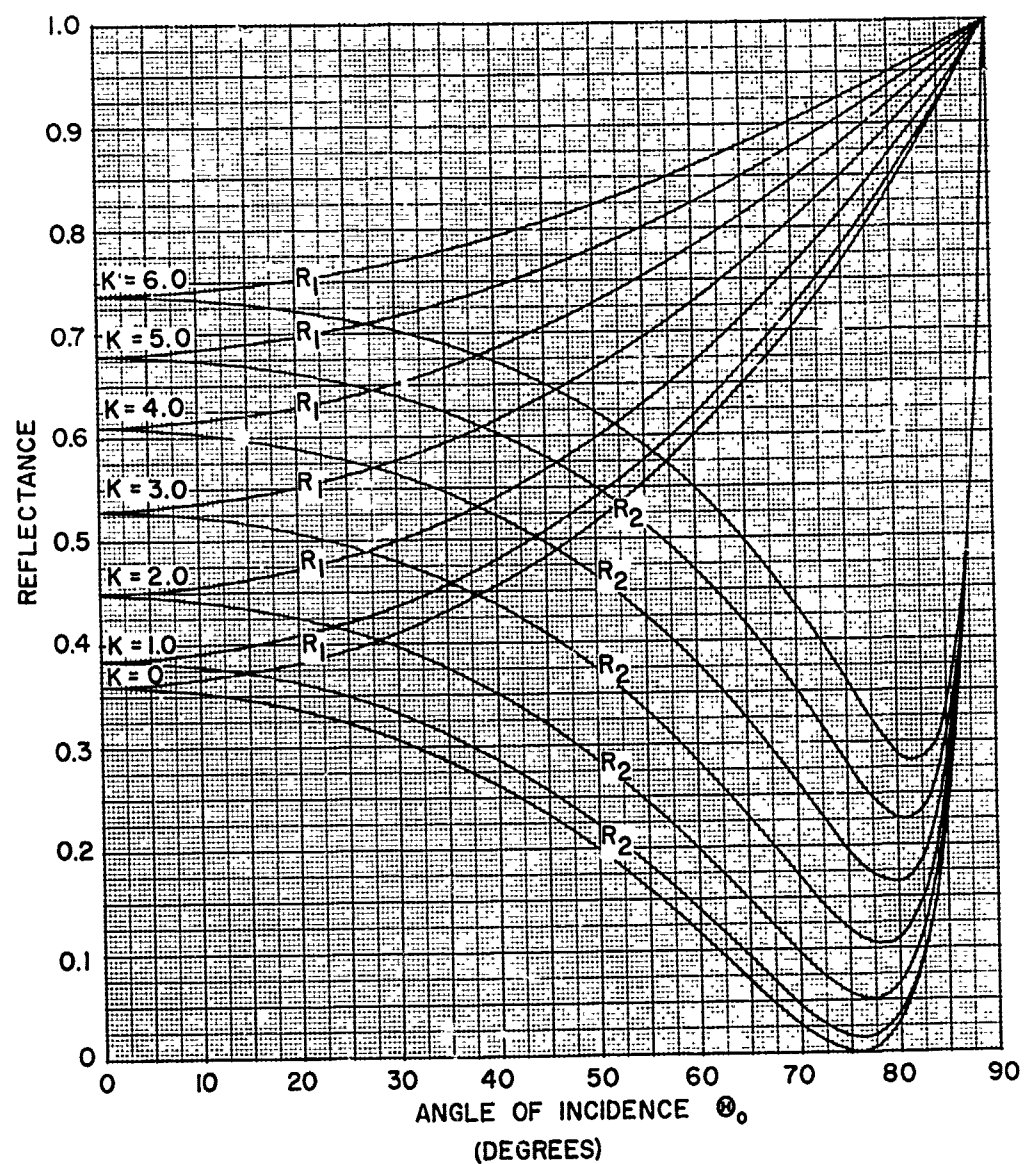


Fig. 10. REFLECTANCE CURVES  $R_1$  AND  $R_2$  FOR  $N = 4.0 - ki$ ;  
 $k = 0$  (1.0) 6.0

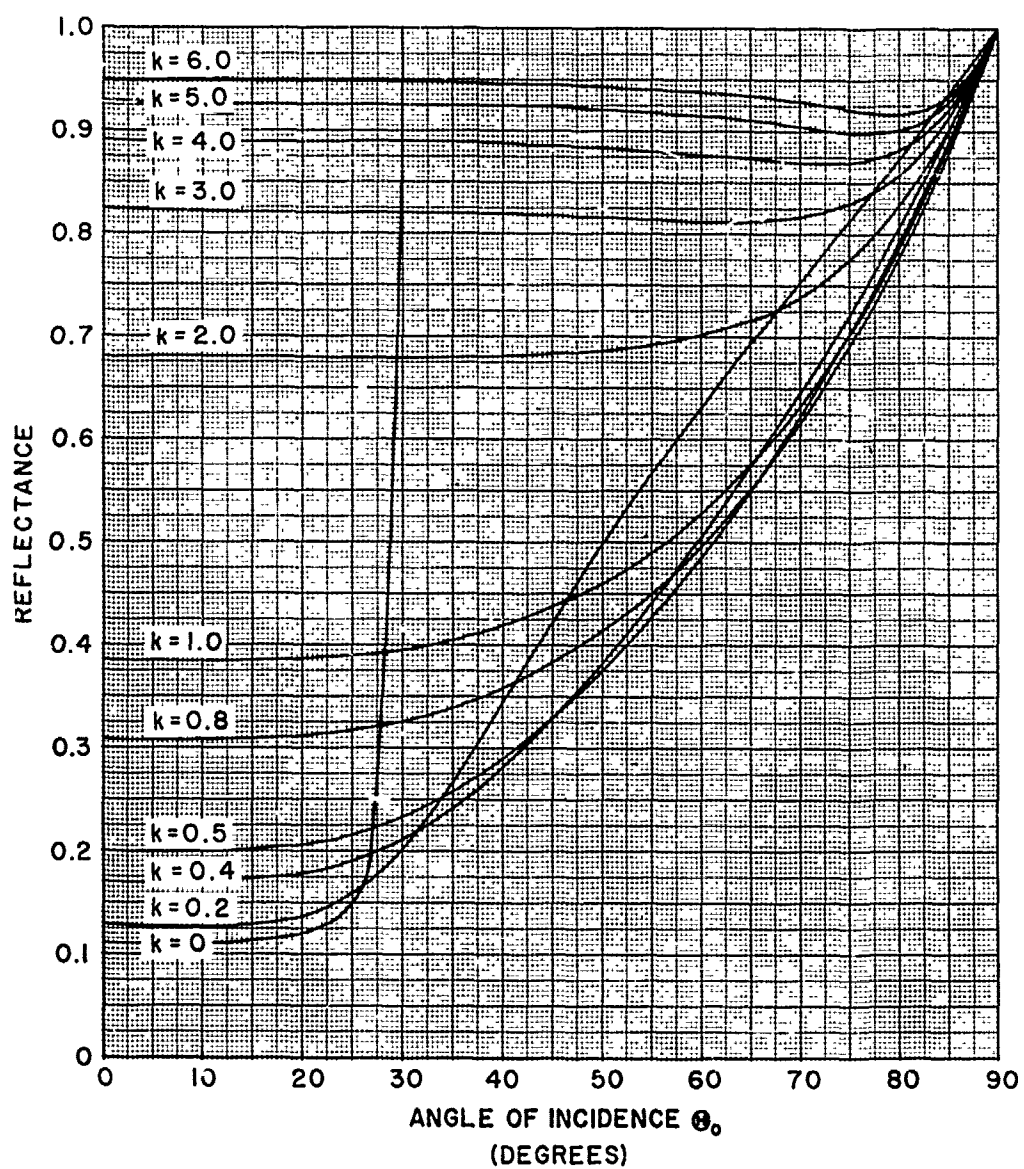


Fig. 11. REFLECTANCE CURVES  $R = \frac{1}{2} (R_1 + R_2)$  FOR  $N = 0.5 - ki$ ;  
 $k = 0, 0.2, 0.4, 0.5, 0.8, 1.0 (1.0) 6.0$

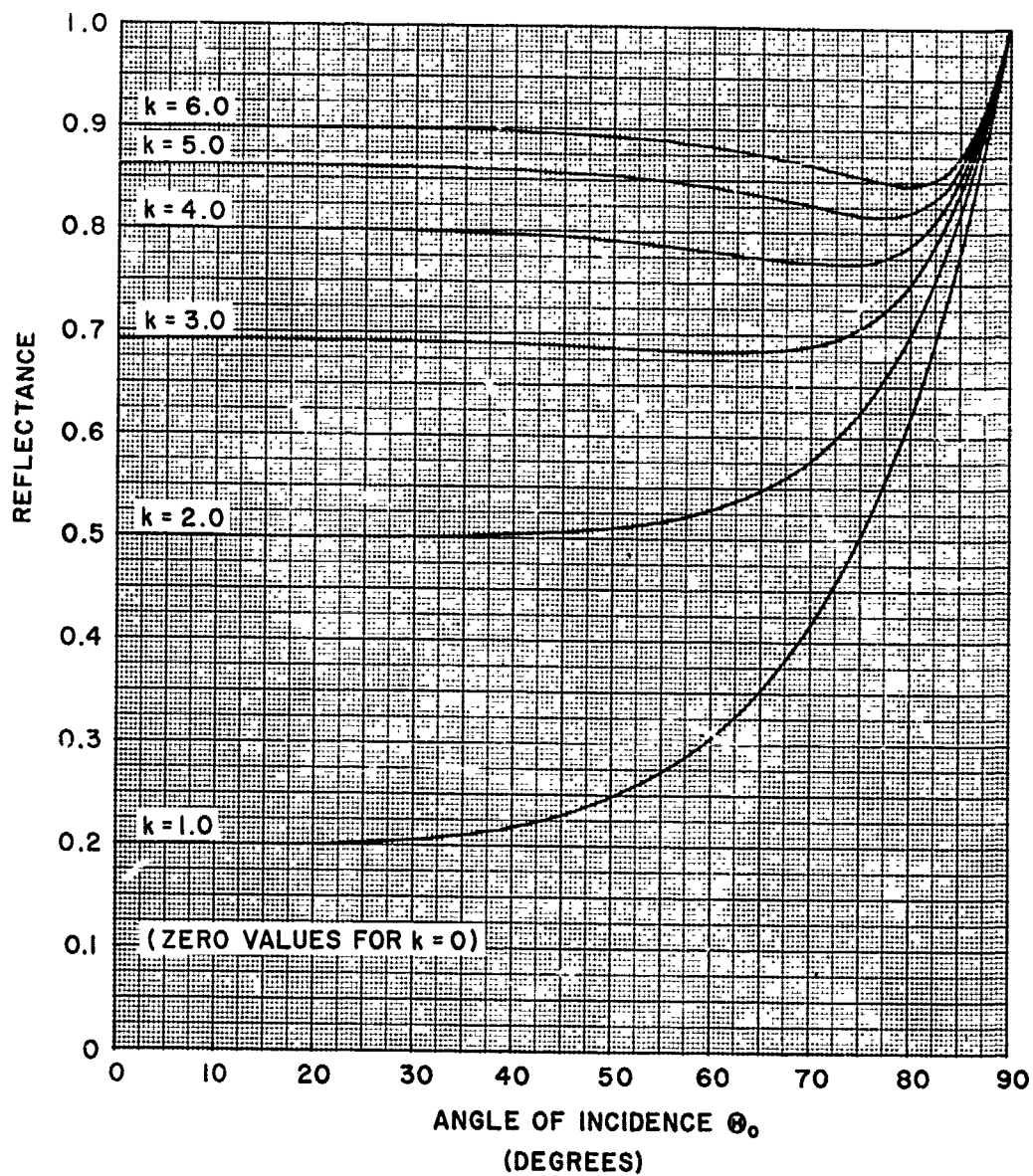


Fig. 12. REFLECTANCE CURVES  $R = \frac{1}{2} (R_1 + R_2)$  FOR  $N = 1.0 - ki$ ;  
 $k = 0$  (1.0) 6.0

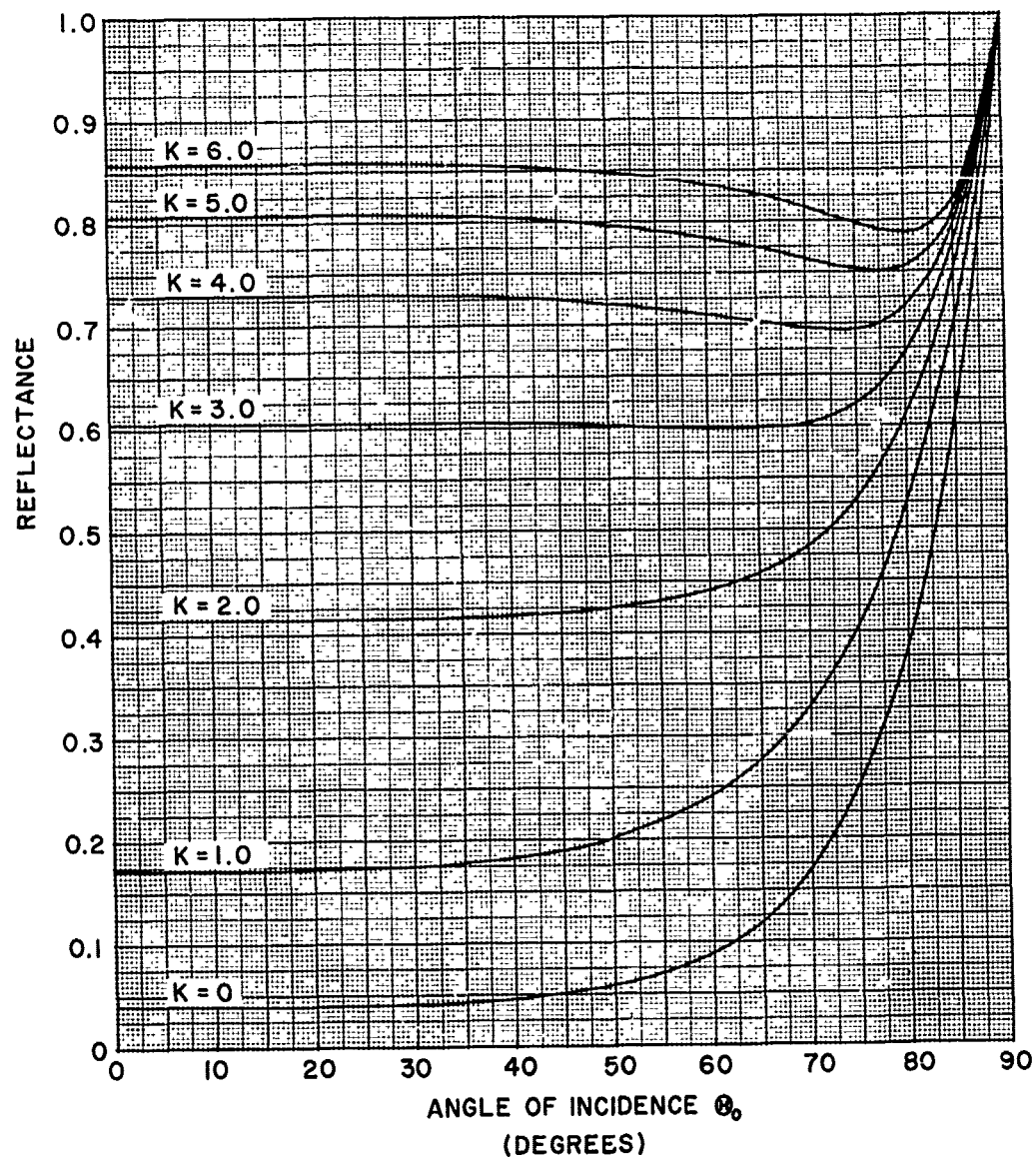


Fig. 13. REFLECTANCE CURVES  $\bar{r} = \frac{1}{2} (R_1 + R_2)$  FOR  $n = 1.5 - ki$ ;  
 $k = 0$  (1.0) 6.0

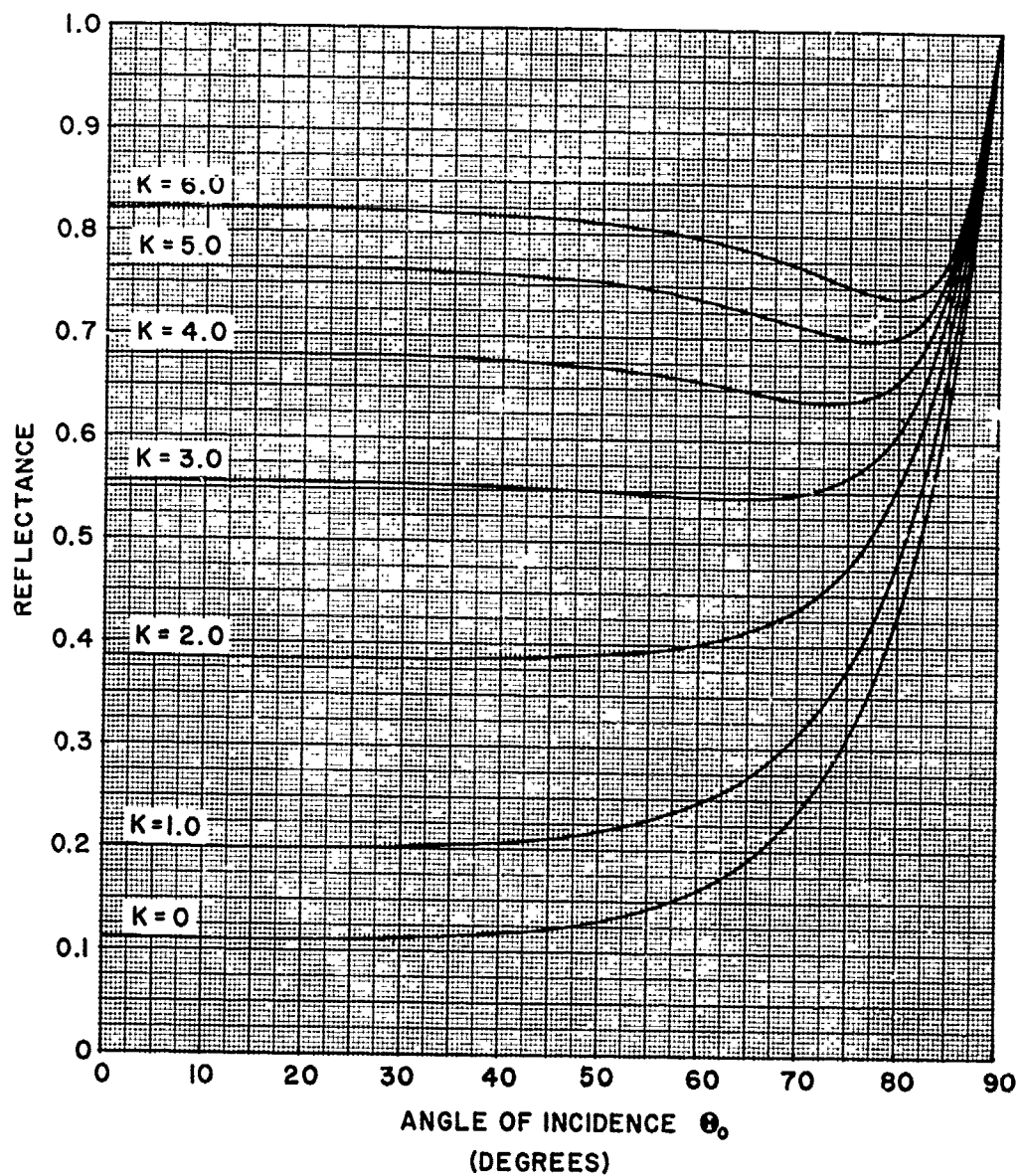


Fig. 14. REFLECTANCE CURVES  $R = \frac{1}{2} (R_1 + R_2)$  FOR  $N = 2.0 - ki$ ;  
 $k = 0 (1.0) 6.0$

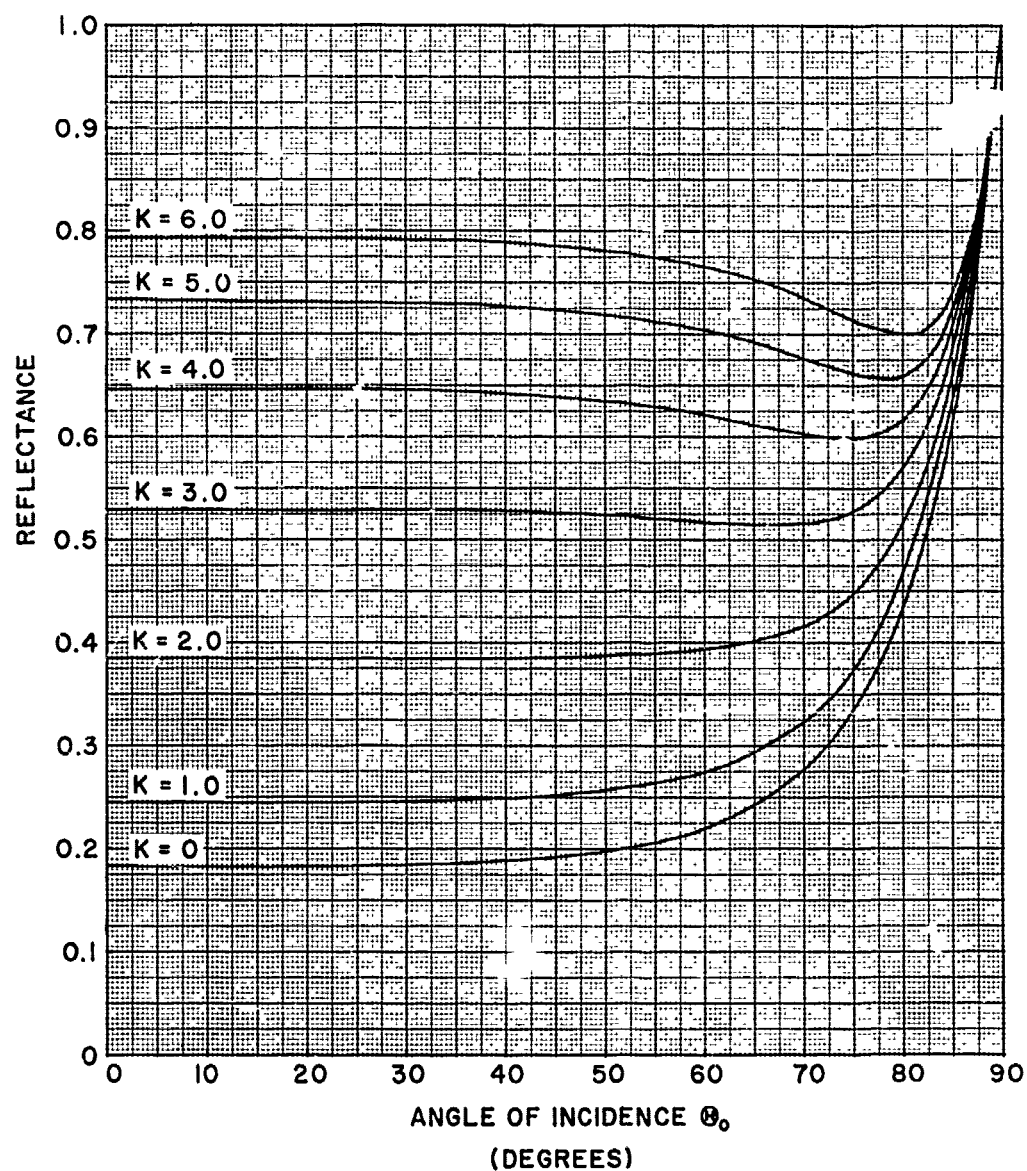


Fig. 15. REFLECTANCE CURVES  $R = \frac{1}{2} (R_1 + R_2)$  FOR  $N = 2.5 - ki$ ;  
 $k = 0 (1.0) 6.0$

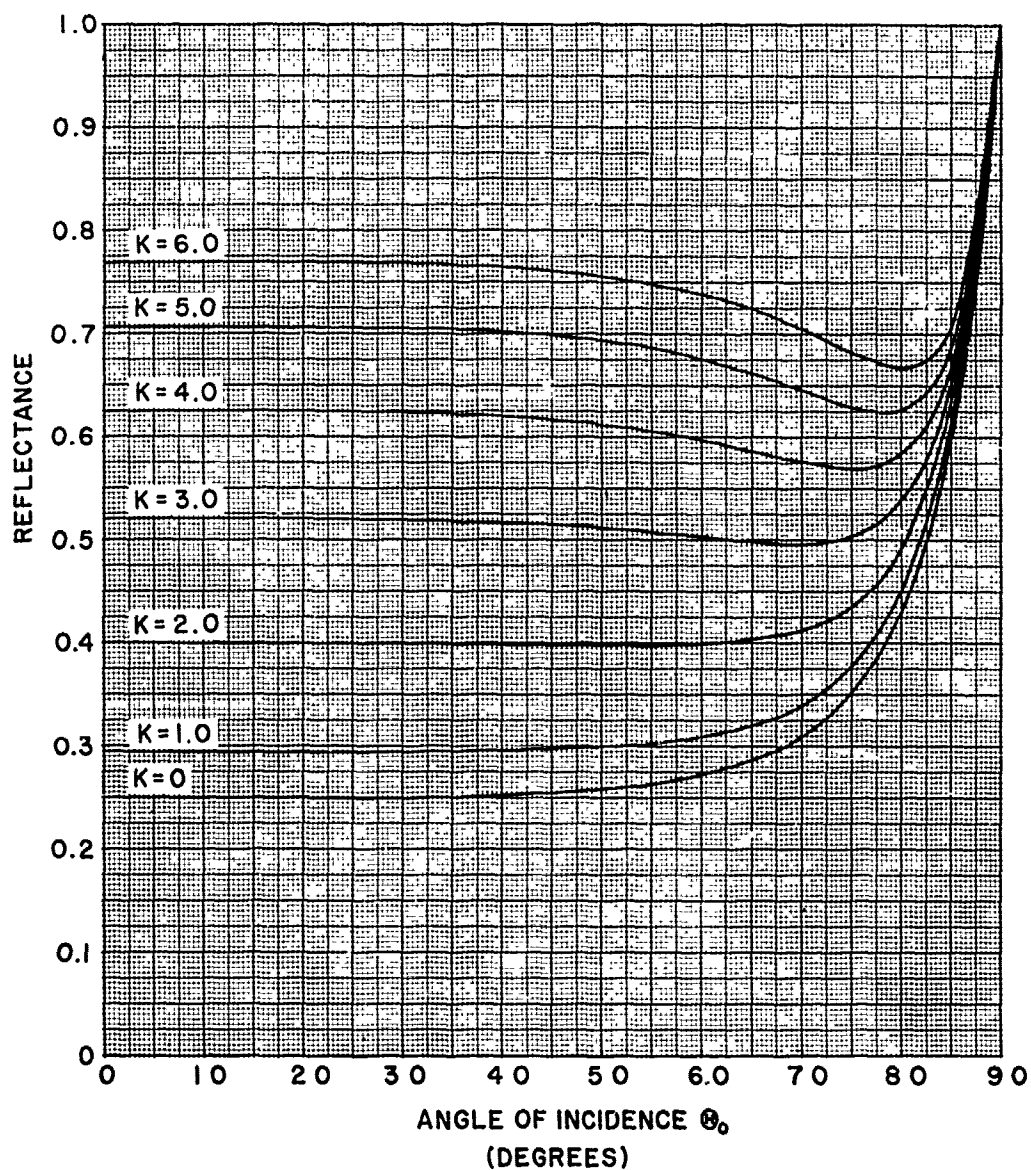


Fig. 16. REFLECTANCE CURVES  $R = \frac{1}{2} (R_1 + R_2)$  FOR  $N = 3.0 - ki$ ;  
 $k = 0$  (1.0) 6.0

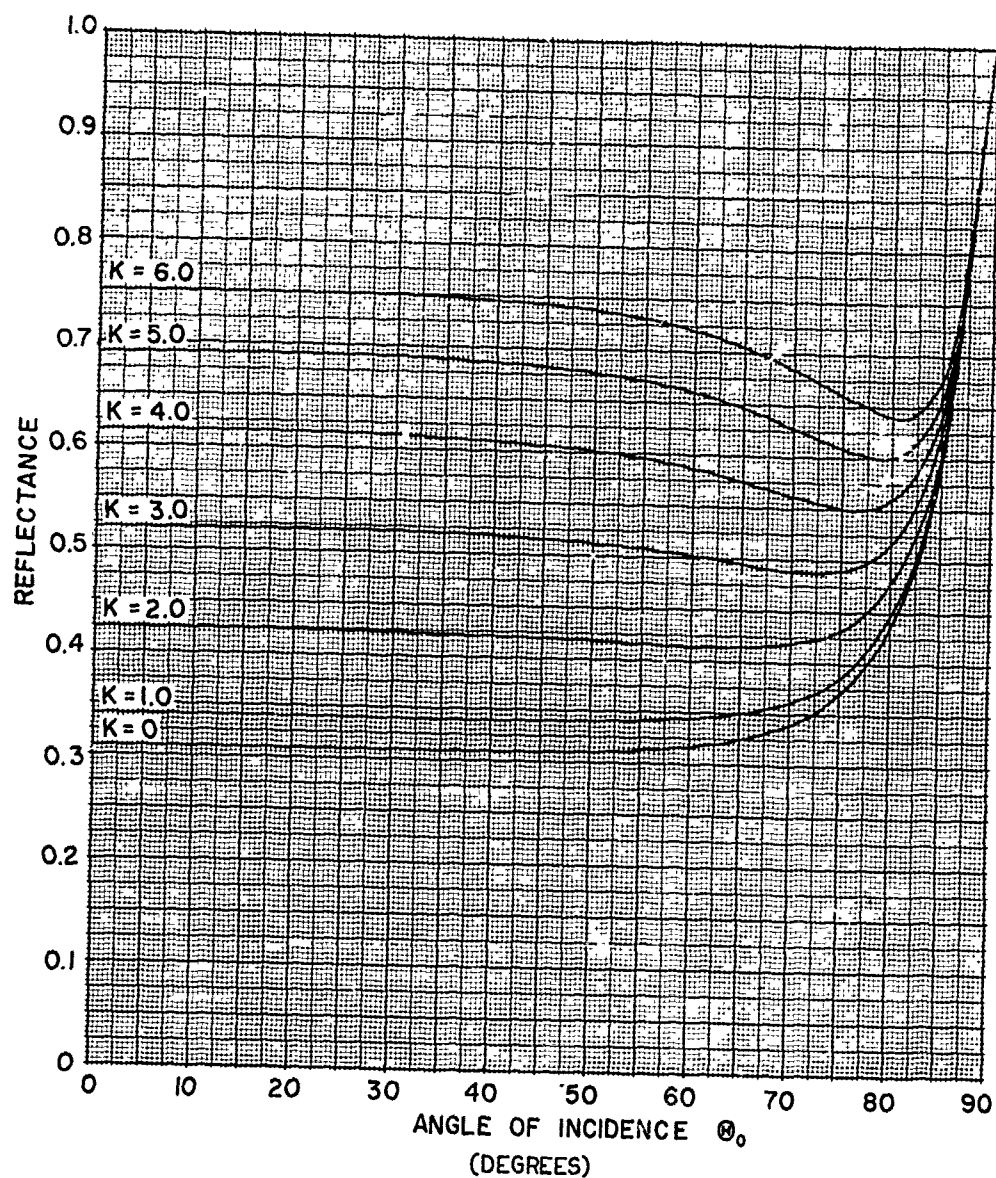


Fig. 17. REFLECTANCE CURVES  $R = \frac{1}{2} (R_1 + R_2)$  FOR  $N = 3.5 - ki$ ;  
 $k = 0$  (1.0) 6.0

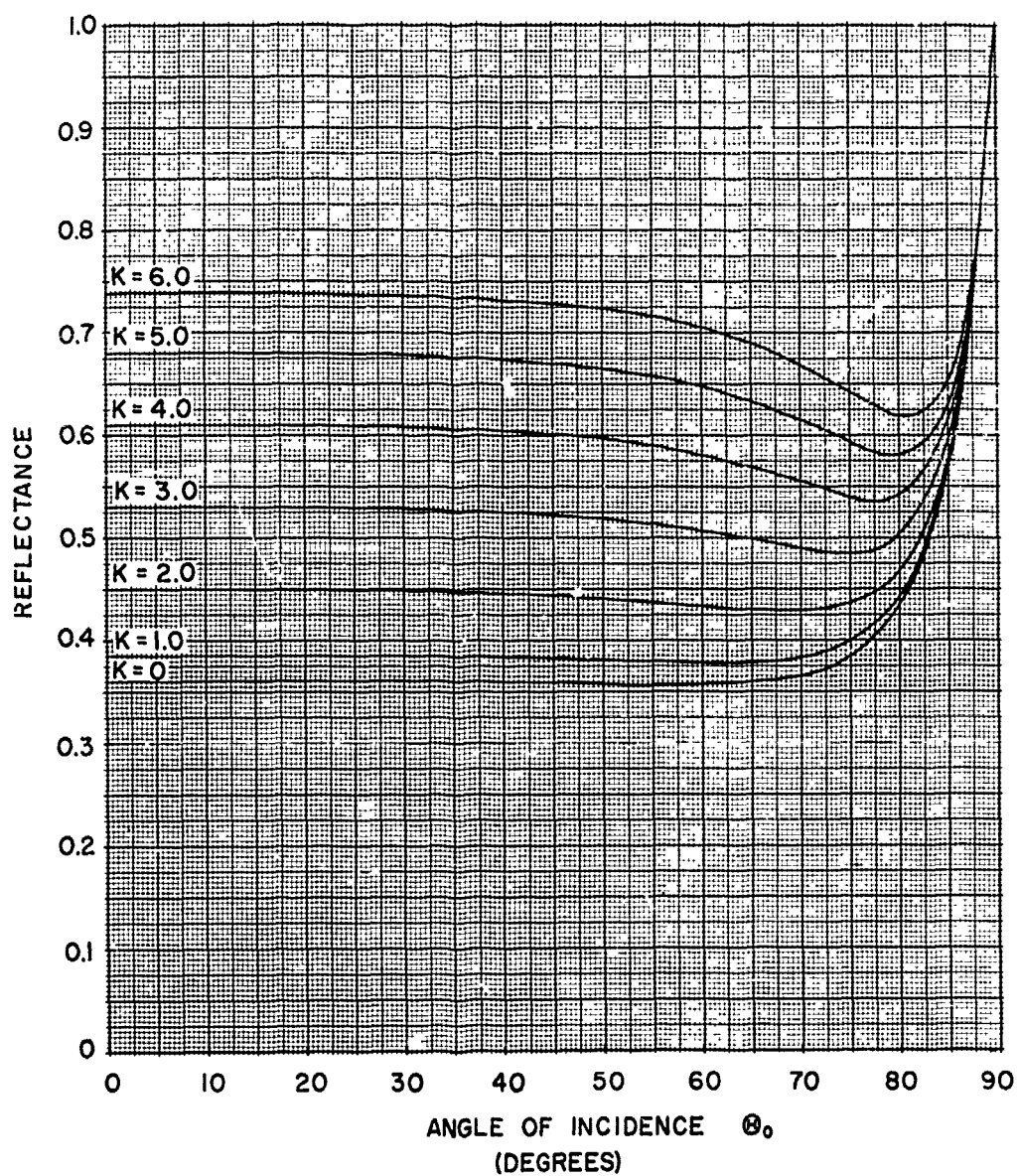


Fig. 18. REFLECTANCE CURVES  $R = \frac{1}{2} (R_1 + R_2)$  FOR  $N = 4.0 - ki$ ;  
 $k = 0 (1.0) 6.0$

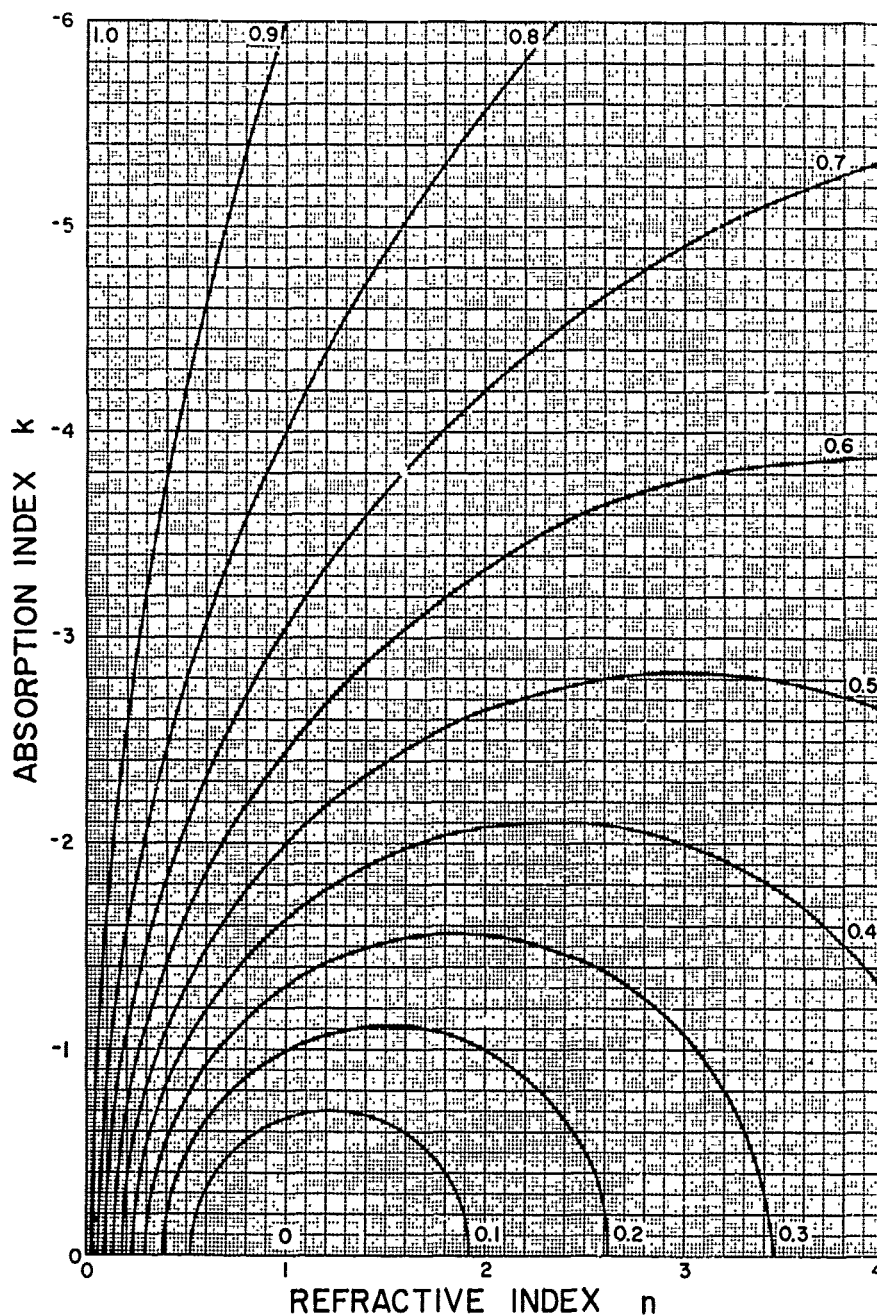


Fig. 19. RELATION BETWEEN THE REFLECTANCE  $R$  OF ELECTROMAGNETIC RADIATION AND THE COMPLEX INDEX OF REFRACTION  $N = n - ki$  FOR ANGLE OF INCIDENCE  $\theta_0 = 0^\circ$  (NORMAL INCIDENCE)

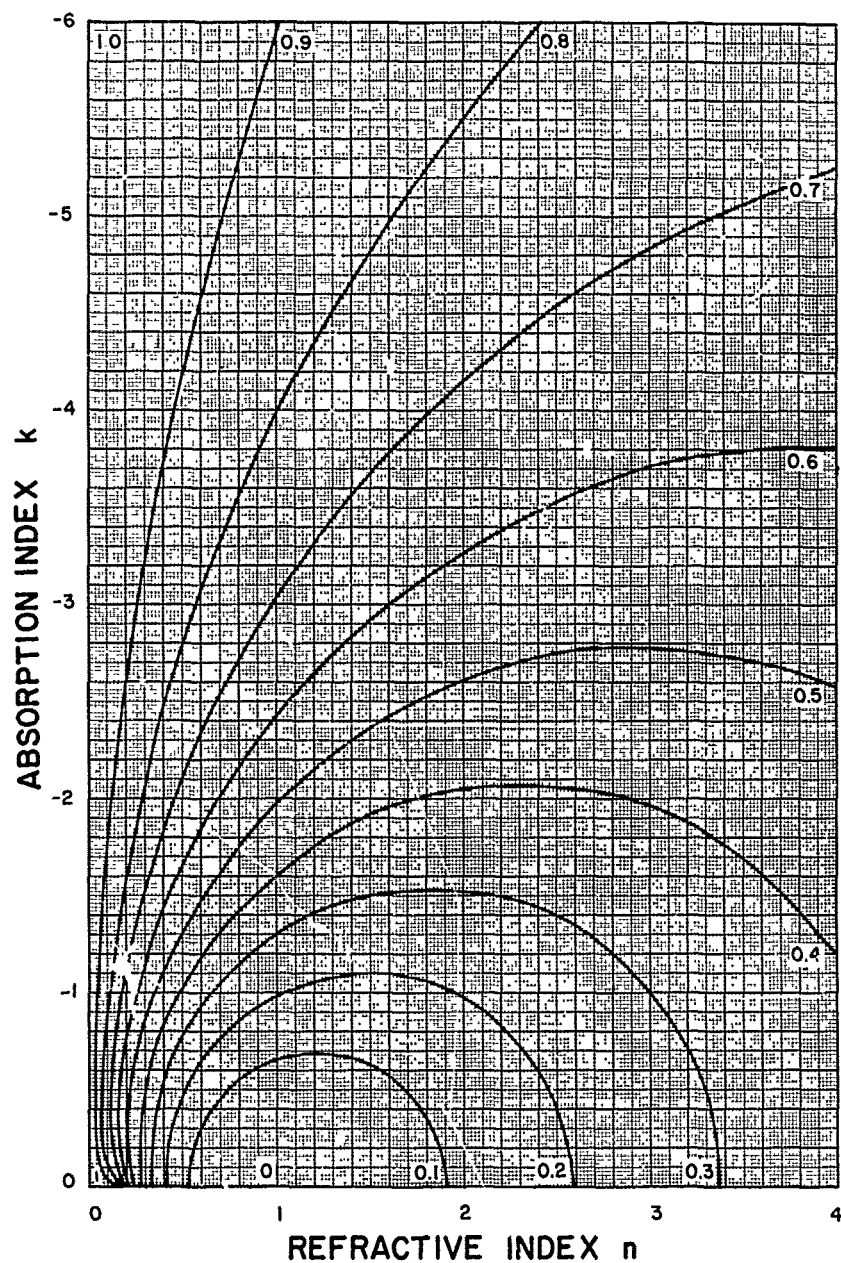


Fig. 20. RELATION BETWEEN THE REFLECTANCE  $R_1$  OF ELECTROMAGNETIC RADIATION AND THE COMPLEX INDEX OF REFRACTION  $N = n - ki$  FOR OBLIQUE INCIDENCE  $\theta_0 = 10^\circ$  WITH RESPECT TO THE SURFACE NORMAL

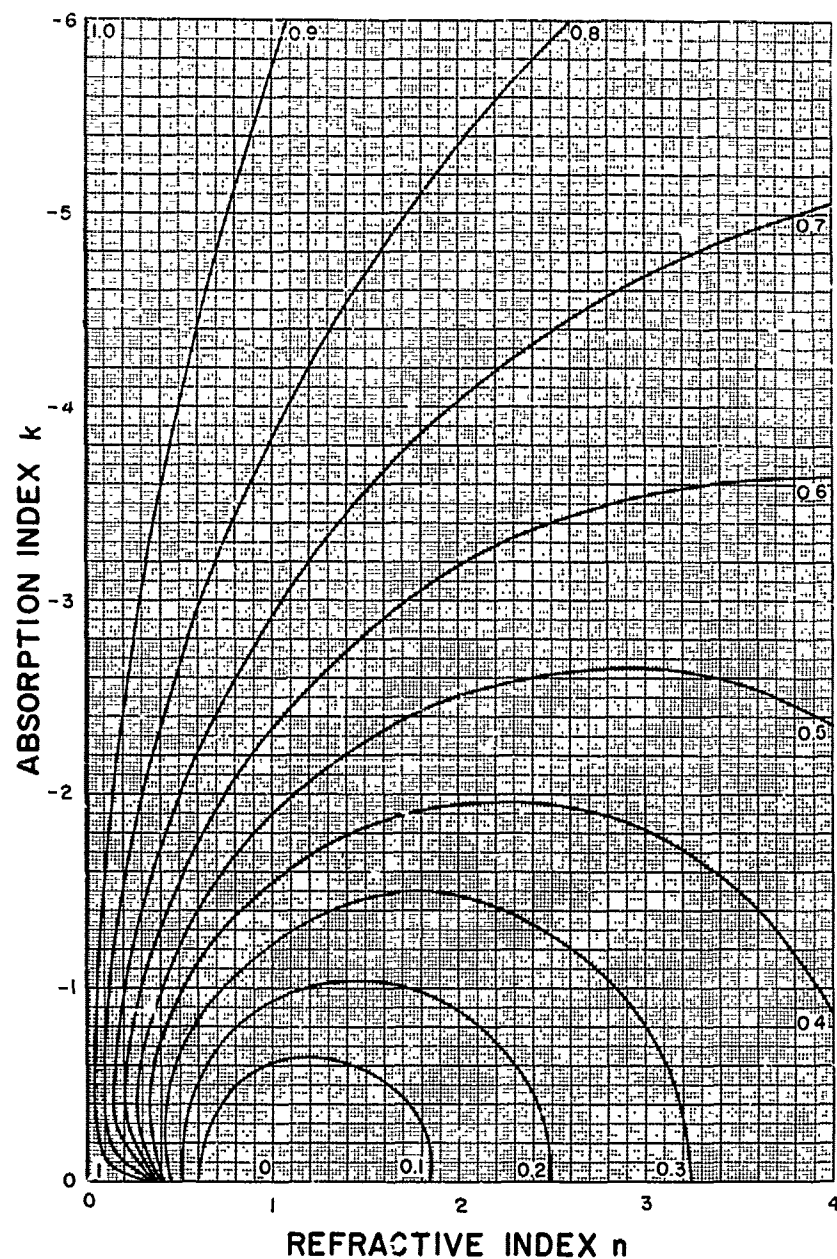


Fig. 21. RELATION BETWEEN THE REFLECTANCE  $R_1$  OF ELECTROMAGNETIC RADIATION AND THE COMPLEX INDEX OF REFRACTION  $N = n - ki$  FOR OBLIQUE INCIDENCE  $\theta_0 = 20^\circ$  WITH RESPECT TO THE SURFACE NORMAL

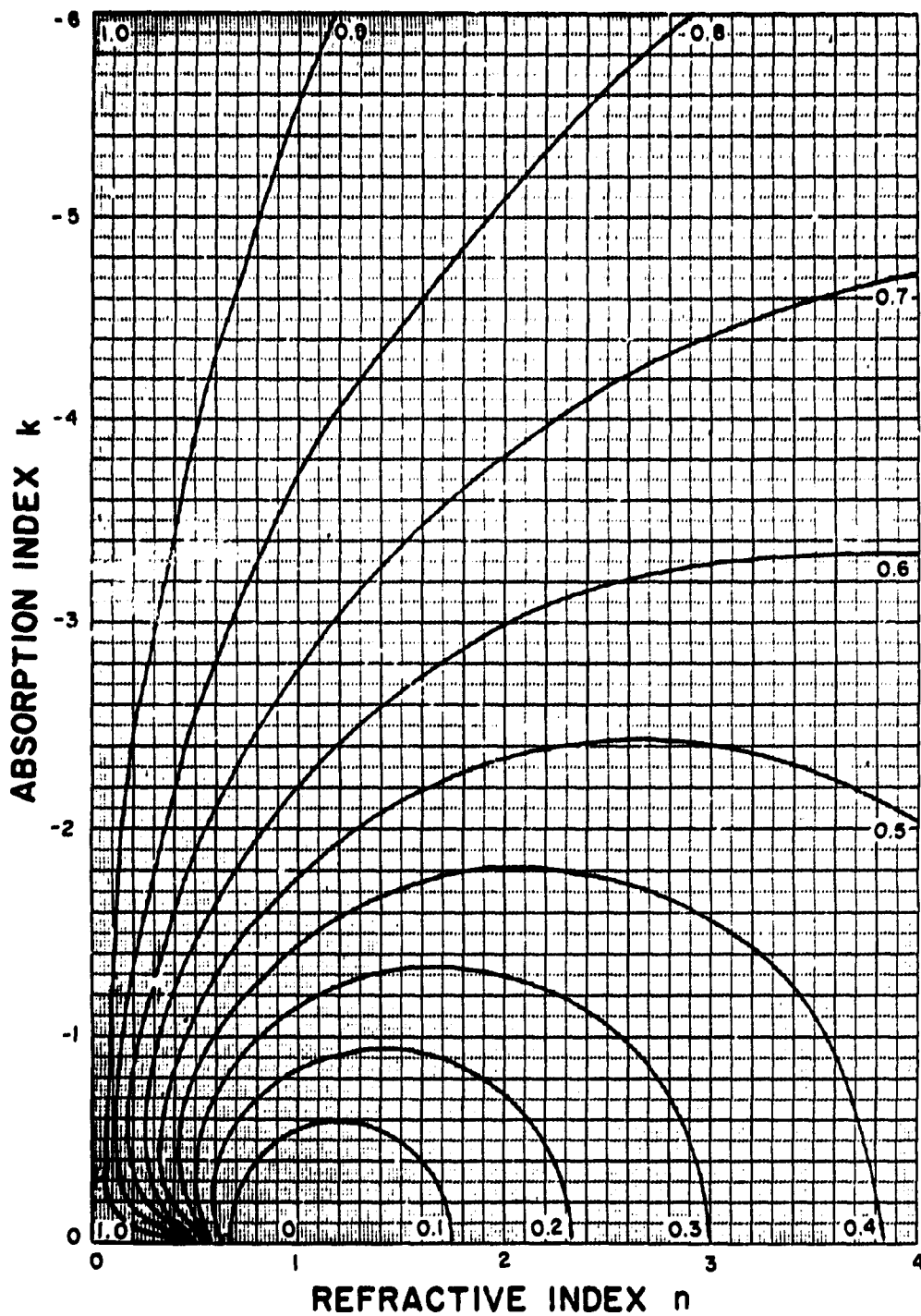


Fig. 22. RELATION BETWEEN THE REFLECTANCE  $R_1$  OF ELECTROMAGNETIC RADIATION AND THE COMPLEX INDEX OF REFRACTION  $N = n - ki$  FOR OBLIQUE INCIDENCE  $\theta_0 = 30^\circ$  WITH RESPECT TO THE SURFACE NORMAL

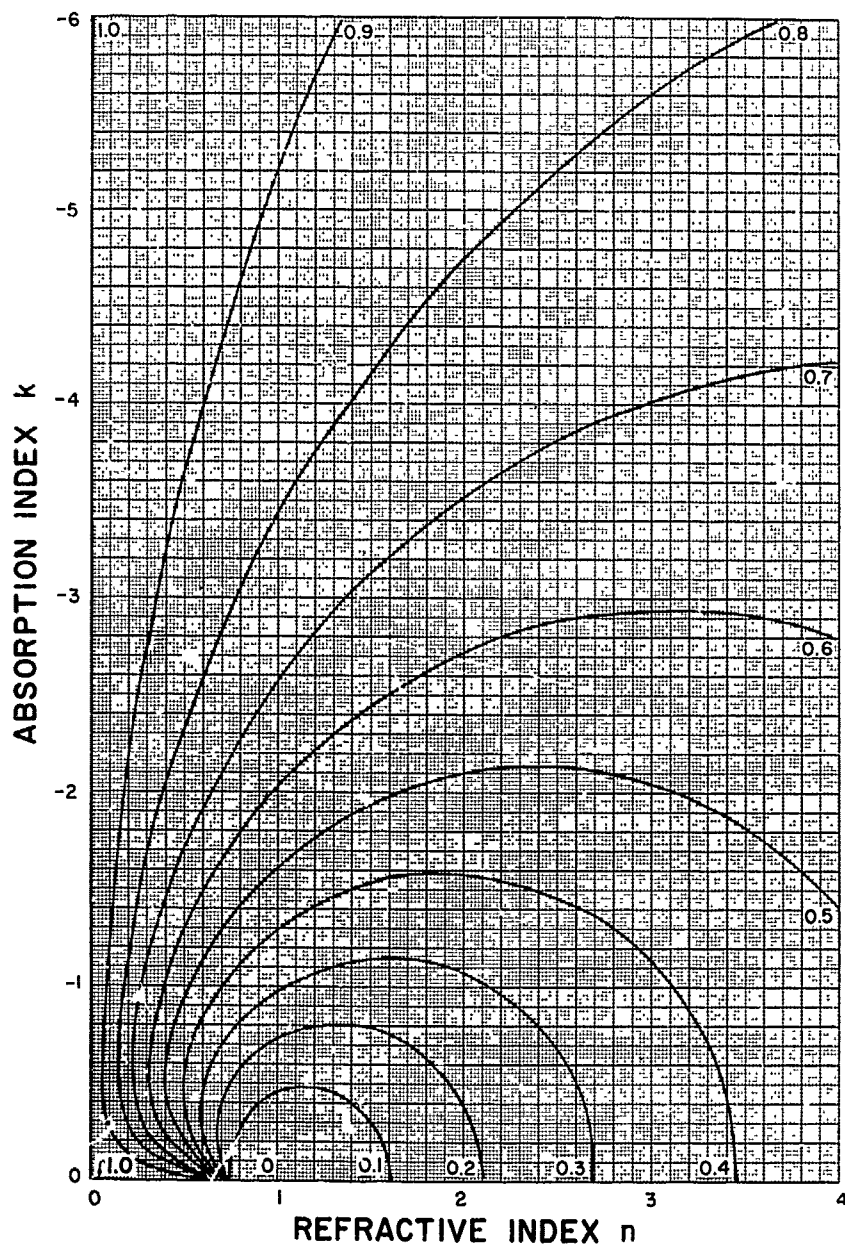


Fig. 23. RELATION BETWEEN THE REFLECTANCE  $R_1$  OF ELECTROMAGNETIC RADIATION AND THE COMPLEX INDEX OF REFRACTION  $N = n - ki$  FOR OBLIQUE INCIDENCE  $\theta_0 = 40^\circ$  WITH RESPECT TO THE SURFACE NORMAL

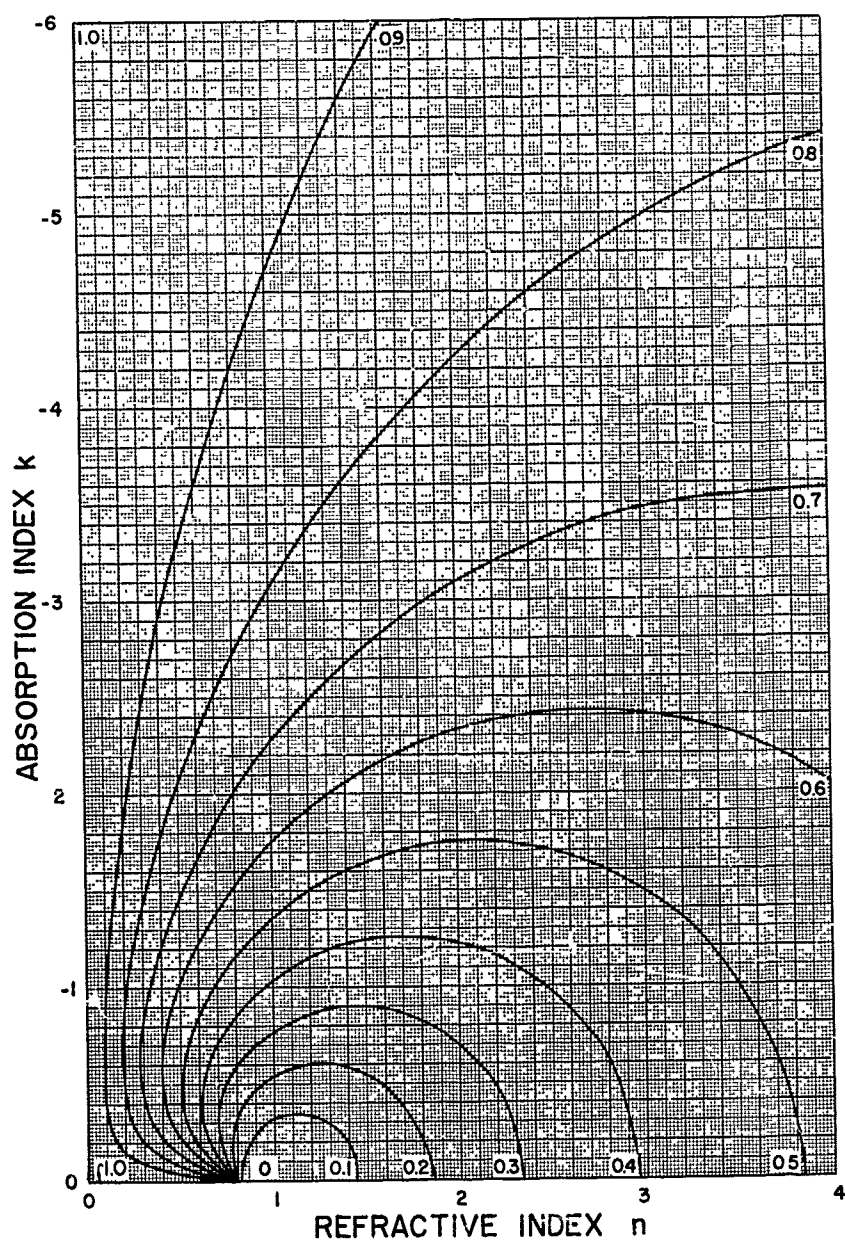


Fig. 24. RELATION BETWEEN THE REFLECTANCE  $R_1$  OF ELECTROMAGNETIC RADIATION AND THE COMPLEX INDEX OF REFRACTION  $N = n - ki$  FOR OBLIQUE INCIDENCE  $\theta_0 = 50^\circ$  WITH RESPECT TO THE SURFACE NORMAL

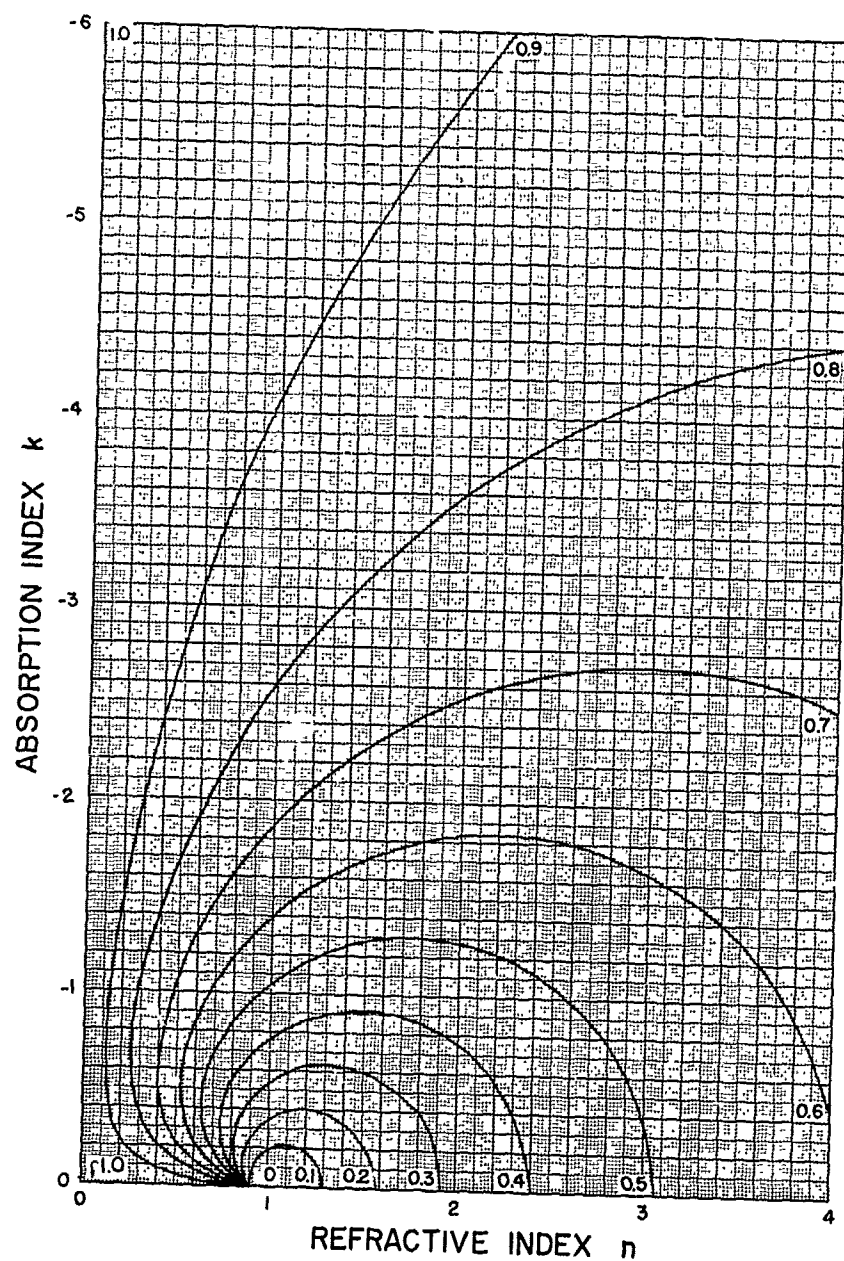


Fig. 25. RELATION BETWEEN THE REFLECTANCE  $R_1$  OF ELECTROMAGNETIC RADIATION AND THE COMPLEX INDEX OF REFRACTION  $N = n - ki$  FOR OBLIQUE INCIDENCE  $\theta_0 = 60^\circ$  WITH RESPECT TO THE SURFACE NORMAL

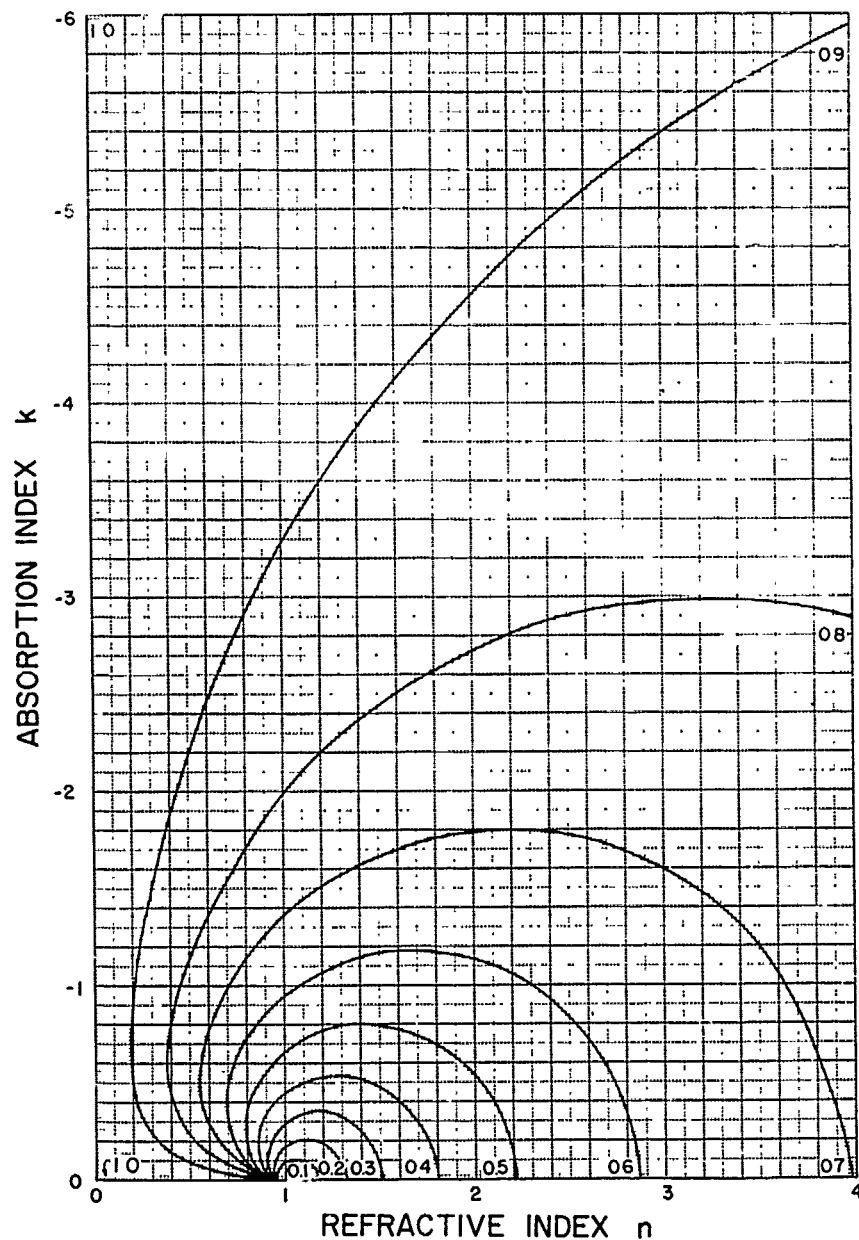


Fig. 26. RELATION BETWEEN THE REFLECTANCE  $R_1$  OF ELECTROMAGNETIC RADIATION AND THE COMPLEX INDEX OF REFRACTION  $N = n - ki$  FOR OBLIQUE INCIDENCE  $\theta_0 = 70^\circ$  WITH RESPECT TO THE SURFACE NORMAL

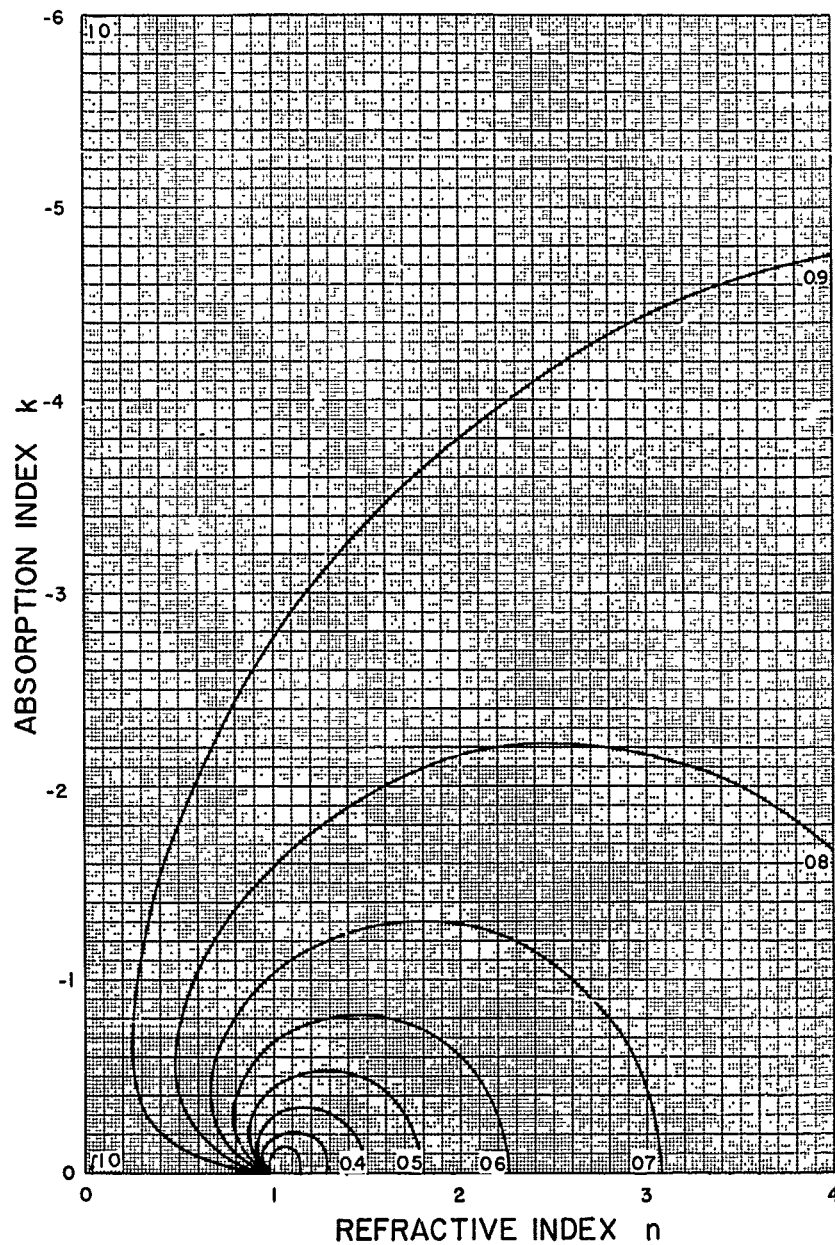


Fig. 27. RELATION BETWEEN THE REFLECTANCE  $R_1$  OF ELECTROMAGNETIC RADIATION AND THE COMPLEX INDEX OF REFRACTION  $N = n - ki$  FOR OBLIQUE INCIDENCE  $\theta_0 = 75^\circ$  WITH RESPECT TO THE SURFACE NORMAL

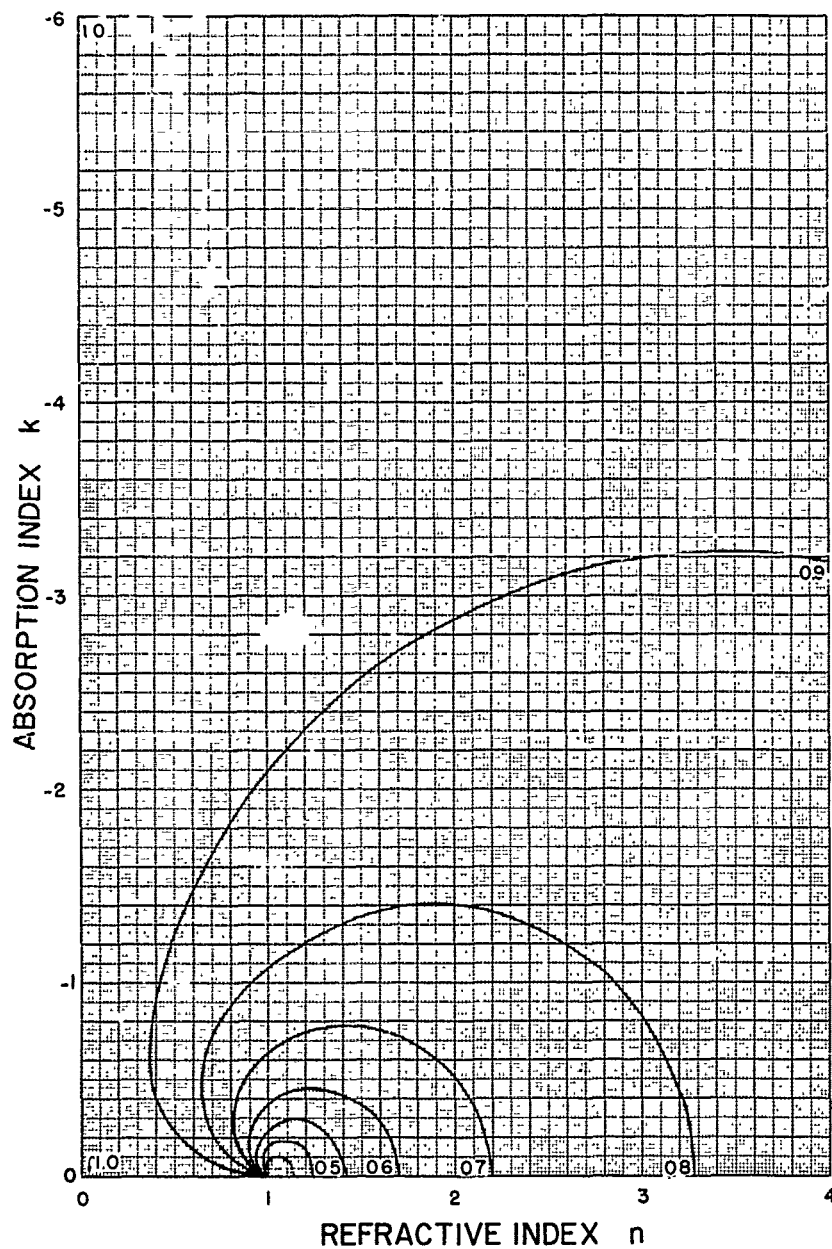


Fig. 28. RELATION BETWEEN THE REFLECTANCE  $R_1$  OF ELECTROMAGNETIC RADIATION AND THE COMPLEX INDEX OF REFRACTION  $N = n - ki$  FOR OBLIQUE INCIDENCE  $\theta_0 = 80^\circ$  WITH RESPECT TO THE SURFACE NORMAL

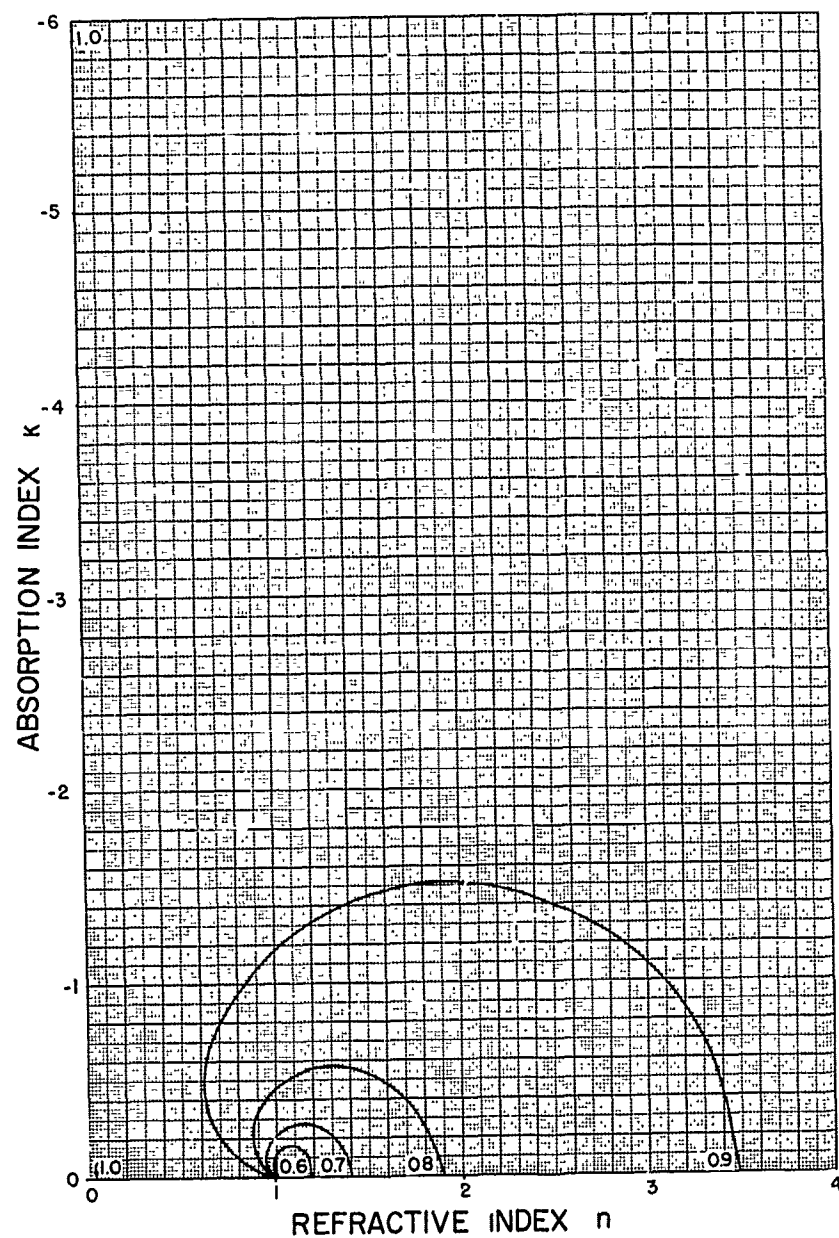


Fig. 29. RELATION BETWEEN THE REFLECTANCE  $R_1$  OF ELECTROMAGNETIC RADIATION AND THE COMPLEX INDEX OF REFRACTION  $N = n - ki$  FOR OBLIQUE INCIDENCE  $\theta_0 = 85^\circ$  WITH RESPECT TO THE SURFACE NORMAL

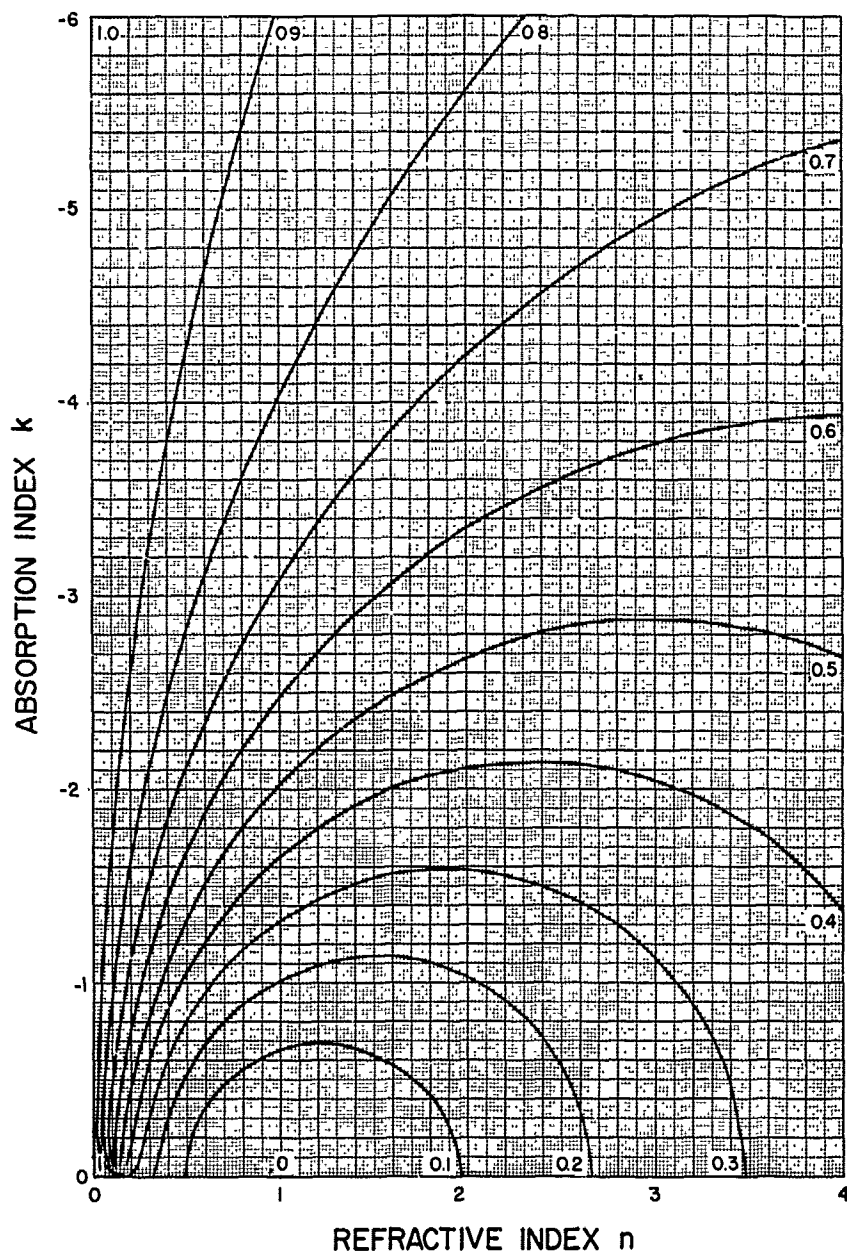


Fig. 30. RELATION BETWEEN THE REFLECTANCE  $R_2$  OF ELECTROMAGNETIC RADIATION AND THE COMPLEX INDEX OF REFRACTION  $N = n - ki$  FOR OBLIQUE INCIDENCE  $\theta_0 = 10^\circ$  WITH RESPECT TO THE SURFACE NORMAL

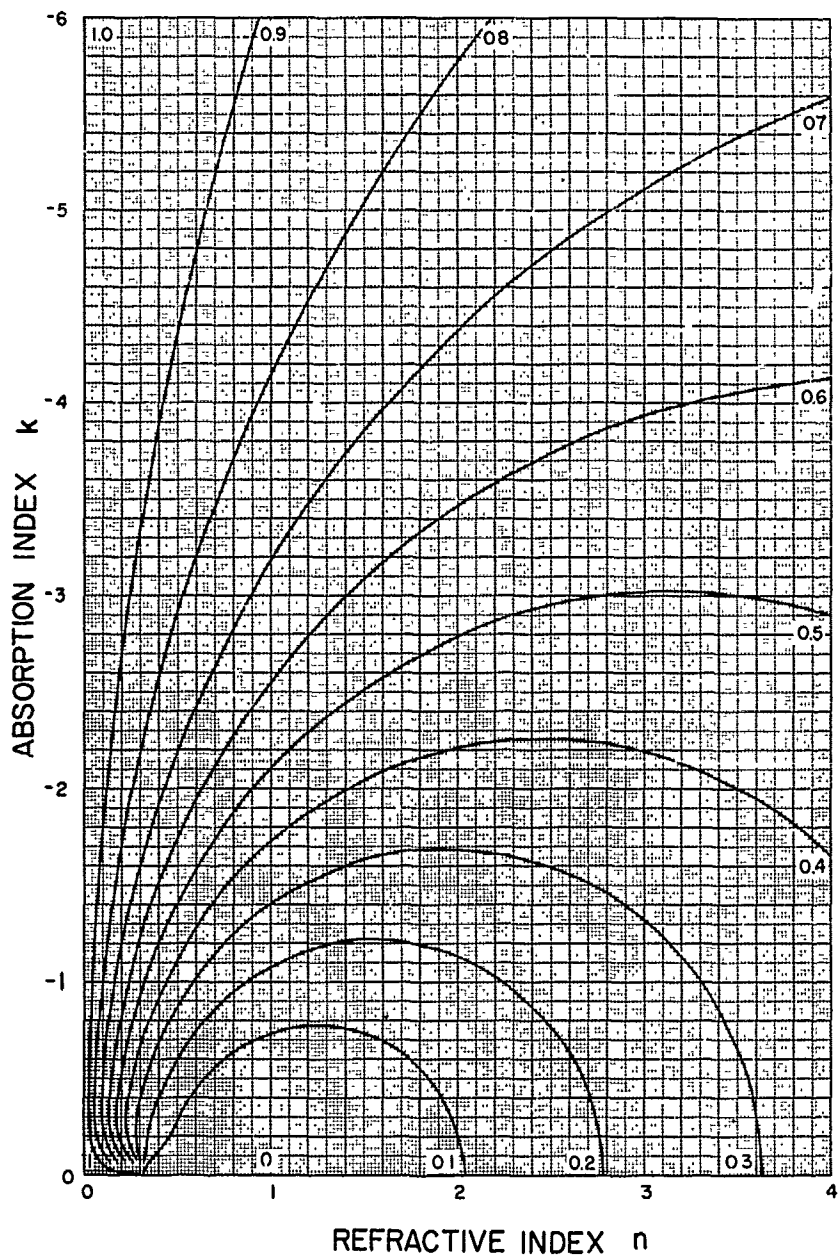


Fig. 31. RELATION BETWEEN THE REFLECTANCE  $R_2$  OF ELECTROMAGNETIC RADIATION AND THE COMPLEX INDEX OF REFRACTION  $N = n - ki$  FOR OBLIQUE INCIDENCE  $\Theta_0 = 20^\circ$  WITH RESPECT TO THE SURFACE NORMAL

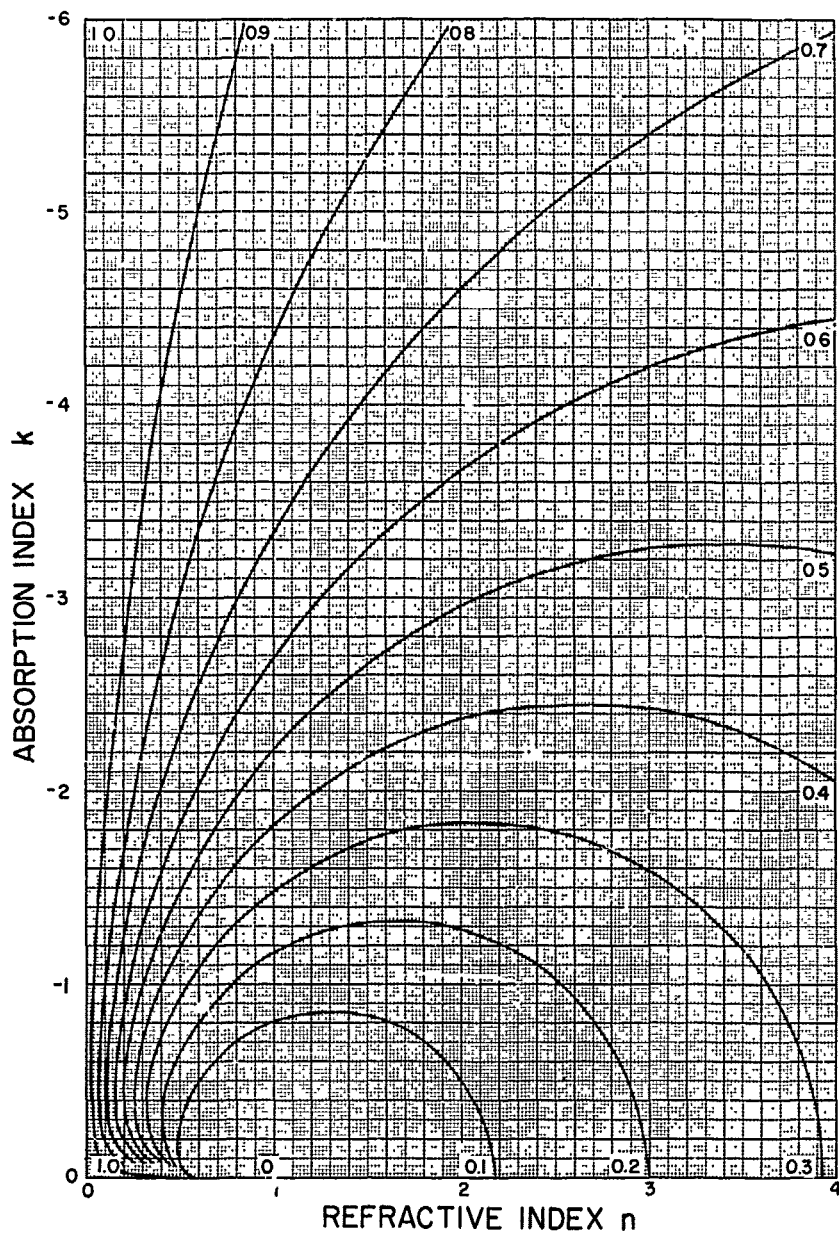


Fig. 32. RELATION BETWEEN THE REFLECTANCE  $R_2$  OF ELECTROMAGNETIC RADIATION AND THE COMPLEX INDEX OF REFRACTION  $N = n - ki$  FOR OBLIQUE INCIDENCE  $\theta_0 = 30^\circ$  WITH RESPECT TO THE SURFACE NORMAL

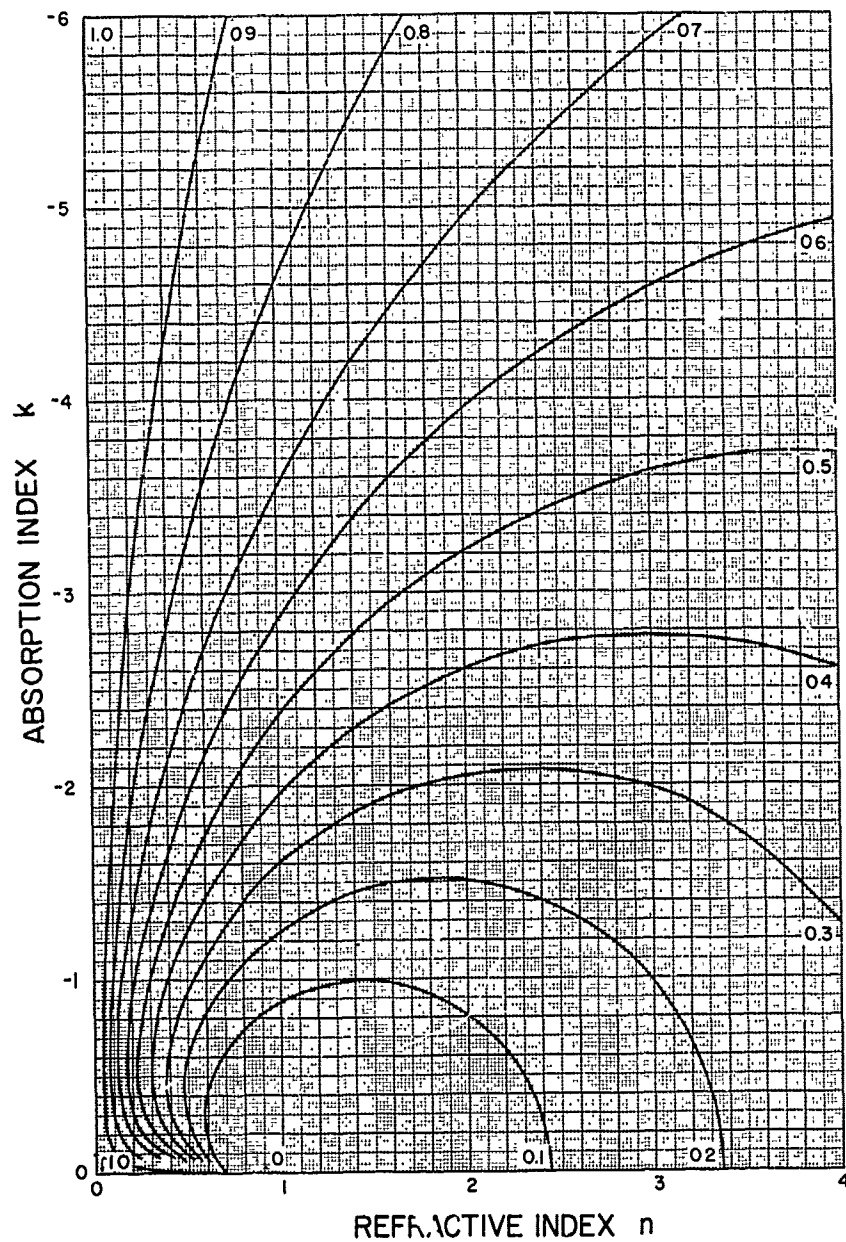


Fig. 33. RELATION BETWEEN THE REFLECTANCE  $R_2$  OF ELECTROMAGNETIC RADIATION AND THE COMPLEX INDEX OF REFRACTION  $N = n - ki$  FOR OBLIQUE INCIDENCE  $\Theta_0 = 40^\circ$  WITH RESPECT TO THE SURFACE NORMAL

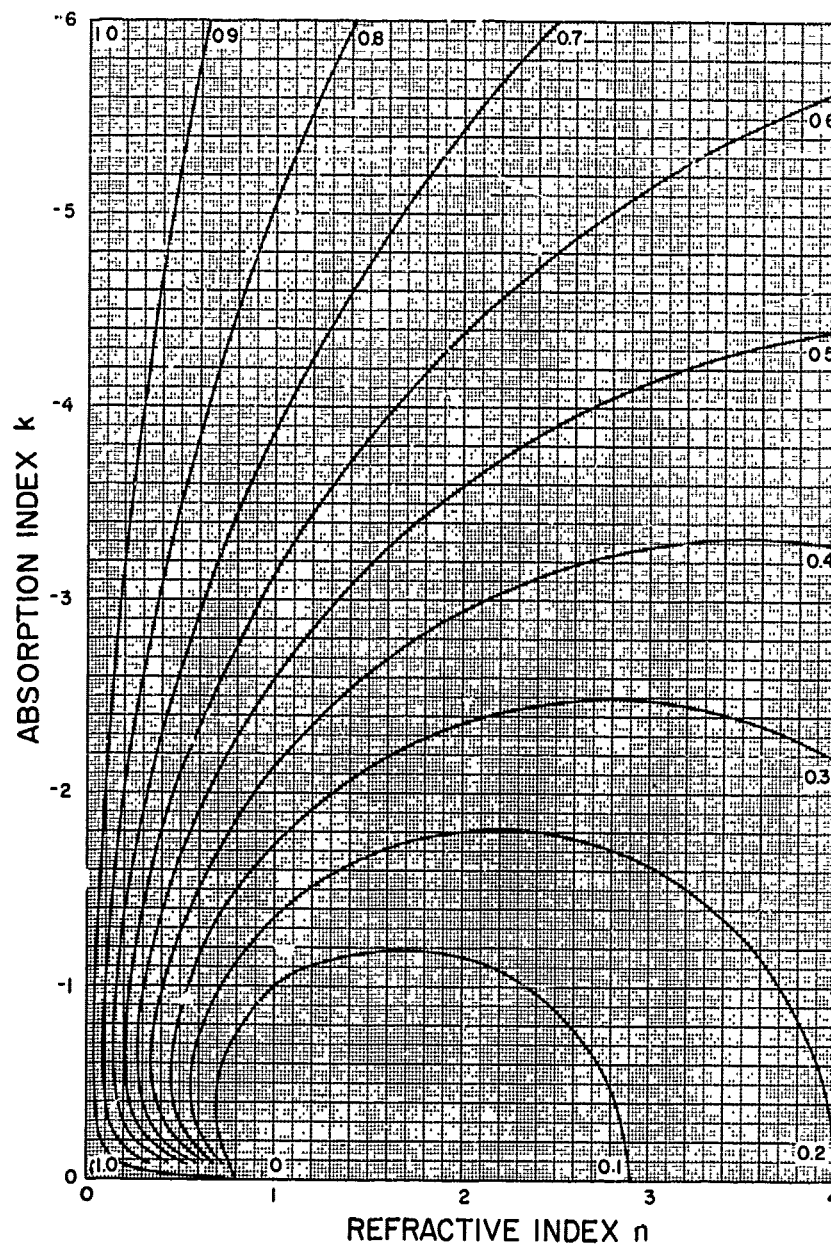


Fig. 34. RELATION BETWEEN THE REFLECTANCE  $R_2$  OF ELECTROMAGNETIC RADIATION AND THE COMPLEX INDEX OF REFRACTION  $N = n - ki$  FOR OBLIQUE INCIDENCE  $\Theta_0 = 50^\circ$  WITH RESPECT TO THE SURFACE NORMAL

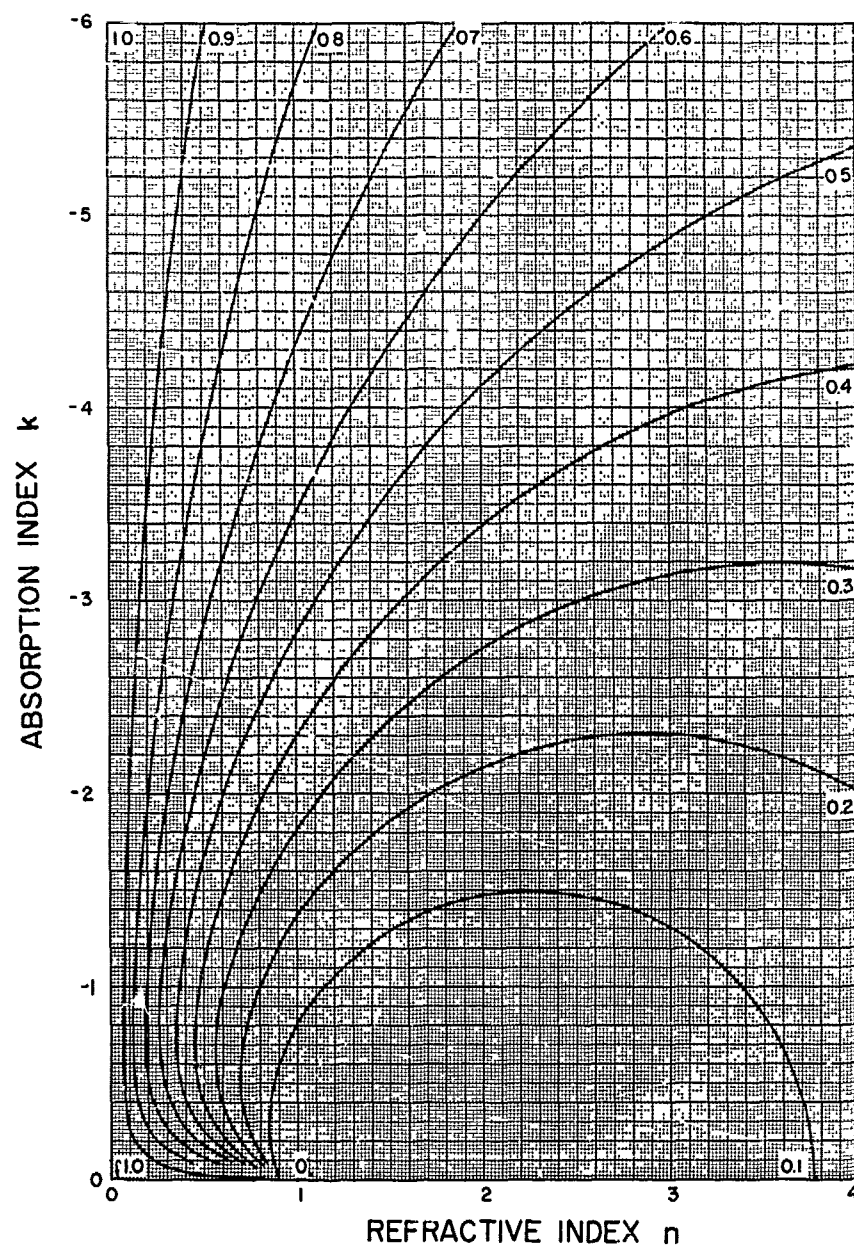


Fig. 35. RELATION BETWEEN THE REFLECTANCE  $R_2$  OF ELECTROMAGNETIC RADIATION AND THE COMPLEX INDEX OF REFRACTION  $N = n - ki$  FOR OBLIQUE INCIDENCE  $\theta_0 = 60^\circ$  WITH RESPECT TO THE SURFACE NORMAL

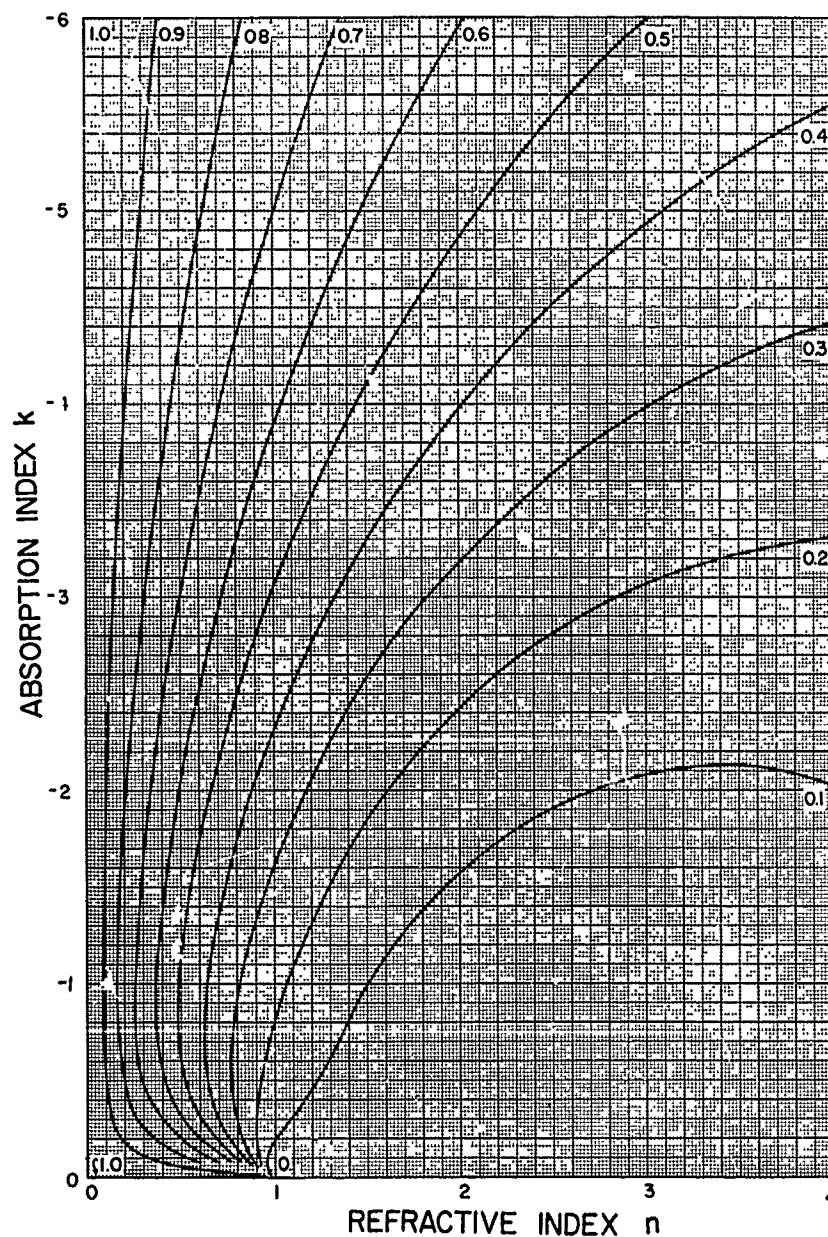


Fig. 36. RELATION BETWEEN THE REFLECTANCE  $R_2$  OF ELECTROMAGNETIC RADIATION AND THE COMPLEX INDEX OF REFRACTION  $N = n - ki$  FOR OBLIQUE INCIDENCE  $\theta_0 = 70^\circ$  WITH RESPECT TO THE SURFACE NORMAL

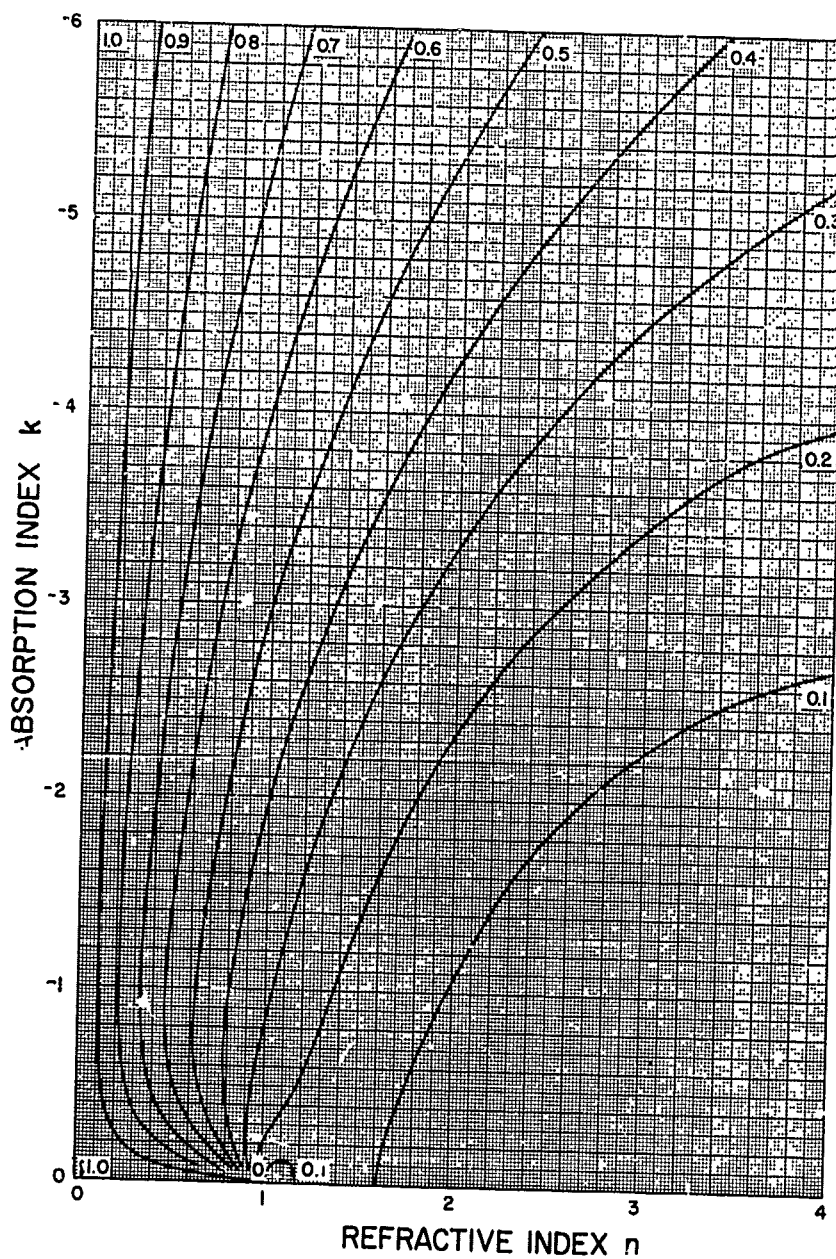


Fig. 37. RELATION BETWEEN THE REFLECTANCE  $R_2$  OF ELECTROMAGNETIC RADIATION AND THE COMPLEX INDEX OF REFRACTION  $N = n - ki$  FOR OBLIQUE INCIDENCE  $\theta_0 = 75^\circ$  WITH RESPECT TO THE SURFACE NORMAL

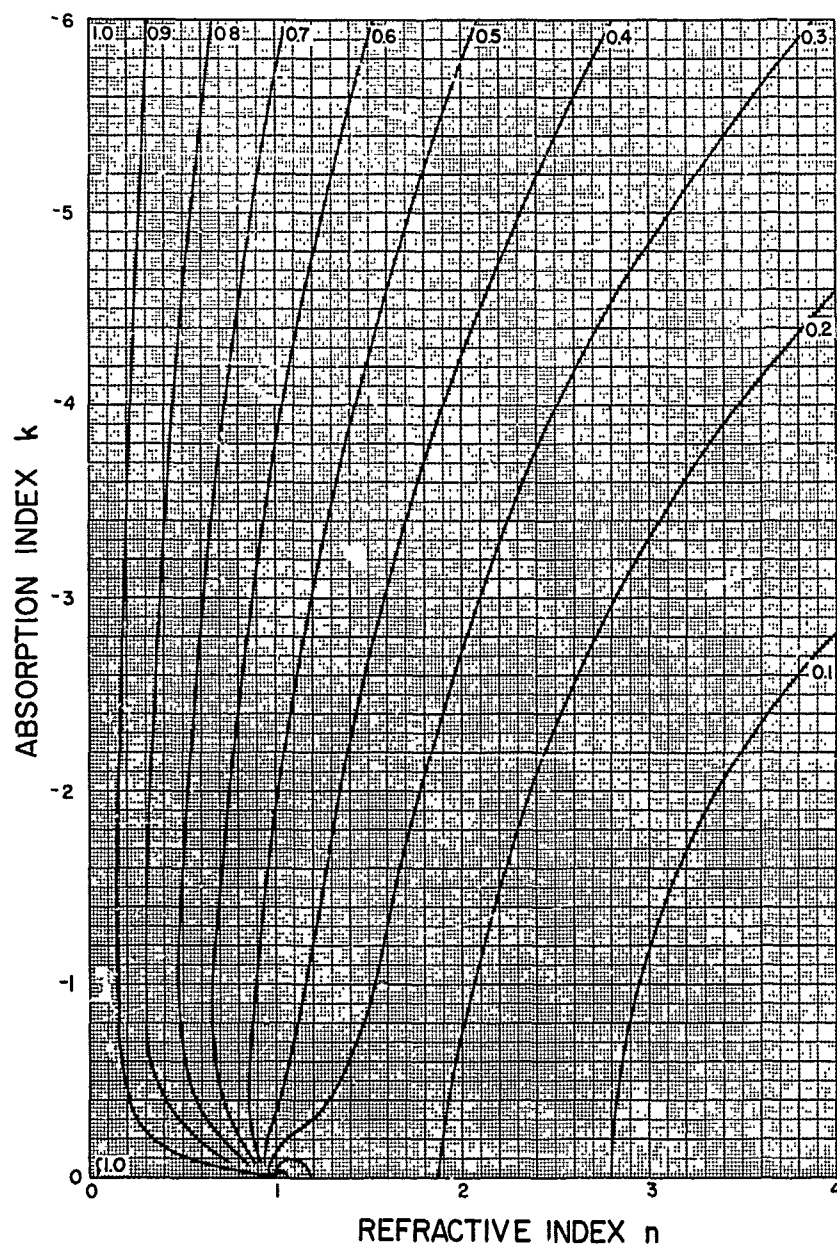


Fig. 38. RELATION BETWEEN THE REFLECTANCE  $R_2$  OF ELECTROMAGNETIC RADIATION AND THE COMPLEX INDEX OF REFRACTION  $N = n - ki$  FOR OBLIQUE INCIDENCE  $\Theta_0 = 80^\circ$  WITH RESPECT TO THE SURFACE NORMAL

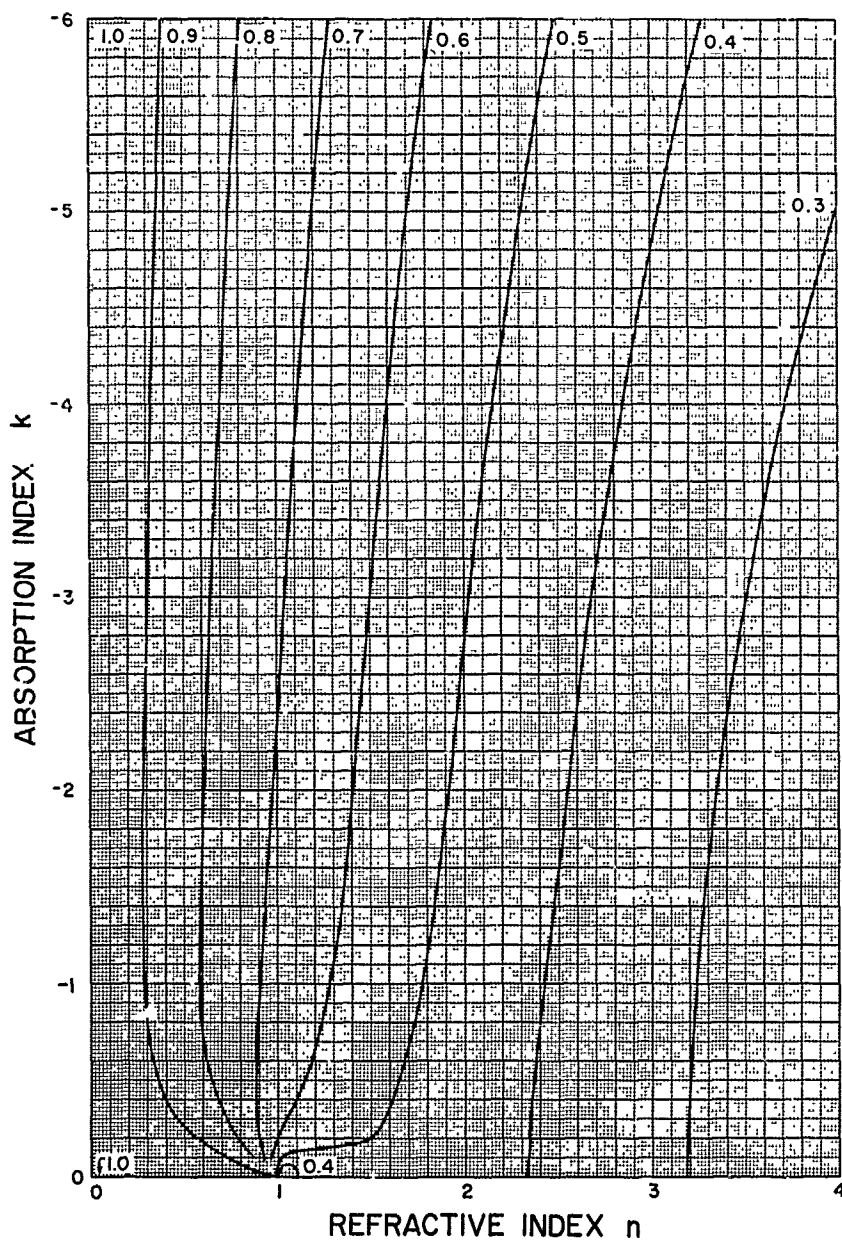


Fig. 39. RELATION BETWEEN THE REFLECTANCE  $R_2$  OF ELECTROMAGNETIC RADIATION AND THE COMPLEX INDEX OF REFRACTION  $N = n - ki$  FOR OBLIQUE INCIDENCE  $\theta_0 = 85^\circ$  WITH RESPECT TO THE SURFACE NORMAL

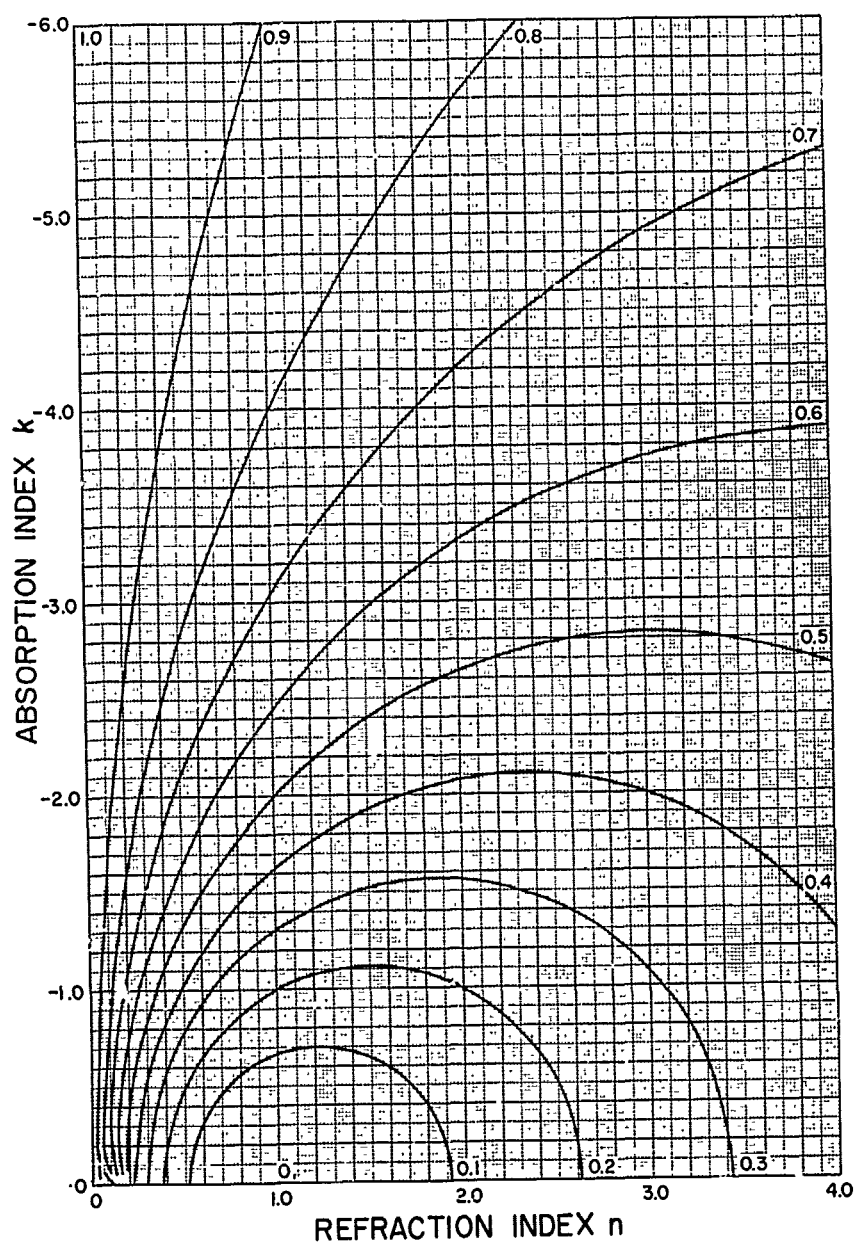


Fig. 40. RELATION BETWEEN THE REFLECTANCE  $R = \frac{1}{2} (R_1 + R_2)$  OF ELECTROMAGNETIC RADIATION AND THE COMPLEX INDEX OF REFRACTION  $N = n - ki$  FOR OBLIQUE INCIDENCE  $\theta_0 = 10^\circ$  WITH RESPECT TO THE SURFACE NORMAL

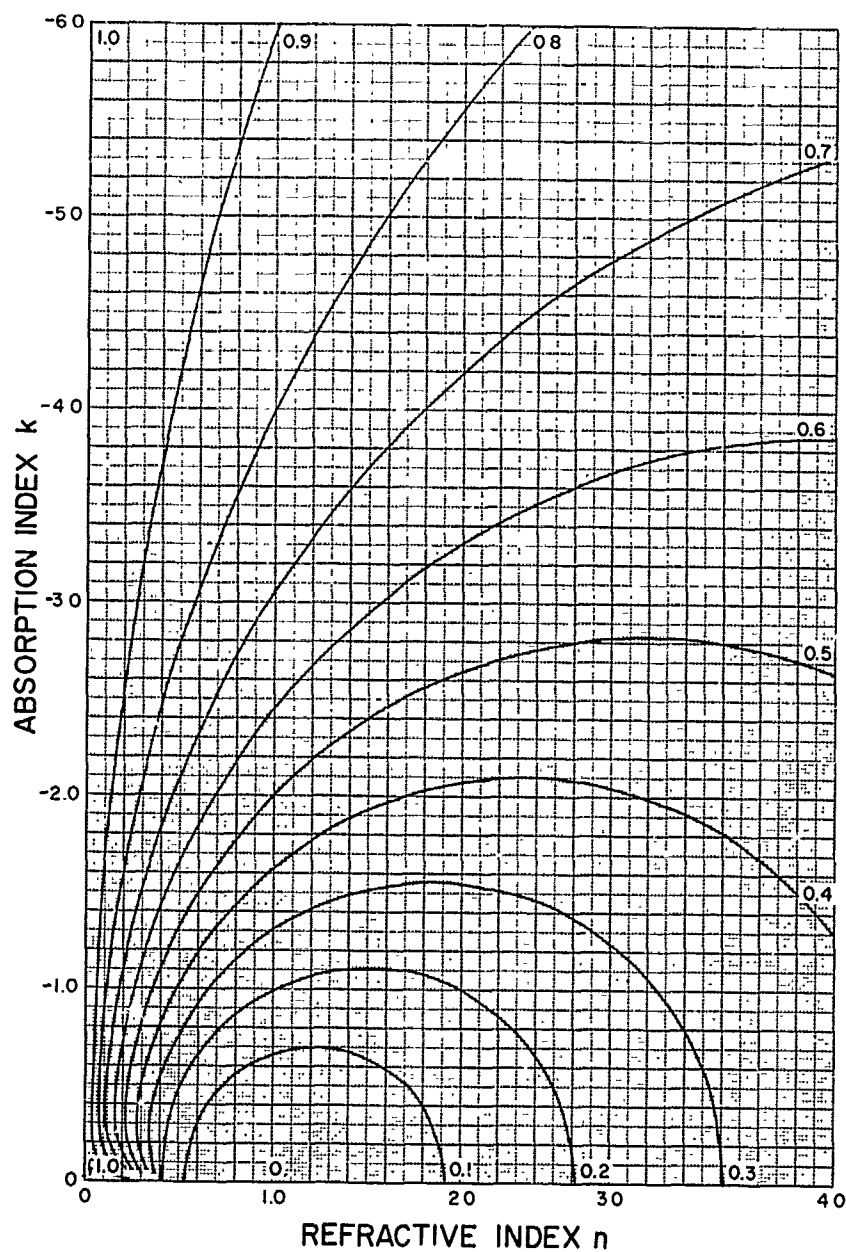


Fig. 41. RELATION BETWEEN THE REFLECTANCE  $R = \frac{1}{2} (R_1 + R_2)$  OF ELECTROMAGNETIC RADIATION AND THE COMPLEX INDEX OF REFRACTION  $N = n - ki$  FOR OBLIQUE INCIDENCE  $\theta_0 = 20^\circ$  WITH RESPECT TO THE SURFACE NORMAL

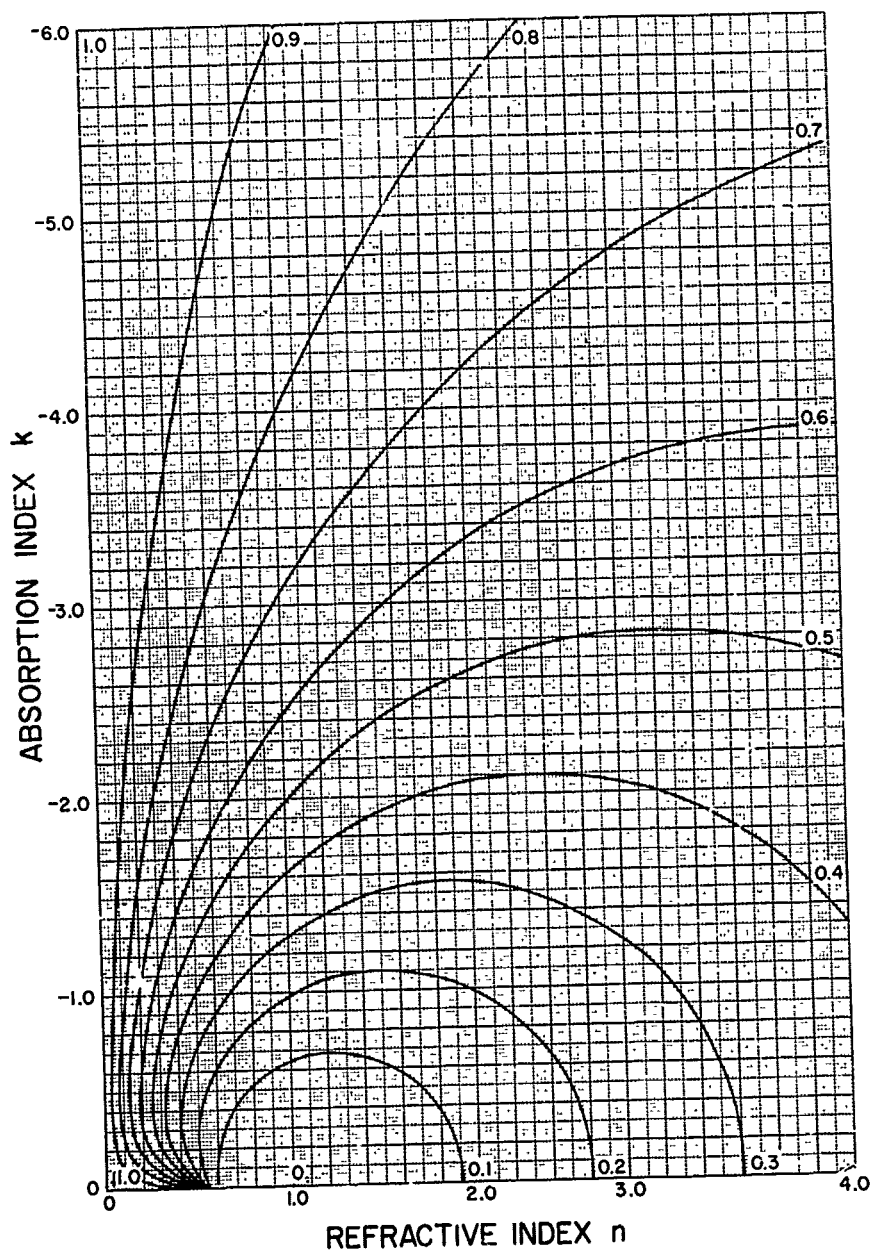


Fig. 42. RELATION BETWEEN THE REFLECTANCE  $R = \frac{1}{2} (R_1 + R_2)$  OF ELECTROMAGNETIC RADIATION AND THE COMPLEX INDEX OF REFRACTION  $N = n - ki$  FOR OBLIQUE INCIDENCE  $\theta_0 = 30^\circ$  WITH RESPECT TO THE SURFACE NORMAL

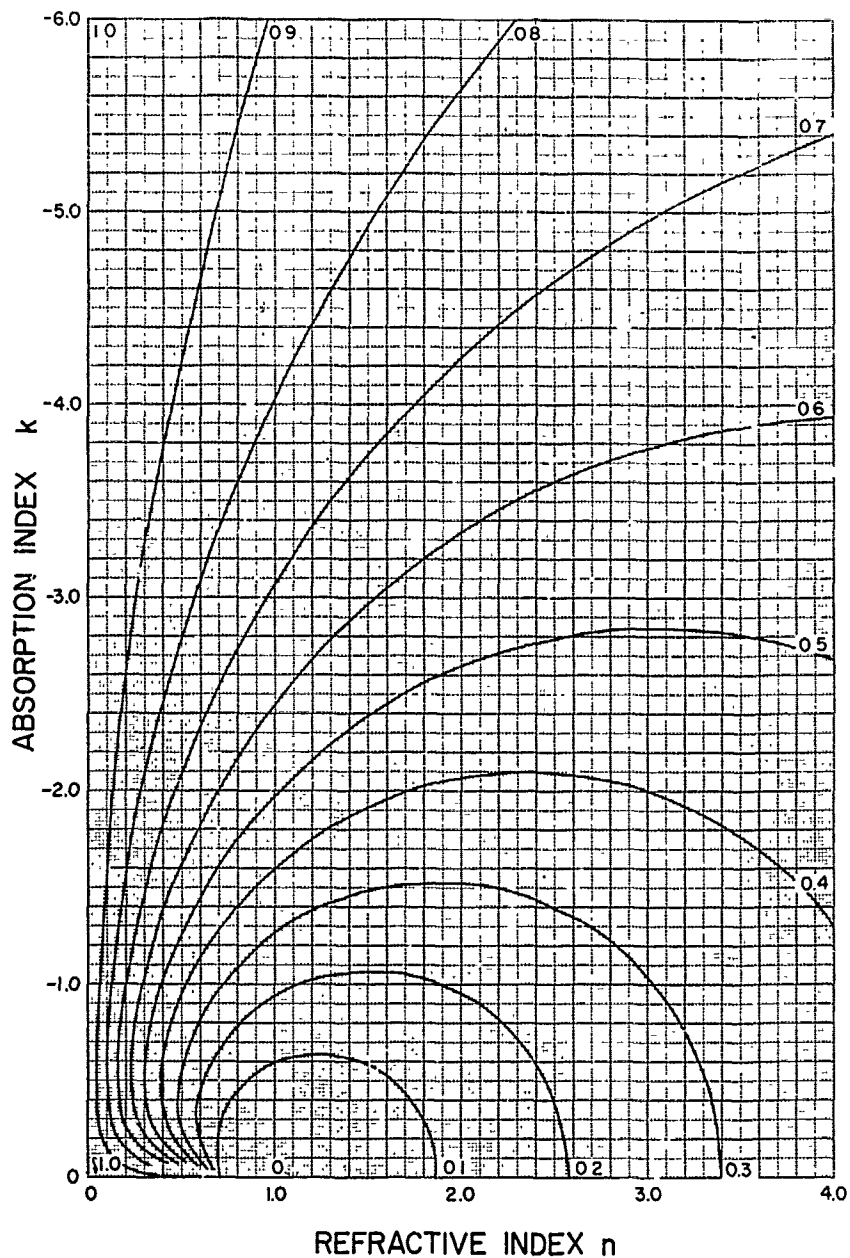


Fig. 43. RELATION BETWEEN THE REFLECTANCE  $R = \frac{1}{2} (R_1 + R_2)$  OF ELECTROMAGNETIC RADIATION AND THE COMPLEX INDEX OF REFRACTION  $N = n - ki$  FOR OBLIQUE INCIDENCE  $\theta_0 = 40^\circ$  WITH RESPECT TO THE SURFACE NORMAL

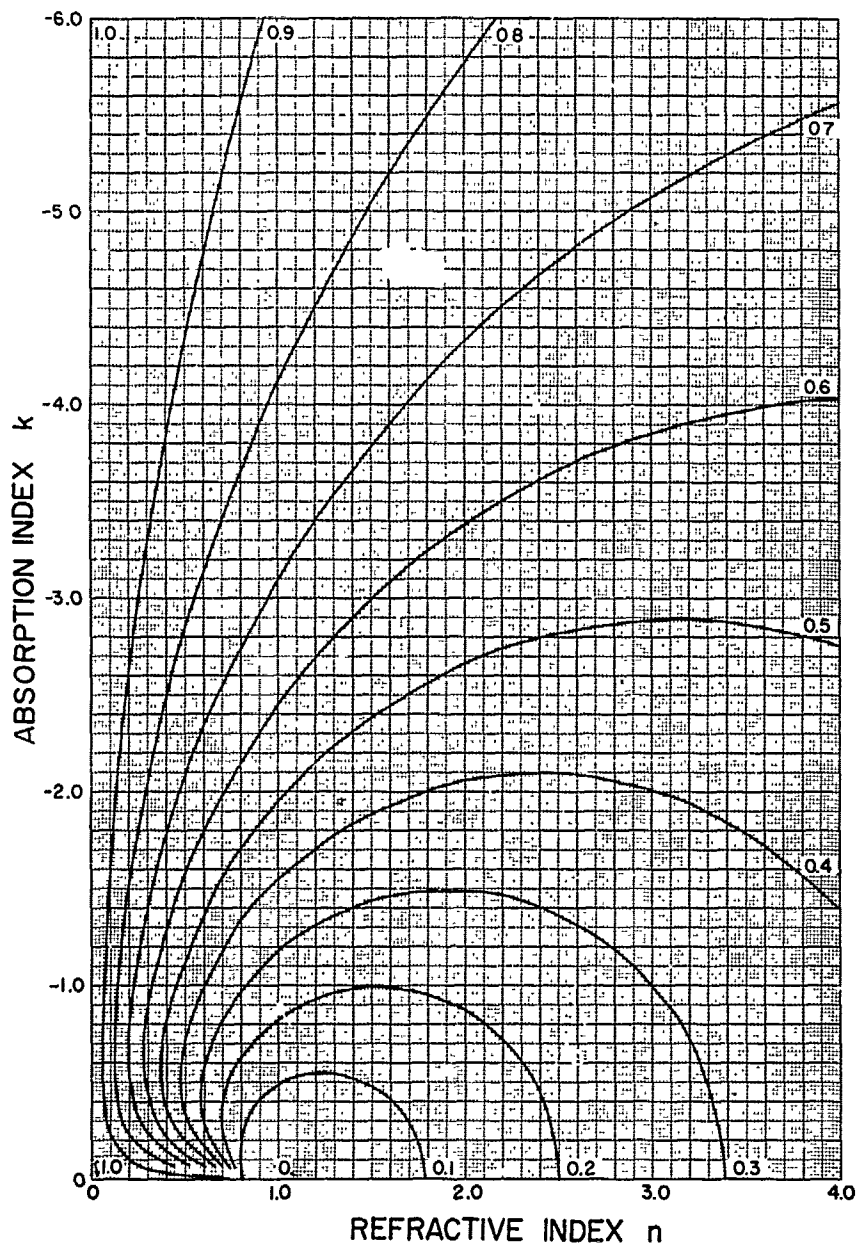


Fig. 44. RELATION BETWEEN THE REFLECTANCE  $R = \frac{1}{2} (R_1 + R_2)$  OF ELECTROMAGNETIC RADIATION AND THE COMPLEX INDEX OF REFRACTION  $N = n - ki$  FOR OBLIQUE INCIDENCE  $\theta_0 = 50^\circ$  WITH RESPECT TO THE SURFACE NORMAL

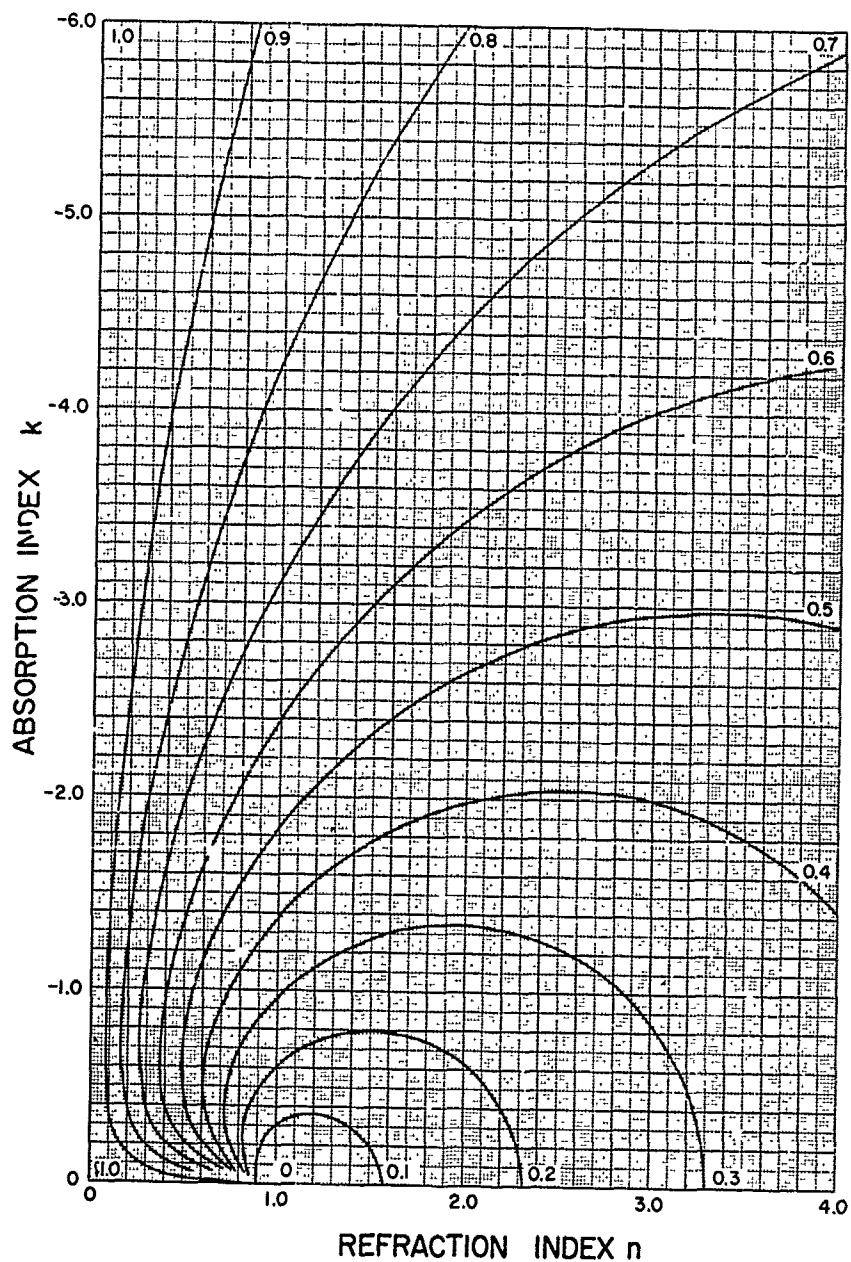


Fig. 45. RELATION BETWEEN THE REFLECTANCE  $R = \frac{1}{2} (R_1 + R_2)$  OF ELECTROMAGNETIC RADIATION AND THE COMPLEX INDEX OF REFRACTION  $N = n - ik$  FOR OBLIQUE INCIDENCE  $\theta_0 = 60^\circ$  WITH RESPECT TO THE SURFACE NORMAL

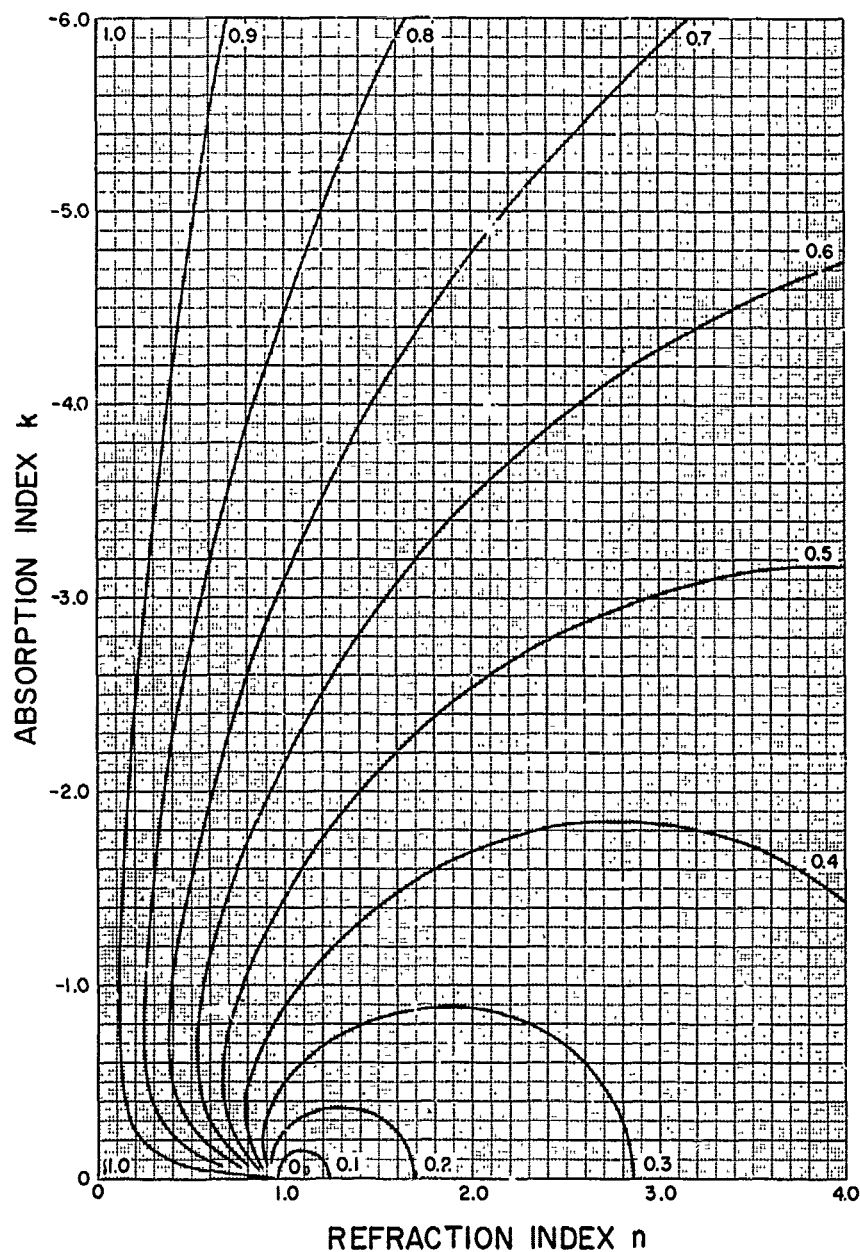


Fig. 46. RELATION BETWEEN THE REFLECTANCE  $R = \frac{1}{2} (R_1 + R_2)$  OF ELECTROMAGNETIC RADIATION AND THE COMPLEX INDEX OF REFRACTION  $N = n - ki$  FOR OBLIQUE INCIDENCE  $\theta_0 = 70^\circ$  WITH RESPECT TO THE SURFACE NORMAL

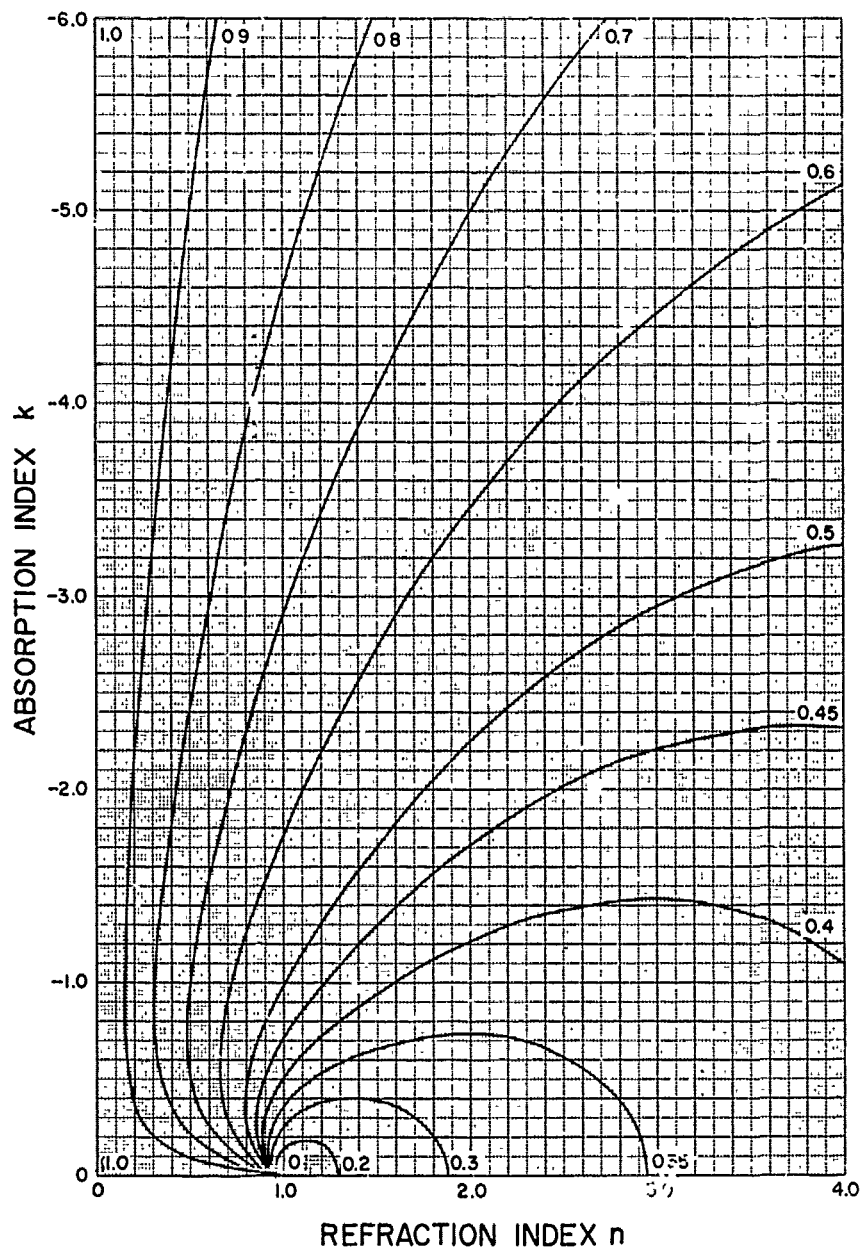


Fig. 47. RELATION BETWEEN THE REFLECTANCE  $R = \frac{1}{2} (R_1 + R_2)$  OF ELECTROMAGNETIC RADIATION AND THE COMPLEX INDEX OF REFRACTION  $N = n - ki$  FOR OBLIQUE INCIDENCE  $\theta_0 = 75^\circ$  WITH RESPECT TO THE SURFACE NORMAL

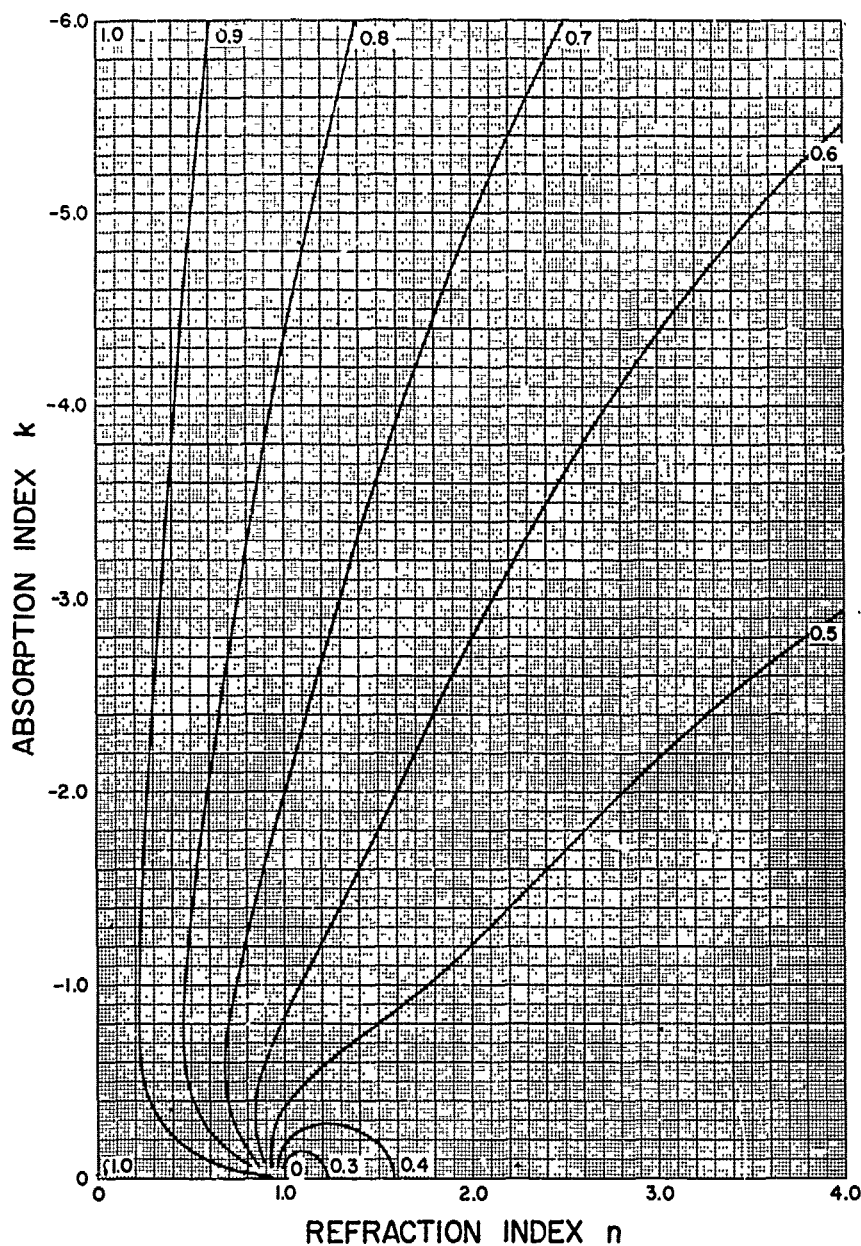


Fig. 48. RELATION BETWEEN THE REFLECTANCE  $R = \frac{1}{2} (R_1 + R_2)$  OF ELECTROMAGNETIC RADIATION AND THE COMPLEX INDEX OF REFRACTION  $N = n - ki$  FOR OBLIQUE INCIDENCE  $\theta_0 = 80^\circ$  WITH RESPECT TO THE SURFACE NORMAL

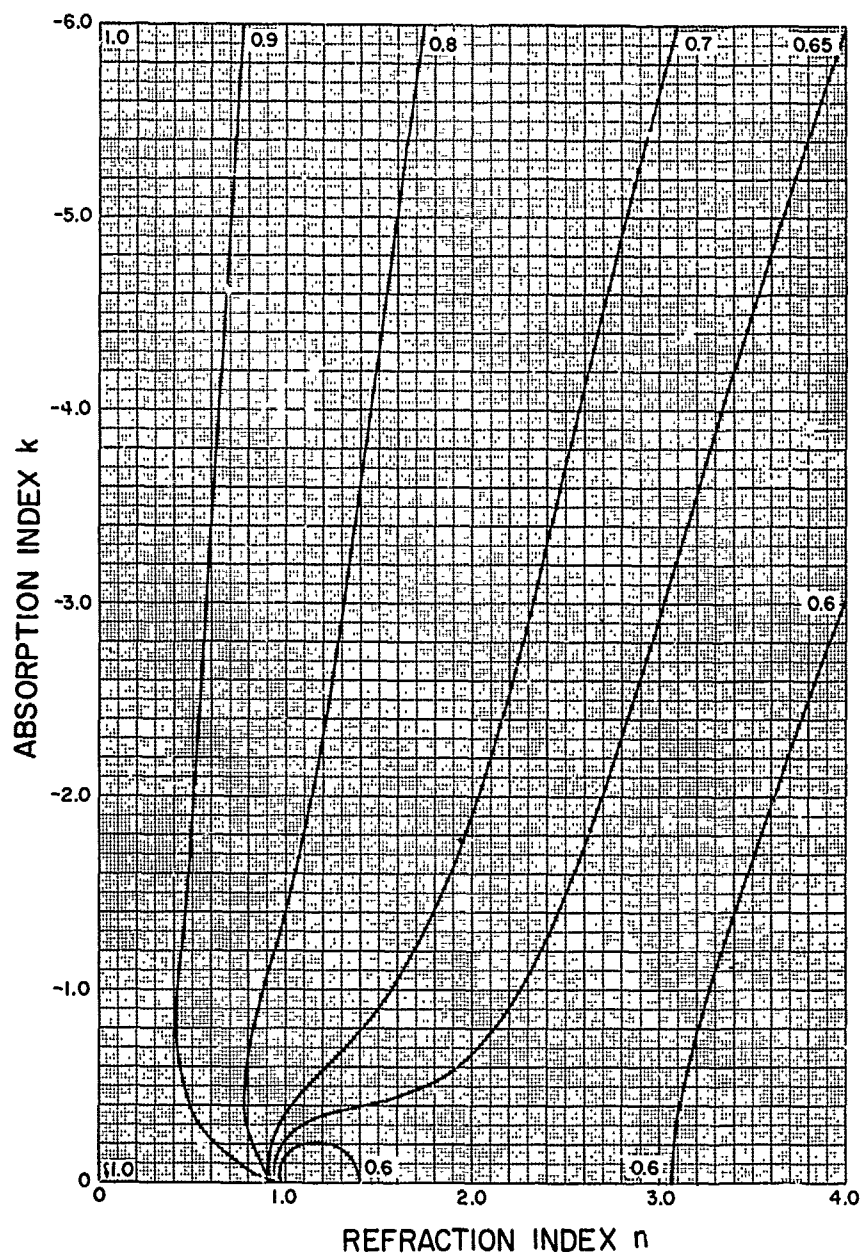


Fig. 49. RELATION BETWEEN THE REFLECTANCE  $R = \frac{1}{2} (R_1 + R_2)$  OF ELECTROMAGNETIC RADIATION AND THE COMPLEX INDEX OF REFRACTION  $N = n - ki$  FOR OBLIQUE INCIDENCE  $\theta_0 = 85^\circ$  WITH RESPECT TO THE SURFACE NORMAL

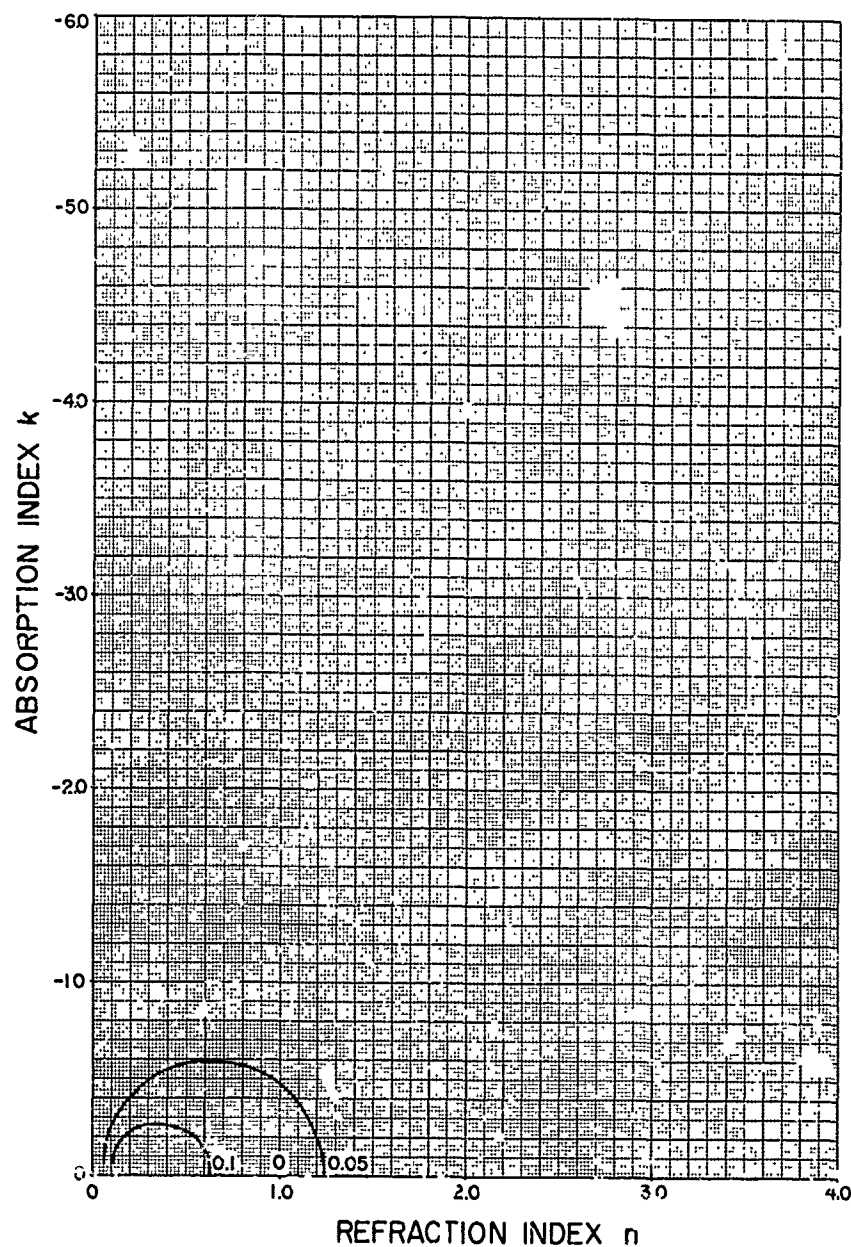


Fig. 50. RELATION BETWEEN THE DEGREE OF POLARIZATION  $P = \frac{R_1 - R_2}{R_1 + R_2}$   
 OF ELECTROMAGNETIC RADIATION AND THE COMPLEX INDEX OF  
 REFRACTION  $N = n - ki$  FOR OBLIQUE INCIDENCE  $\theta_0 = 10^\circ$   
 WITH RESPECT TO THE SURFACE NORMAL

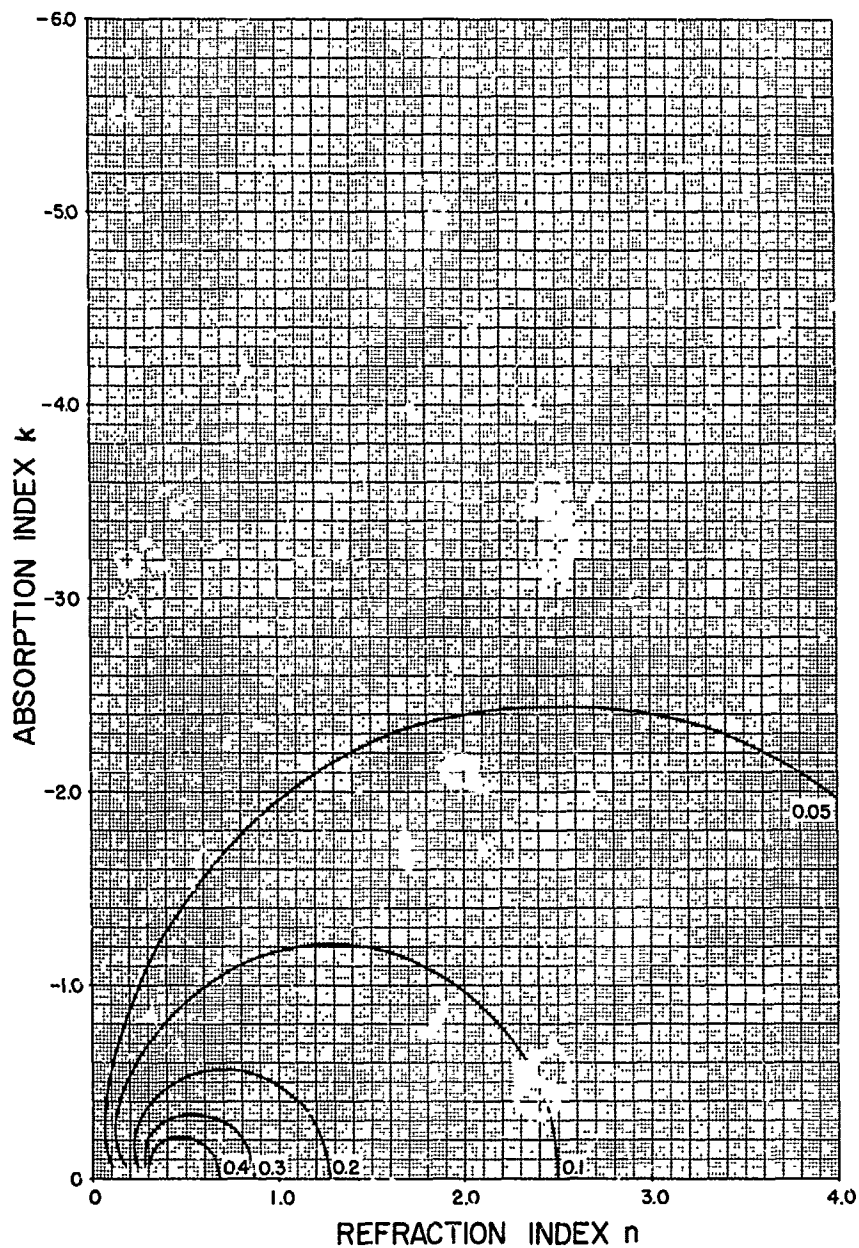


Fig. 51. RELATION BETWEEN THE DEGREE OF POLARIZATION  $P = \frac{R_1 - R_2}{R_1 + R_2}$

OF ELECTROMAGNETIC RADIATION AND THE COMPLEX INDEX OF REFRACTION  $N = n - ki$  FOR OBLIQUE INCIDENCE  $\theta_0 = 20^\circ$  WITH RESPECT TO THE SURFACE NORMAL

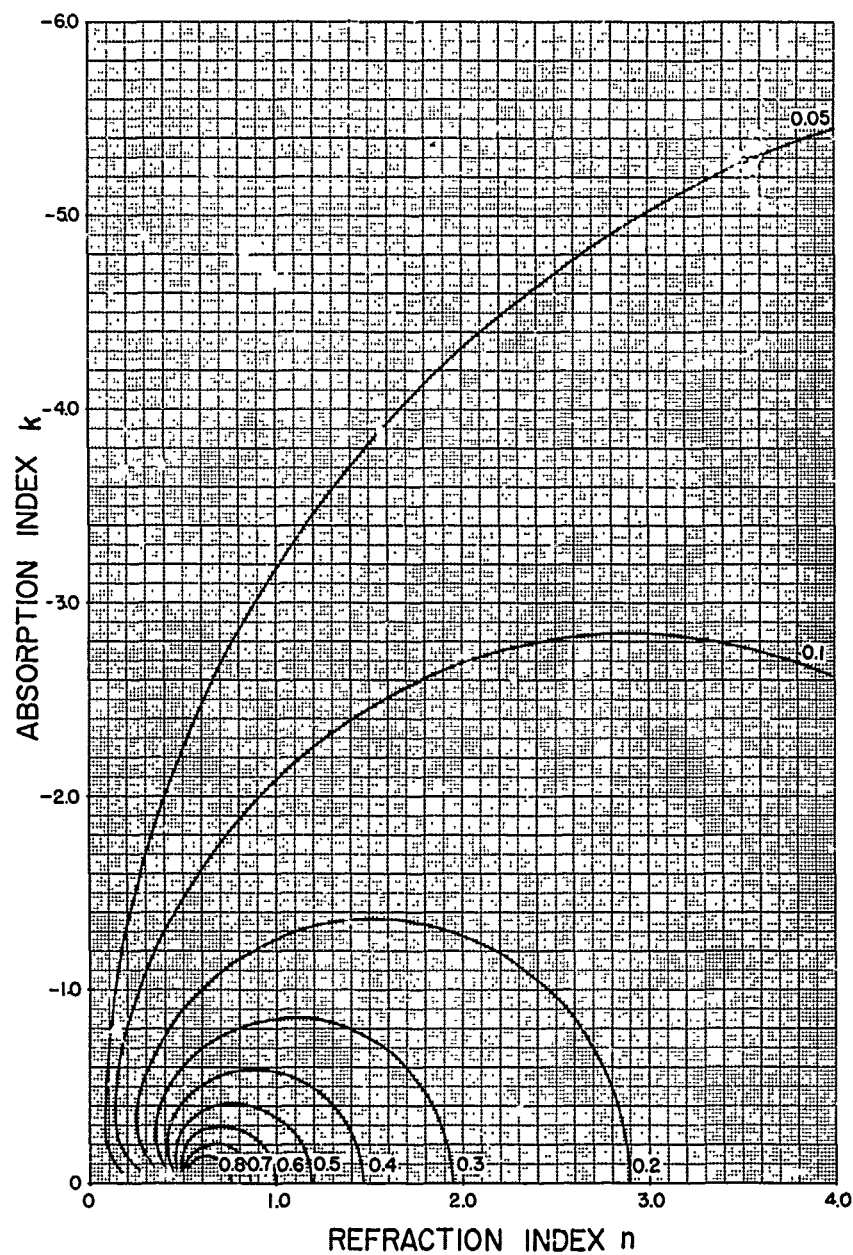


Fig. 52. RELATION BETWEEN THE DEGREE OF POLARIZATION  $P = \frac{R_1 - R_2}{R_1 + R_2}$  OF ELECTROMAGNETIC RADIATION AND THE COMPLEX INDEX OF REFRACTION  $N = n - ki$  FOR OBLIQUE INCIDENCE  $\theta_0 = 30^\circ$  WITH RESPECT TO THE SURFACE NORMAL

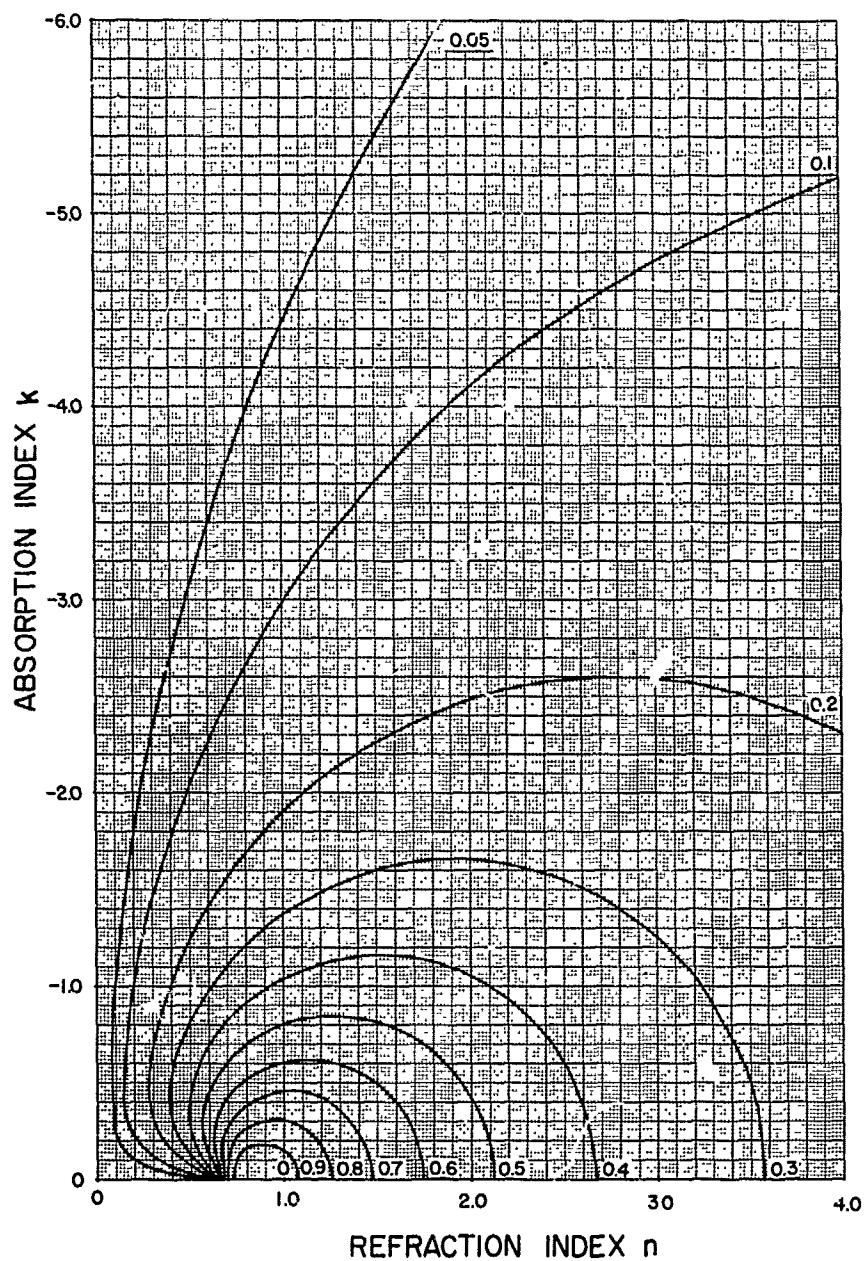


Fig. 53. RELATION BETWEEN THE DEGREE OF POLARIZATION  $P = \frac{R_1 - R_2}{R_1 + R_2}$   
 OF ELECTROMAGNETIC RADIATION AND THE COMPLEX INDEX OF  
 REFRACTION  $N = n - ki$  FOR OBLIQUE INCIDENCE  $\theta_0 = 40^\circ$   
 WITH RESPECT TO THE SURFACE NORMAL

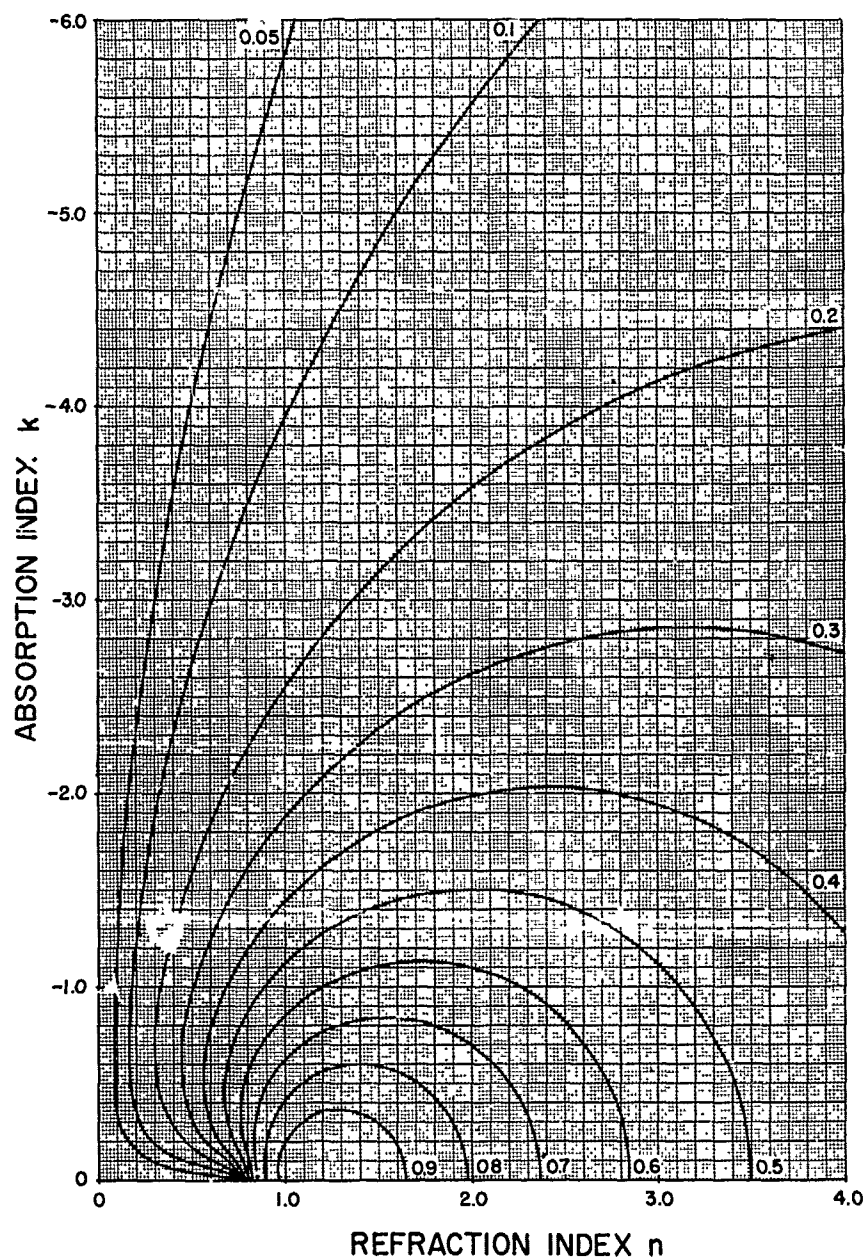


Fig. 54. RELATION BETWEEN THE DEGREE OF POLARIZATION  $P = \frac{R_1 - R_2}{R_1 + R_2}$  OF ELECTROMAGNETIC RADIATION AND THE COMPLEX INDEX OF REFRACTION  $N = n - ki$  FOR OBLIQUE INCIDENCE  $\theta_0 = 50^\circ$  WITH RESPECT TO THE SURFACE NORMAL

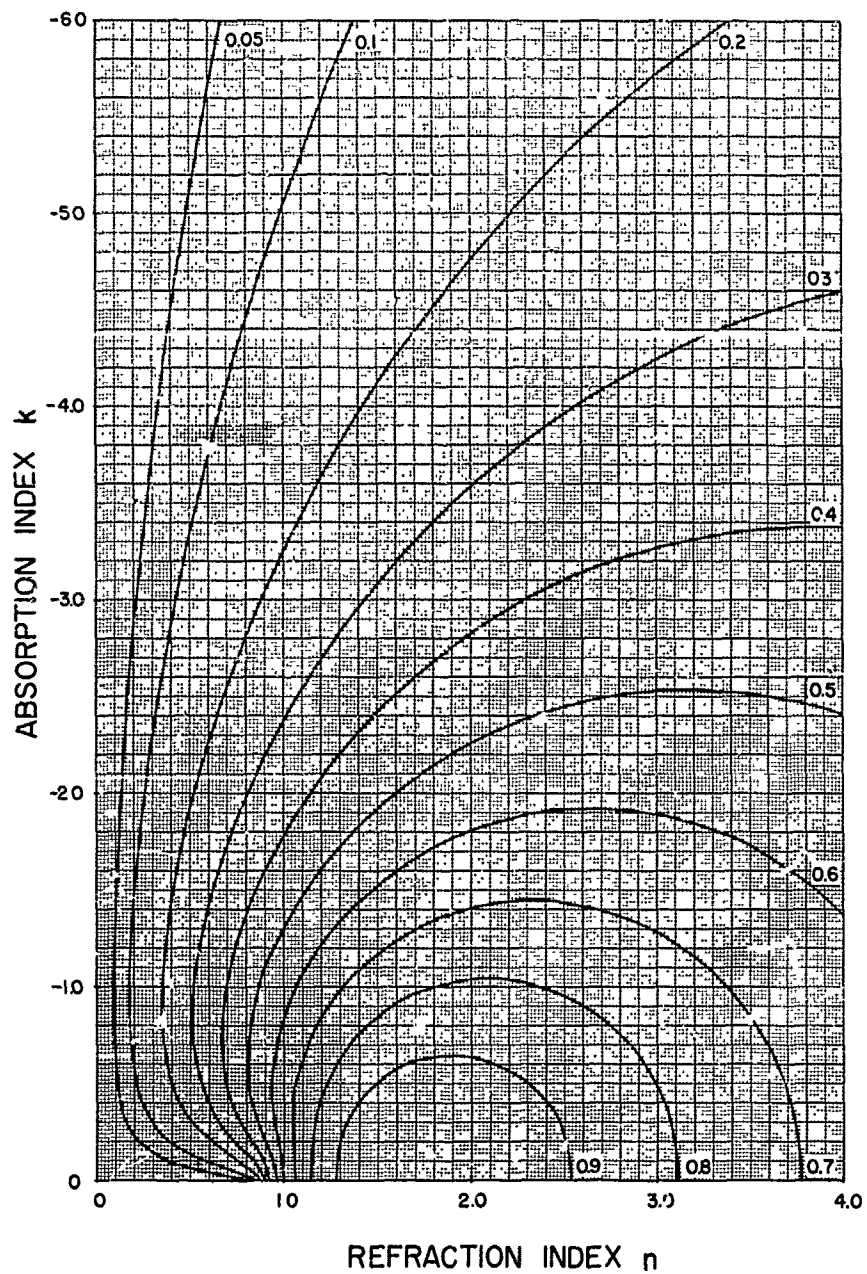


Fig. 55. RELATION BETWEEN THE DEGREE OF POLARIZATION  $P = \frac{R_1 - R_2}{R_1 + R_2}$   
 OF ELECTROMAGNETIC RADIATION AND THE COMPLEX INDEX OF  
 REFRACTION  $N = n - ki$  FOR OBLIQUE INCIDENCE  $\theta_0 = 60^\circ$   
 WITH RESPECT TO THE SURFACE NORMAL

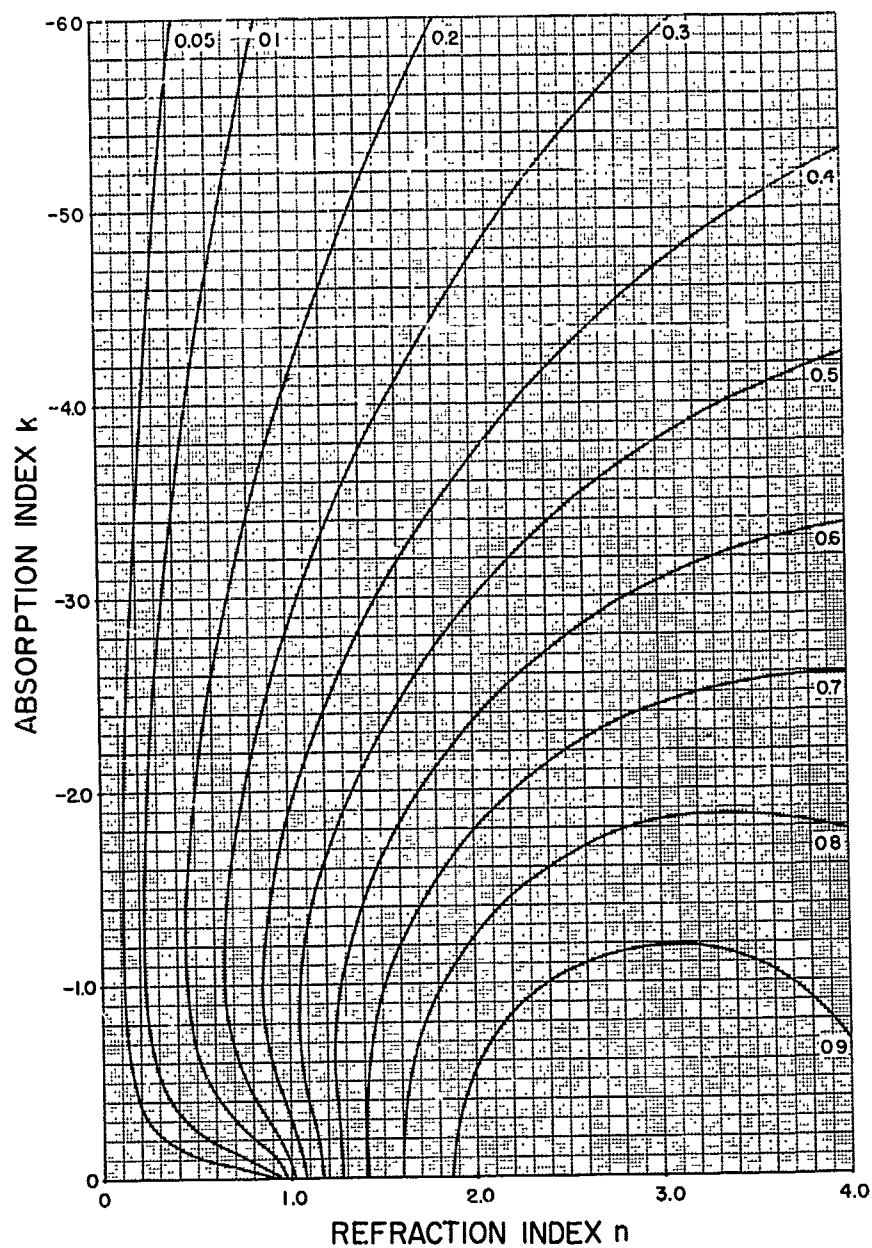


Fig. 56. RELATION BETWEEN THE DEGREE OF POLARIZATION  $P = \frac{R_1 - R_2}{R_1 + R_2}$  OF ELECTROMAGNETIC RADIATION AND THE COMPLEX INDEX OF REFRACTION  $N = n - ki$  FOR OBLIQUE INCIDENCE  $\theta_0 = 70^\circ$  WITH RESPECT TO THE SURFACE NORMAL

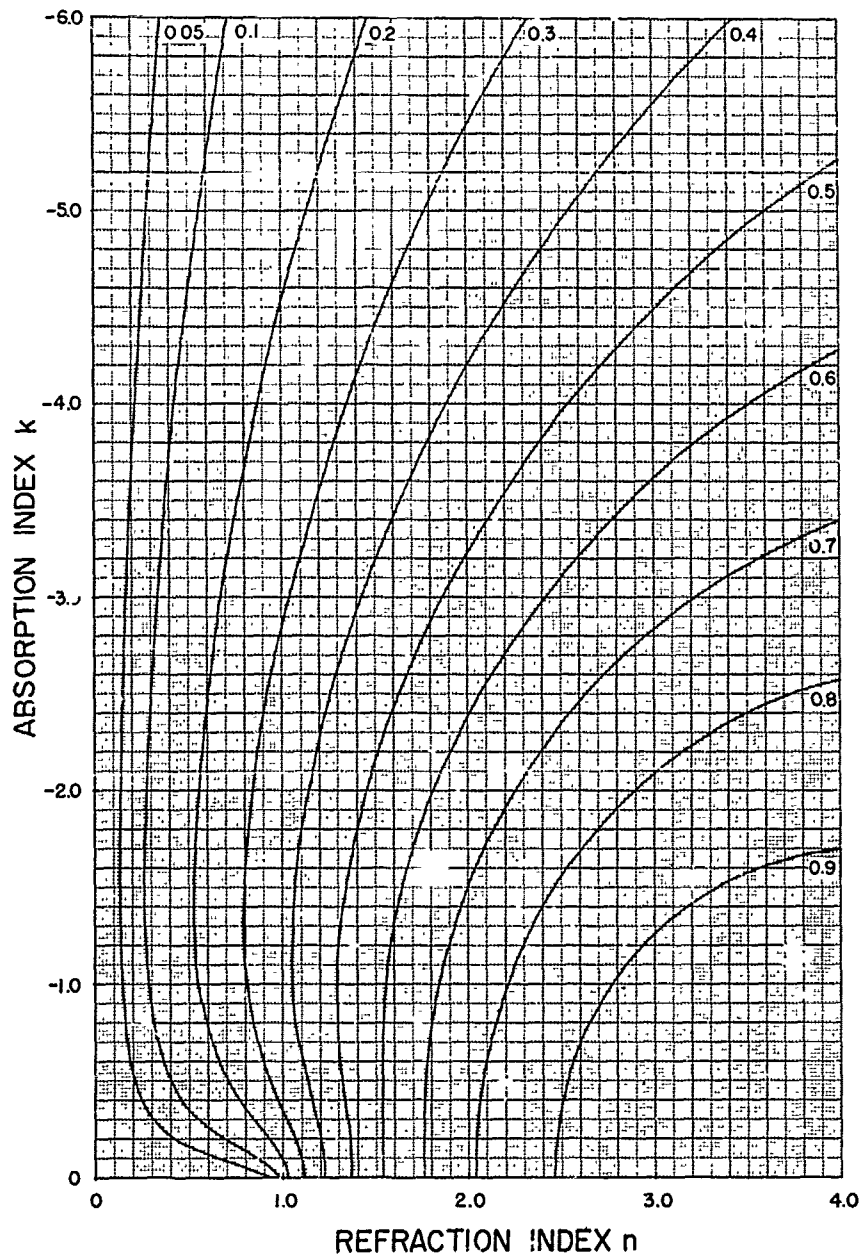


Fig. 57. RELATION BETWEEN THE DEGREE OF POLARIZATION  $P = \frac{R_1 - R_2}{R_1 + R_2}$  OF ELECTROMAGNETIC RADIATION AND THE COMPLEX INDEX OF REFRACTION  $N = n - ki$  FOR OBLIQUE INCIDENCE  $\theta_0 = 75^\circ$  WITH RESPECT TO THE SURFACE NORMAL

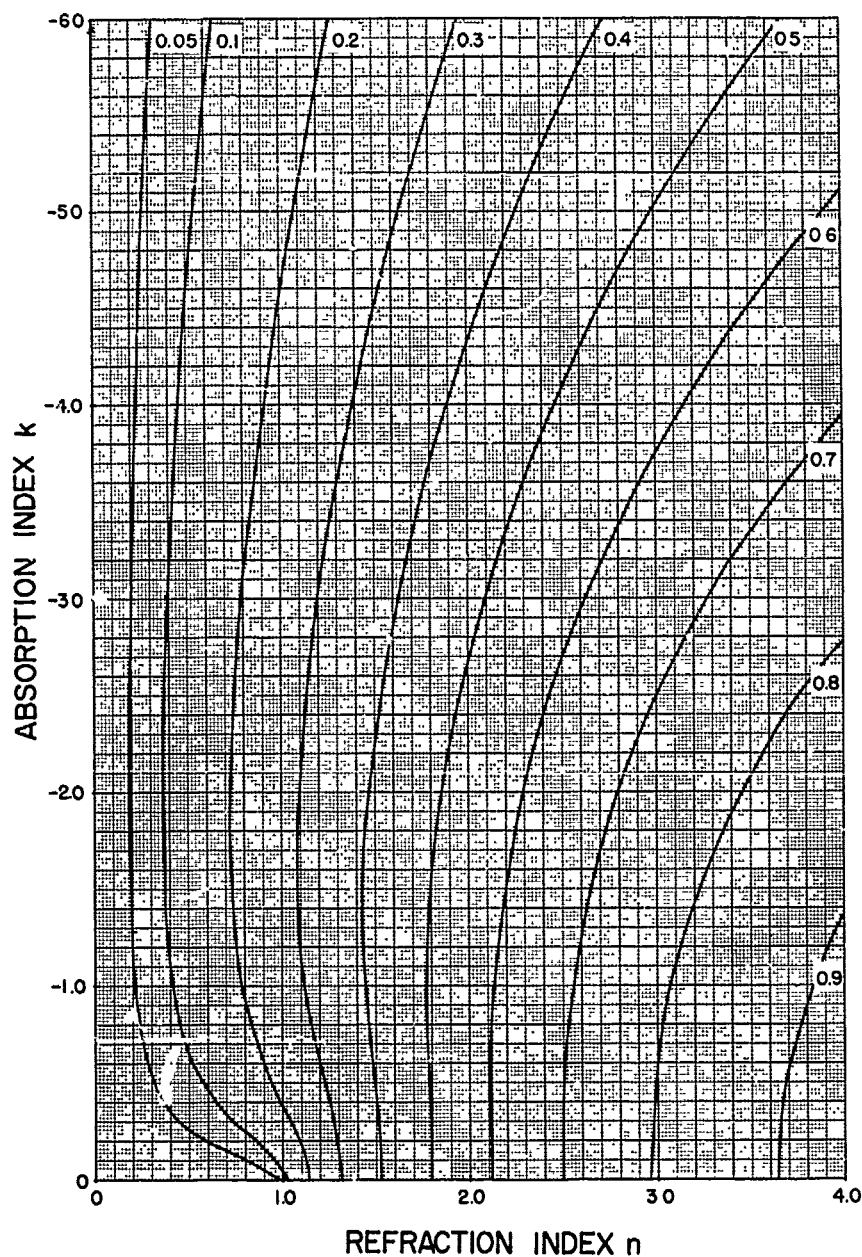


Fig. 58. RELATION BETWEEN THE DEGREE OF POLARIZATION  $P = \frac{R_1 - R_2}{R_1 + R_2}$  OF ELECTROMAGNETIC RADIATION AND THE COMPLEX INDEX OF REFRACTION  $N = n - ki$  FOR OBLIQUE INCIDENCE  $\theta_0 = 80^\circ$  WITH RESPECT TO THE SURFACE NORMAL

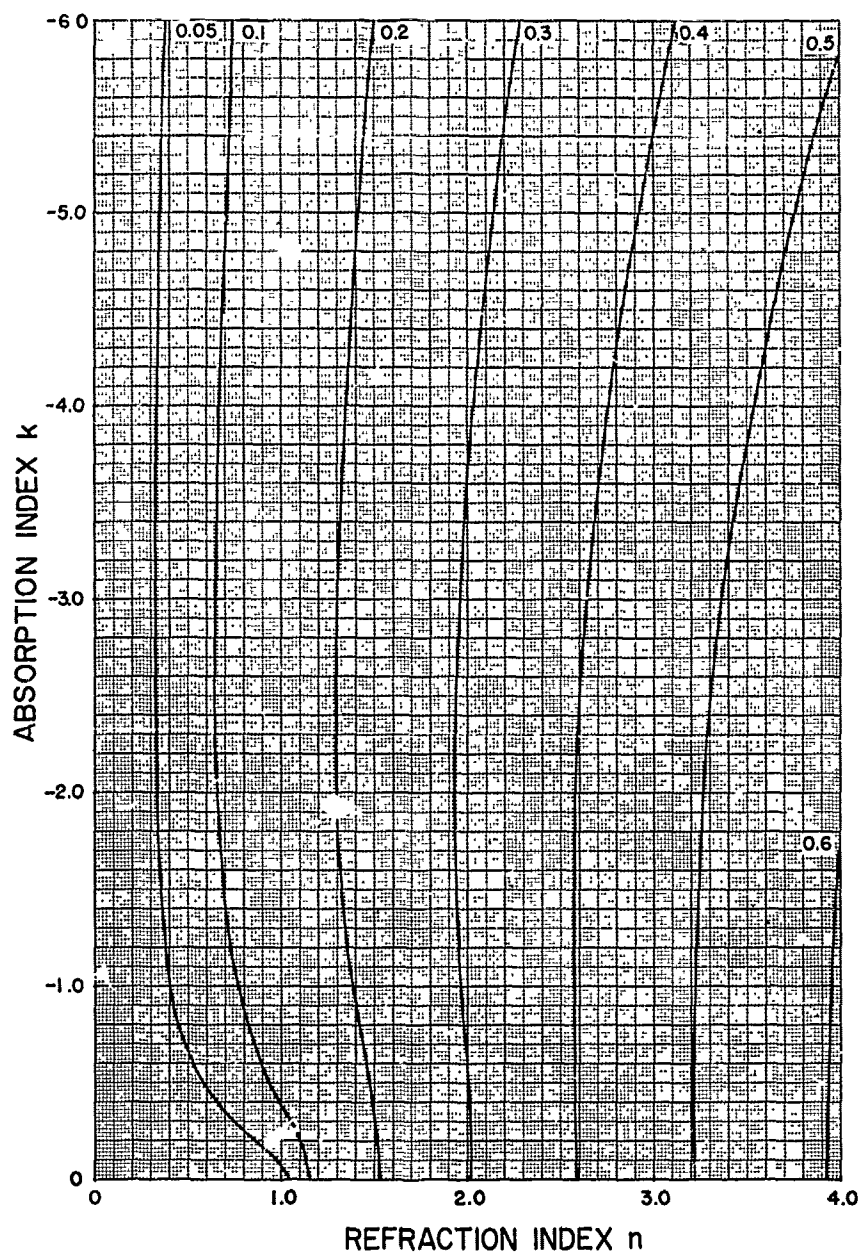


Fig. 59. RELATION BETWEEN THE DEGREE OF POLARIZATION  $P = \frac{R_1 - R_2}{R_1 + R_2}$  OF ELECTROMAGNETIC RADIATION AND THE COMPLEX INDEX OF REFRACTION  $N = n - ki$  FOR OBLIQUE INCIDENCE  $\theta_0 = 85^\circ$  WITH RESPECT TO THE SURFACE NORMAL

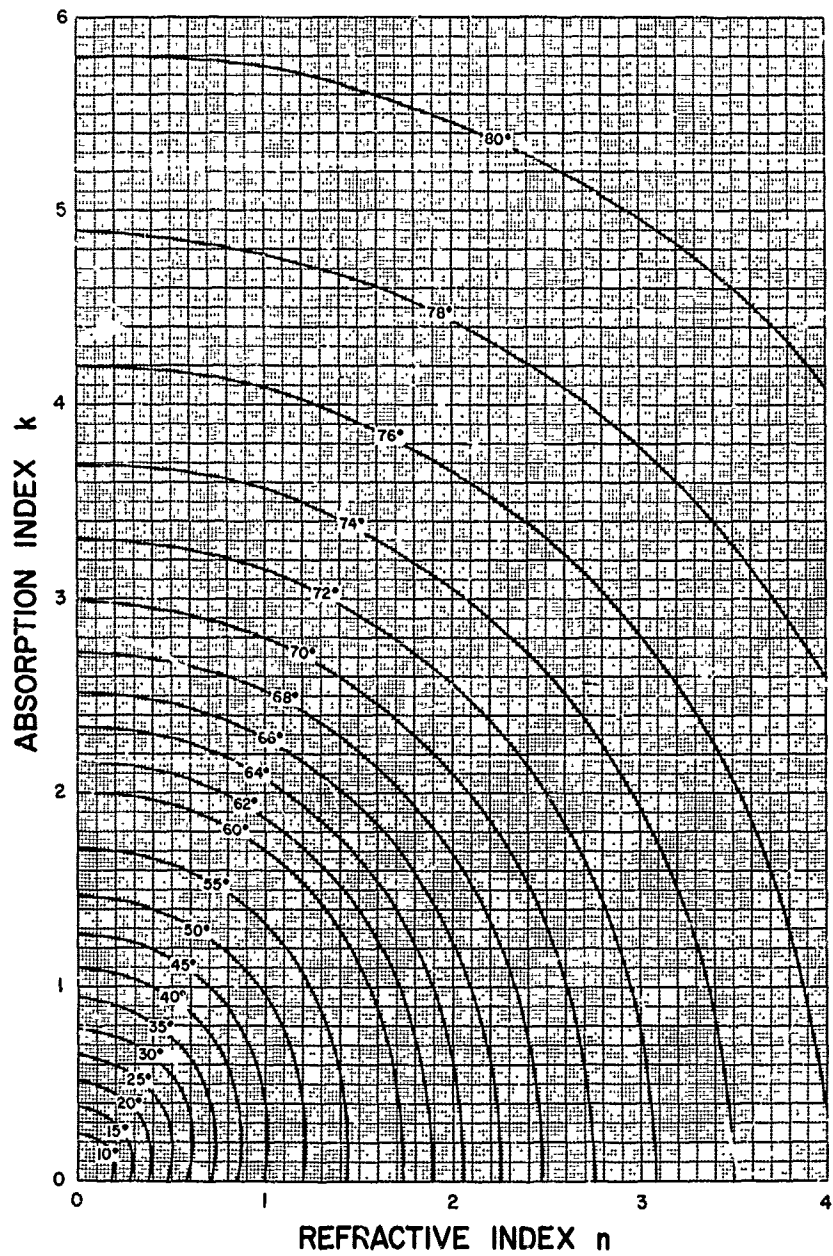


Fig. 60. RELATION BETWEEN THE FIRST BREWSTER ANGLE (WHERE  $R_2$  IS A MINIMUM) AND THE COMPLEX INDEX OF REFRACTION  $N = n - ki$

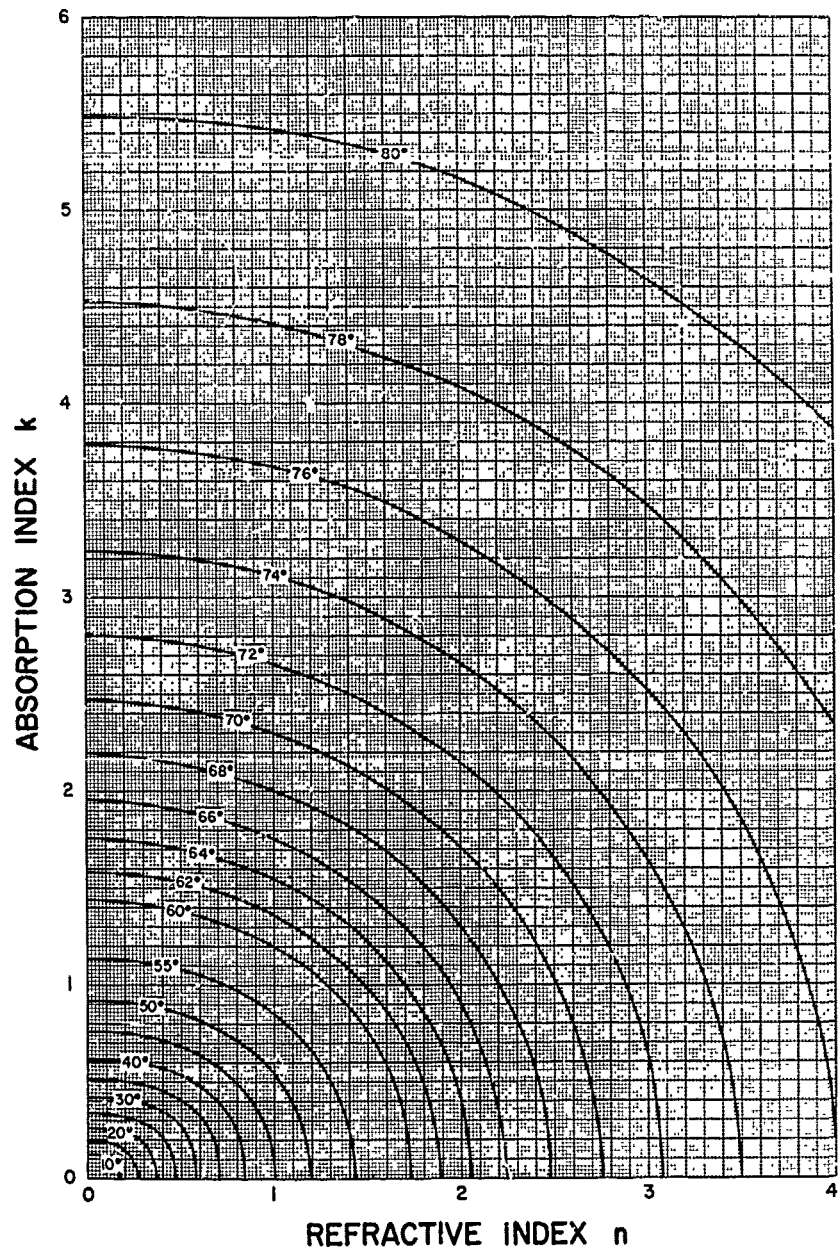


FIG. 61. RELATION BETWEEN THE SECOND BREWSTER ANGLE (WHERE  $P$  IS A MAXIMUM) AND THE COMPLEX INDEX OF REFRACTION  $N = n - ki$

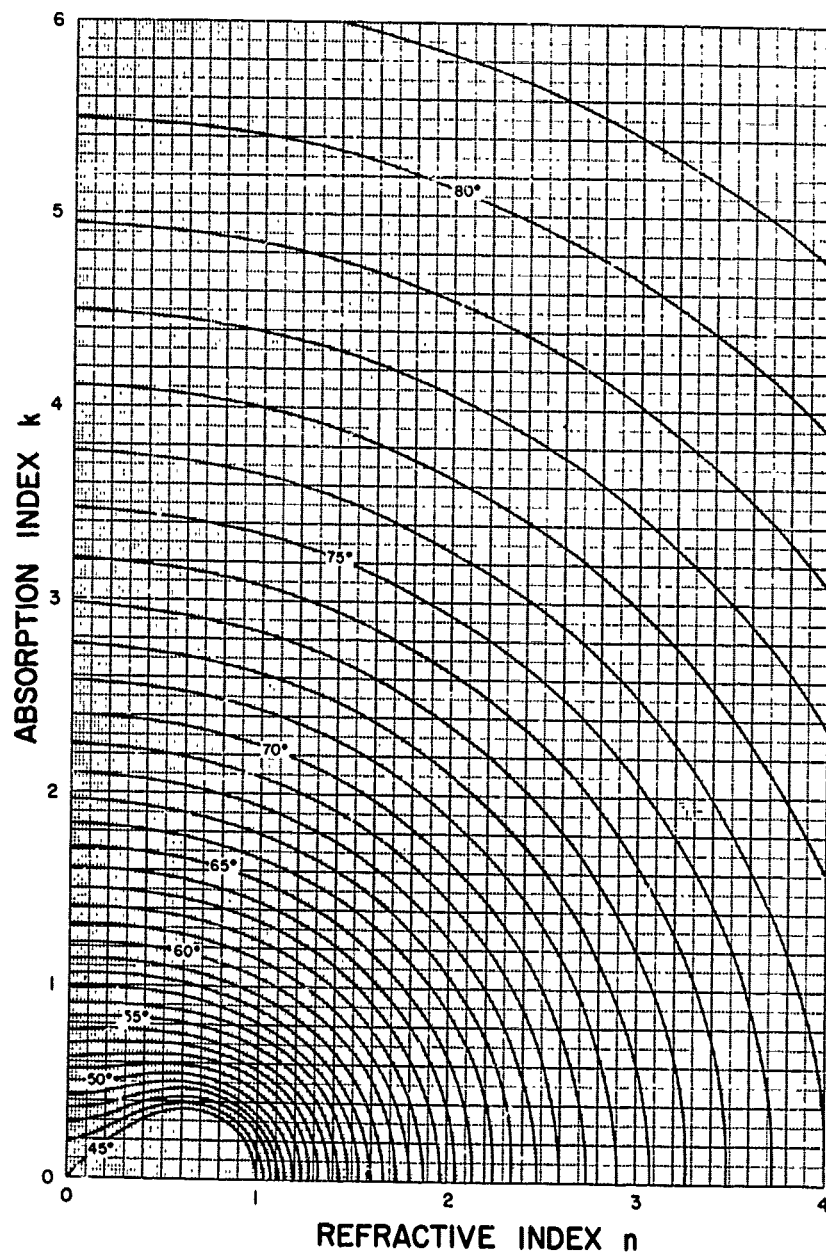


Fig. 62. RELATION BETWEEN THE THIRD BREWSTER ANGLE = PRINCIPAL ANGLE OF INCIDENCE (WHERE THE PHASE DIFFERENCE  $\delta$  IS  $90^\circ$ ) AND THE COMPLEX INDEX OF REFRACTION  $N = n - ki$

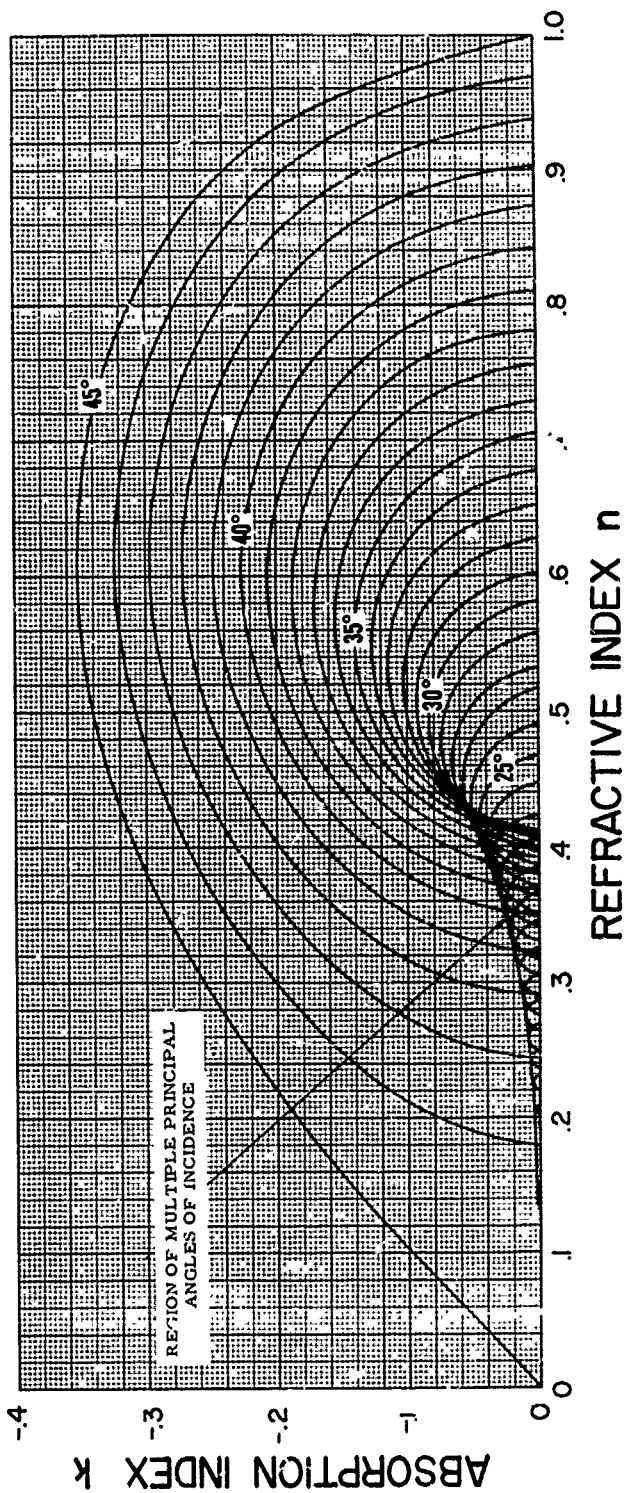


Fig. 63. THE THIRD BREWSTER ANGLE OF INCIDENCE = PRINCIPAL ANGLE OF INCIDENCE, FOR SMALL VALUES OF THE INDEX OF REFRACTION  $N = n - ki$

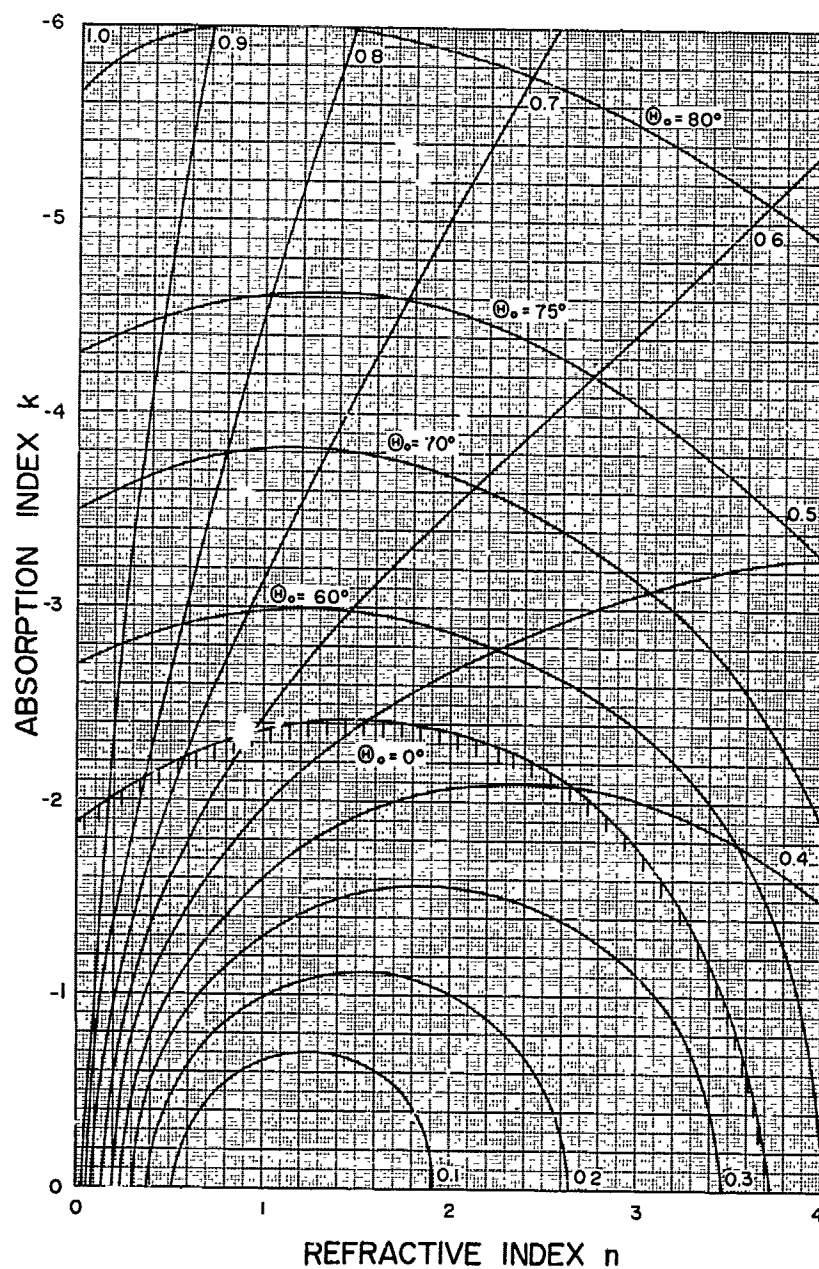


Fig. 64. RELATION AMONG THE ANGLE OF INCIDENCE  $\Theta_0$  WHERE THE REFLECTANCE  $R = \frac{1}{2} (R_1 + R_2)$  IS A MINIMUM, THE REFLECTANCE  $R_{\min}$ , AND THE COMPLEX INDEX OF REFRACTION  $N = n - ki$

## Chapter 3

### SUPPLEMENTARY REMARKS AND REVIEW OF THE NUMERICAL VALUES

The numerical values which are given in Tables A through D are the power intensities of the reflected radiation that are the absolute squares of the amplitudes. If the numerical values of the amplitudes are wanted, one must take into consideration that  $r_1 = r_\perp$  is always negative and that  $r_2 = r_\parallel$  is negative if the angle of incidence  $\theta_i$  is larger than that for which the minimum of  $R_2$  occurs (See Eq. 29). The proper values of  $\theta_0$  where  $R_2 = \text{minimum}$  and of  $(R_2)_{\text{min}}$  itself are given in Table E. Directions for the use of the data presented in this paper are included in Section 4.1 with the proposed applications.

Since the reflectivity is expressed as a function of a combination of  $\theta_0$ ,  $n$ , and  $k$ , there are different ways to illustrate the relations among them. One method we will use is the customary one of plotting the reflection coefficient versus the angle of incidence. In order to give a good survey, a set of graphs is provided, with each plot representing a system of curves for which the real part of the index of refraction  $n$  is held constant and  $k$  is varied from 0 to 6. Figures 3-10 illustrate the tendencies of  $R_1$  and  $R_2$ , whereas Figs. 11-18 consider the reflectivity  $R$  for natural or unpolarized radiation. It will be noted from the curves of the reflectivities  $R$ ,  $R_1$ , and  $R_2$  that each index of refraction has its own peculiar curve which is always different from that for another index of refraction.

Another very useful method is to plot the numerical results of the Fresnel equations obtained for a constant angle of incidence  $\theta_0$ , and to consider each of  $R_1$ ,  $R_2$ ,  $R$ ,  $R_2/R_1$ , or  $P$  separately versus  $n$ , for constant values of  $k$ . Such graphs were drawn and used to prepare Argand diagrams. They also proved to be the most economical method for determining material constants from experimental results, as will be discussed in Section 4.2 (Fig. 69). The majority of the illustrations make use of the Argand diagram, which plots the reflectivities  $R_1$ ,  $R_2$ , and  $R$  and the degree of polarization  $P$ , for a constant angle of incidence. These "isorefectance" curves are shown in Figs. 19-49, while the degrees of polarization are given in Figs. 50-59.

As stated in the preface, the resulting graphs and tables are valid both for  $N = n + ki$ , and  $N = n - ki$ , ( $n \geq 0$ ,  $k \geq 0$ ).

### 3.1. Reflectivities $R_1$ and $R_2$ at Air-Dielectric Interface Versus $\theta_0$

This is the case where  $k = 0$ . From Figs. 3-10 we learn that  $R_1$  and  $R_2$  are equal to each other at normal incidence. Without exception, the curves for  $R_1$  have their minimum at normal incidence; as the angle of incidence is increased, the curves tend monotonously toward unity. The curves for  $R_2$ , however, first decrease to smaller values until they reach their minimum  $R_2 = 0$ , then as the angle of incidence is further increased they also tend monotonously toward  $R_2 = 1$  (total reflectance), which they reach for  $\theta_0 = 90^\circ$ , if  $n > 1$ .

Those cases in which  $n < 1$  (internal reflection) are peculiar in that total reflection occurs from incident angles smaller than  $90^\circ$  beginning with  $\theta_0 = \sin^{-1} n$ . The particular incident angle for which  $R_2$  becomes zero is named Brewster angle, and for this angle the relation  $\tan \theta_0 = n$ , called Brewster's law, is valid. For the Brewster angle the degree of polarization  $P$  becomes unity, or 100%, because there exists only the reflected wave, which oscillates perpendicularly to the plane of incidence. The reflection at the Brewster angle is the only instance where the reflected radiation is completely polarized in one single plane, which means that the incoming radiation has to be a harmonic oscillation.

### 3.2. Reflectivities $R_1$ and $R_2$ at Air-Conductor Interface Versus $\theta_0$

The only difference between the reflection curves (see Figs. 3-10) for conducting material ( $k > 0$ ) and the curves for dielectrics ( $k = 0$ ) is that in the former the curves for the reflectivity  $R_2$  never reach the value zero regardless of what the real angle of incidence may be. The angle of incidence at which the minimum of  $R_2 \neq 0$  occurs with conducting material is called "pseudo Brewster angle," because here the Brewster law has only a formal meaning and the angle does not have the physical significance it does in the case of dielectrics. As a matter of fact, we observe in this (1) only partial polarization occurs, (2) the maximum degree of polarization does not occur for this angle, and (3) the electric field vectors of the reflected and diffracted radiation are no longer perpendicular to each other. The direction of the diffracted wave, which is of limited penetration depth, is given by the angle  $\theta_1$  which follows from

$$\frac{\sin \theta_0}{\sin \theta_1} = n(\theta_0) \quad (53)$$

where the real index of refraction  $n = n(\theta_0)$  is defined by

$$n(\theta_0) = \left( \frac{q(\theta_0)}{\alpha_2} \right)^2 + \sin^2 \theta_0 \quad (54)$$

The term  $\frac{q(\theta_0)}{\alpha_2}$  is the same as that which appears in the Fresnel equations in Chapter 1. The angle of incidence  $\theta_0$ , at which the reflectivity  $R_2$  becomes a minimum, is discussed in more detail later in this chapter.

Associated with the reflection, of which we considered hitherto only the energy loss by absorption and transparency for both amplitudes, there is also a delay in the phases of the amplitudes. As stated in the first chapter, it is assumed that the incoming radiation consists of two harmonic waves, in phase with each other and polarized in two planes perpendicular to each other. Therefore, the graphic representation of the resultant of the two amplitudes is a straight line, intersecting the origin with an angle  $\psi$  (in this case  $\psi = 45^\circ$ ) with respect to the amplitudes. The angle  $\psi$  is called the azimuth of the vibration and is defined by

$$\tan \psi_i = \frac{E_{\perp}^i}{E_{\parallel}^i} \quad (55)$$

This definition is arbitrary, and certain textbooks prefer to designate the complement angle of  $\psi$  as the azimuth. The azimuth of the reflected vibration is given by

$$\tan \psi_r = \frac{E_{\perp}^r}{E_{\parallel}^r} = \sqrt{\frac{R_1}{R_2}} \quad (56)$$

We know from physics that in reflection on dielectrics the wave oscillating perpendicularly to the plane of incidence experiences a phase shift of  $180^\circ$  with respect to the original wave for any angle of incidence. The amplitude perpendicular to the plane of incidence, however, will remain unchanged for all angles of incidence which are smaller than the Brewster angle. If the angle of incidence is beyond the Brewster angle, the amplitude  $E_{\parallel}$  of the electric field vector  $E$  will show a phase shift of  $180^\circ$ , and, consequently, both reflected waves will be in phase again.

In the case of a conducting material, there is a monotonous decrease of the phase difference  $\delta = 180^\circ$  at normal incidence down to  $\delta = 0^\circ$  at grazing incidence. This means the two amplitudes will never become zero at the same time unless  $\delta = 180^\circ$ . The geometric picture of the end of the electric (or magnetic) field vector will be a circle or an ellipse. The phase shift can be calculated by the equation

$$\tan \delta = \frac{2 \frac{P(\theta_0)}{\alpha_2} \sin \theta_0 \tan \theta_0}{\sin^2 \theta_0 \tan^2 \theta_0 - \left( \frac{q^2(\theta_0)}{\alpha_2^2} + \frac{p^2(\theta_0)}{\alpha_2^2} \right)} \quad (57)$$

and is a function of the index of refraction and the angle of incidence  $\theta_0$ . This study considers the determination of material constants from reflection measurements only, and it should be stressed that the knowledge of reflected amplitudes alone can tell nothing about the phase shift. From the data on  $R_1$  and  $R_2$  we can obtain only the lengths of the axes of the quadrant or rectangle which are circumscribed about the circle or ellipse of polarization. These curves have four points of contact with the frame, which are given by

$$P_{1,2} (\pm \sqrt{R_1}, \pm \sqrt{R_2} \cos \delta), \text{ and}$$

$$P_{3,4} (\pm \sqrt{R_1} \cos \delta, \pm \sqrt{R_2}).$$

In experimental work, particularly in optics, that angle of incidence where the difference in phase is  $90^\circ$  is of special interest, and is called the "principal angle of incidence." For this case the axes of the vibration ellipse are oriented in the direction of the field components of the vector  $E$ . The corresponding azimuth is defined as the "principal azimuth," and is also given by Eq. (56).

Some physics textbooks explain that the principal angle of incidence is the same as the angle at which the reflectance curve of  $R_2$  has a minimum. This is generally not true; the assumption was apparently based on mathematical formulations which are used in metal optics and are of limited validity even when large values of  $n$  and  $k$  are concerned. The approximations employed yield the same angle  $\theta_0$  for  $R_2 = \text{minimum}$  and for  $\delta = 90^\circ$ .

Using the reflection coefficients  $R_1$  and  $R_2$ , the degree of polarization  $P$  is defined as

$$P = \frac{R_1 - R_2}{R_1 + R_2} = \frac{1 - \frac{R_2}{R_1}}{1 + \frac{R_2}{R_1}} = \frac{\tan^2 \psi - 1}{\tan^2 \psi + 1} \quad (58)$$

and as long as we consider specular reflection only, the degree of polarization is always positive. The maximum degree of polarization occurs if  $R_2/R_1$  is a minimum. Contrary to statements appearing in some textbooks, the angle of incidence  $\theta_0$  at which the ratio of  $R_2/R_1$  is a minimum is not identical to either the "pseudo Brewster angle" or the "principal angle of incidence." The  $(R_2)_{\min}$ ,  $(R_2/R_1)_{\min}$  or  $P_{\max}$  and  $\delta = 90^\circ$  each occur for a particular angle of incidence, with a maximum variation in these angles of between  $0^\circ$  and  $45^\circ$ . Only in the case of dielectric materials are the incidence angles  $\theta_0$  for  $(R_2)_{\min}$  and for  $\delta = 90^\circ$  the same. As a visual aid, the case  $N = n - ki = 0.6 - 0.6i$  is graphically illustrated in Fig. 65, with the curves representing  $R_1$ ,  $R_2$ ,  $R_2/R_1$ ,  $P$  and  $\delta$  plotted against  $\theta_0$ . The three distinct angles which appear are considered in more detail in Section 3.10. In order to clarify the distinction it is proposed here to name the above-mentioned characteristic angles of incidence First, Second, and Third Brewster Angles. The following definitions are based on the assumption that the incoming wave consists of two equal amplitudes which oscillate perpendicular to each other, one perpendicular and one parallel to the plane of incidence:

#### First Brewster Angle - Pseudo Brewster Angle:

The angle of incidence  $\theta_0$  for which the amplitude  $\sqrt{R_2}$  of the wave oscillating parallel to the plane of incidence is a minimum.

#### Second Brewster Angle:

The angle of incidence  $\theta_0$  for which the ratio of the reflected intensities  $(R_2/R_1)$  is a minimum, or of the same tenor, for which the degree of polarization  $P = (R_1 - R_2)/(R_1 + R_2)$  is a maximum.

#### Third Brewster Angle - Principal Angle of Incidence:

The angle of incidence  $\theta_0$  at which the two amplitudes of the reflected wave have a difference in phase of  $\delta = 90^\circ$ .

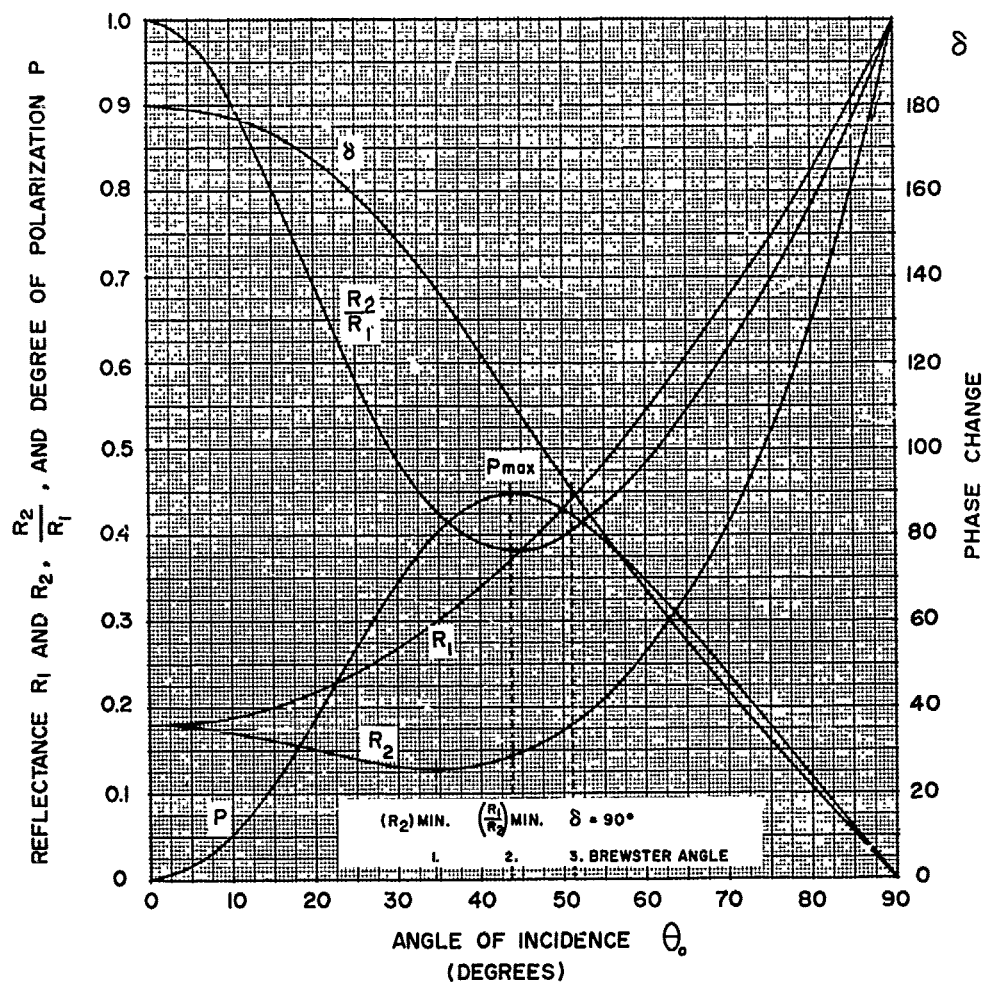


Fig. 65. ILLUSTRATION OF THE DEFINITION OF THE FIRST, SECOND, AND THIRD BREWSTER ANGLE OF INCIDENCE, FOR  $N = 0.6 - 0.61$

### 3.3. Reflectivity R of Unpolarized Radiation Versus $\theta_0$

If a source emits electromagnetic radiation, the vibrations of which oscillate in all transverse directions perpendicular to the wave's path, such radiation is called unpolarized. Natural light is an example of unpolarized radiation. The numerical value of the reflection of such a radiation  $R$  is given by the arithmetic mean of  $R_1$  plus  $R_2$ . Figures 11 to 18 (Chapter 2), which illustrate  $R$  versus  $\theta_0$ , show that as long as  $n$  and  $k$  are small and the angles of incidence are not too large the reflectivity  $R$  is nearly constant; the curves have their minimum at normal incidence. For a real index of refraction, this minimum of the reflectance occurs at normal incidence as long as  $n \leq 3.732$  (see also Refs. 8 and 9, p. 399). If we follow the axis of  $n$  to larger values the incidence angle for  $R = \text{minimum}$  increases very fast at first, reaching  $41^\circ$  for  $n = 3.80$  and  $57.4^\circ$  for  $n = 4.00$ . This angle gradually approaches the Brewster angle, but becomes identical only for  $n = \infty$ . Section 2.8 contains a general discussion of the occurrence of  $R_{\min}$  for the complex plane of  $N$ .

### 3.4. Reflectivity R at Normal Incidence, and N

The reflectance at normal incidence ( $\theta_0 = 0^\circ$ )\* was earlier given by Eq. (45)

$$R = \frac{(n-1)^2 + k^2}{(n+1)^2 + k^2} \quad (59)$$

For the illustration in the Argand diagram, we use the following equation which is derived from Eq. (59) after an elementary transformation:

$$\left(n - \frac{1+R}{1-R}\right)^2 + k^2 = \frac{4R}{(1-R)^2} \quad (60)$$

This develops into the equation of a circle with the radius

$$r = \frac{2\sqrt{R}}{1-R}$$

around the center  $C$  which has the coordinates  $P_c\left(\frac{1+R}{1-R}, 0\right)$ .

---

\* This case was also investigated by T. S. Moss (Ref. 10).

Figure 19 illustrates this case using isorefectance curves representing  $R = 0.1$  (0.1) 1.0 of the incident radiation. Total reflectance occurs only if  $N$  is purely imaginary. Where  $n$  and  $k$  are large in comparison with unity, Eq. (60) can be replaced by

$$\left(n - \frac{1+R}{1-R}\right)^2 + k^2 = \left(\frac{1+R}{1-R}\right)^2 \quad (61)$$

and if  $n = k$  and  $\gg 1$ , Eq. (59) simplifies to

$$R = \frac{n-1}{n+1} \quad (62)$$

### 3.5. Reflectivity $R_1$ and $N$

The curves for  $R_1$  have the same circular shape for small angles of incidence  $\theta_0$  as for normal incidence (Figs. 20-29). As the angle of incidence is increased, the curves draw closer to the point  $P(1.0, 0)$ . With slanting incoming radiation ( $\theta_0$  between approximately  $70^\circ$  and  $90^\circ$ ), all materials exhibit a high reflectance, Total reflectivity occurs also for pure real indices of refraction for which the angles of incidence  $\theta_0$  are defined by the inequality  $0 < n \leq \sin \theta_0$ .

### 3.6. Reflectivity $R_2$ and $N$

All curves for  $R_2 = \text{constant}$  (Figs. 30 to 39) start in the area where  $n < 1$  and  $k$  is very small, reach more or less high values of  $k$  and  $n$ , and then return to the axis of abscissa  $k = 0$ , and enter the adjacent quadrant in which they describe symmetrical curves. For this reason, the illustrations cover only one quadrant of the complex plane. This symmetry exists without any exception for all curves of  $R$ ,  $R_1$ ,  $R_2$ , and  $P$ .

As stated in the preface, a wave propagation across an interface between two absorbing materials results in a relative complex index of refraction of the form  $N = n + ki$  ( $n > 0$ ,  $k \geq 0$ ), if the phase of the complex index of the first medium is smaller than the phase of the second medium.

The curves for  $R_2$  do not have the simple shape of the  $R_1$  curves, being convex in some regions and concave in others. Because of the occurrence of the Brewster angle, the curves for the smaller values of  $R_2$  deviate from the circular form, and the curves for the lower

reflectance degenerate into two branches and have four points of intersection with the axis of the abscissa. If  $\theta_0 < 45^\circ$ , we observe total reflection from  $n > 0$  to  $n = \sin \theta_0$ . For real indices and for complex indices with small values of  $k$ , the reflectivity  $R_2$  decreases from 1 to 0 if  $n$  passes from  $n = \sin \theta_0$  to  $\tan \theta_0 < n \leq 1.0$ . This reflectivity maximum, however, is always smaller than unity.

If  $\theta_0 > 45^\circ$ , the point in the Argand diagram for  $R_2 = 0$  is situated on the axis of abscissa on the right-hand side of the point  $n = 1$ . Remarkable amounts of reflection will occur for indices of refraction close to unity, as the reader can observe in Fig. 39 which represents  $R_2$  for  $\theta_0 = 85^\circ$ . For values of  $n < 1$ , the area close to  $k = 0$  represents internal reflection and the reflection of waves in a plasma. A detailed description of these cases would require numerical values for  $N$  with smaller intervals for  $n$  and  $k$  than the 0.1 used in our tables.\*

### 3.7. Reflectivity R and N

The reflectance  $R$  of unpolarized radiation (e. g. natural light) is shown in Figs. 40 to 49. These graphs contain the combined irregularities of  $R_1$  and  $R_2$  and, therefore, deviate further from the circular shape than do the individual curves for  $R_1$  and  $R_2$ .

### 3.8. Degree of Polarization P and N

The degree of polarization  $P$ , defined by

$$P = \frac{R_1 - R_2}{R_1 + R_2} = \frac{1 - \frac{R_2}{R_1}}{1 + \frac{R_2}{R_1}} \quad (63)$$

is illustrated by Figs. 50 to 59. This equation can be written

$$\frac{R_2}{R_1} = \frac{1 - P}{1 + P}$$

so that the graphs also illustrate the ratio of the reflectivities. A  $P$ -to- $R_2/R_1$  conversion table is provided below.

---

\* Reference 11 presents some graphs for  $R_1$  and  $R_2$  for  $\theta_0 = 20^\circ$  and  $\theta_0 = 67^\circ$ .

P	$\frac{R_2}{R_1}$
0	1
0.1	0.8181
0.2	0.666
0.3	0.53846
0.4	0.42857
0.5	0.333
0.6	0.25
0.7	0.17647
0.8	0.111
0.9	0.05263
1.0	0
$\frac{R_2}{R_1}$	P

The smaller the ratio  $R_2/R_1$ , the greater the degree of polarization. Polarization reaches the maximum value of 100% only for dielectrics. The curves are again similar to circles with one center at  $n = \tan \theta_0$ ,  $k = 0$  (Brewster angle), and another at  $n = 1$ ,  $k = 0$ . The latter is not illustrated in all graphs due to the fact that the curves cannot be distinguished on the chosen scale. It is remarkable that for small angles of incidence polarization occurs only in a small area of the diagrams. If we consider multiple reflection where all the planes of incidence are parallel to each other, we have to take into account the incoming intensities for each wave separately. The degree of polarization is then given by

$$P = \frac{\sum_{v=0}^{\infty} R_1^{(v)} - \sum_{v=0}^{\infty} R_2^{(v)}}{\sum_{v=0}^{\infty} R_1^{(v)} + \sum_{v=0}^{\infty} R_2^{(v)}} \quad (64)$$

where  $R_1^{(0)}$  and  $R_2^{(0)}$  stand for the squares of  $E_1^i$  and  $E_2^i$ , respectively, which are the components of the electric field vector of the original wave. The absolute values of  $E_1^i$  and  $E_2^i$  are always considered unity. Since  $R_2$  is always smaller than  $R_1$ , we can see from the above equation that multiple reflection is a good means to obtain a radiation with a high degree of polarization from a given source.

### 3.9. Occurrence of the Characteristic Angles of Incidence

Section 3.2 mentions three characteristic incidence angles, defined as the First, Second, and Third Brewster angles. We obtain numerical expressions for the First and Second Brewster angles by differentiation based on application of Eqs. (32) and (33). To do this requires tedious analytical labor and leads to immense and unwieldy equations.\* In order to discuss the three angles in the whole complex area of the index of refraction, we chose a technique which avoids these complications. This method is described below for the First Brewster angle.

#### 3.9.1. First Brewster Angle and N

The problem here was to illustrate the relation between the angle of incidence  $\theta_0$ , at which  $R_2$  is a minimum, and this minimum itself. For this purpose, the Argand diagram was again selected. A first sketch was prepared by taking the minimum values of  $R_2$  and the corresponding angles  $\theta_0$  from Figs. 3 to 10 and similar graphs and from special tables which are not published in this paper. This method does not give sufficient accuracy to prepare a serviceable plot of the subject, since (1) the minima of the  $R_2$  curves are often very flat, and (2) in many of the cases the  $R_2$  curves change so rapidly with the angle of incidence that it would not be feasible to tabulate all the data required to find the exact values of  $\theta_0$ ; even the special  $2^\circ$ -tables [ $\theta_0 = 0^\circ(2^\circ)88^\circ$ ] which served to supplement the published  $5^\circ$ -tables [ $\theta_0 = 0^\circ(5^\circ)85^\circ$ ] were not sufficient for this purpose. It was necessary to use computer methods to obtain the desired numerical values of  $(R_2)_{\min}$  and  $\theta_0$  for given indices of refraction by successive approximation. Since these data have not been published and are of special interest, the results are

---

\* One of the known methods for approximating the angle of minimum of reflectance is that proposed by Quincke. However it was found that it holds only if  $n$  and  $k$  are large and then only in special cases. C. Boeckner (Ref. 12) considers it impossible to solve this problem explicitly for  $n$  and  $k$ .

presented in Table E (Volume II) of this report. This table contains  $(R_2)_{\min}$  and the corresponding angle of incidence  $\theta_0$  for all combinations of  $n = 0.1(0.1)4.0$  and  $k = 0.1(0.1)6.0$ . The corresponding graphical illustrations are given in Figs. 60 and 70.

The curves for  $\theta_0 = \text{constant}$  ( $\theta_0 > 50^\circ$ ) are of oval shape with the major axis in the direction of the ordinate axis. For smaller angles they lose the oval shape and cross the ordinate axes obliquely. The crossing angles are smaller for curves closer to the origin, with the shape of the curves resembling a clover leaf.

### 3.9.2. Second Brewster Angle and N

The case where the degree of polarization  $P$  has its maximum was investigated in the same manner as the First Brewster Angle; using a corresponding set of graphs and tables. The same problems were encountered. The ratio  $R_2/R_1$ , which has to be a minimum and is easier to handle, was used instead of  $P$  for the final calculations, performed by computer. The results are given in Table F (Volume II) and Figs. 61 and 71. The curves have an oval shape but differ in that the major axis lies in the direction of the axis of abscissa.

### 3.9.3. Third Brewster Angle and N

For the principal angle of incidence there exists a rigorous equation which is given in the literature as (Ref. 13, p. 363)

$$\sin^4 \theta_0 \tan^4 \theta_0 = n^4(1 + \kappa^2)^2 - 2n^2(1 - \kappa^2) \sin^2 \theta_0 + \sin^4 \theta_0 \quad (65)$$

Since  $n^2 + k^2$  is generally much greater than unity, optics of metals takes into account only the first term of the right-hand side of this equation using the form

$$n^2 + k^2 = \sin^2 \theta_0 \tan^2 \theta_0. \quad (66)$$

This study, however, seeks a thorough discussion of the reflection characteristics for all kinds of materials and will use the exact expression. On this basis Eq. (65) can be written

$$(n^2 + k^2)^2 - 2 \sin^2 \theta_0 (n^2 - k^2) = \sin^4 \theta_0 \tan^4 \theta_0 - \sin^4 \theta_0 \quad (*) \quad (67)$$

or

$$(n^2 - \sin^2 \theta_0)^2 + (k^2 + \sin^2 \theta_0)^2 + 2n^2 k^2 = \sin^4 \theta_0 (\tan^4 \theta_0 + 1). \quad (68)$$

These equations represent Cassinian curves in the Argand diagram (Fig. 62) for each constant angle of incidence. The curves are defined by the bipolar equation  $rr^1 = a^2$ , or expressed in words, they are the loci of all points of which the product of the distances from two fixed loci, separated by a distance of  $2c$ , has the constant value  $a^2$ . Using our nomenclature, the curves have the equations

$$(n^2 + k^2)^2 - 2c^2 (n^2 - k^2) = a^4 - c^4 \quad (69)$$

\*) The curves  $\delta = f(n, k, \theta_0)$ , where  $n$  and  $k$  are considered as parameters, all have two common points, i. e.  $\delta = 180^\circ$  for  $\theta_0 = 0^\circ$  and  $\delta = 0^\circ$  for  $\theta_0 = 90^\circ$ . Each one of the curves, therefore, crosses the line  $\delta = 90^\circ$  an odd number of times to the right of  $\theta_0 = 0^\circ$ . For physical reasons, we are interested in reading these intersection points, and must consider either one or three values  $\theta_0$  for  $\delta = 90^\circ$ . Those values satisfy the equation

$$\tan^8 \theta_0 - (A - 2B + 1) \tan^4 \theta_0 - 2(A - B) \tan^2 \theta_0 - A = 0 \quad (67a)$$

which is obtained from Eq. (67) by substituting  $\tan \theta_0 / \sqrt{1 + \tan^2 \theta_0}$  for  $\sin \theta_0$ , where

$$A = (n^2 + k^2)^2$$

$$B = n^2 - k^2$$

As is seen, this equation of the 8th order contains only even powers of the unknown. For the reason given above, it follows that Eq. (67a) has either one or three positive roots in  $\tan \theta_0$ . In the case of three positive roots, two of them may coincide. This case is physically better described by the words: "We have two different values for  $\tan \theta_0$ ." Thus we distinguish three cases:

- (a) one single positive root  $\theta_0$ ;
- (b) two distinct positive values satisfying Eq. (67a); and
- (c) three distinct roots.

where

$$c = \sin \theta_0$$

$$a = \sin \theta_0 \tan \theta_0$$

In the interval of the angle of incidence  $0 \leq \theta_0 \leq 90^\circ$ , the Cassinian curves take on different shapes. We can distinguish three cases:

$$(a) \sin \theta_0 = \sin \theta_0 \tan \theta_0$$

$$(b) \sin \theta_0 < \sin \theta_0 \tan \theta_0$$

$$(c) \sin \theta_0 > \sin \theta_0 \tan \theta_0$$

Case (a) occurs if  $a = c$ , i. e.  $\theta_0 = 45^\circ$ ; this is the lemniscate of Bernoulli with the pole at the origin. Case (b) occurs if  $c < a$ , i. e.  $\theta_0 > 45^\circ$ . For values of  $\theta_0$  between  $\theta_0 = 45^\circ$  and  $\tan \theta_0 = \sqrt{2}$ , the curves are general lemniscates with their two saddle points at the ordinate axes; for greater values of  $\theta_0$  the curves are Cassinian ovals, with their longer axes along the axis of abscissa. Case (c) occurs if  $c > a$ , i. e.  $\theta_0 < 45^\circ$ . The curves for  $\theta_0 < 45^\circ$  are within the lemniscate of Bernoulli, and each branch has two points of intersection with the axis of abscissa. This case is illustrated by a special drawing (Fig. 63). It will be observed that the unequal relation between the principal angle of incidence and the index of refraction no longer holds for a certain region of small indices. This "region of multiple principal angles of incidence" is bounded by three curves: (1) the axis of abscissa, (2) the envelope of the curves  $\theta_0 = \text{constant}$ , and (3) approximately the curve for  $\theta_0 = 33^\circ$ . (More precise investigation of the nature of this third boundary does not seem to be worth the amount of work involved). From an inspection of numerical results it was observed that materials with an index of refraction located on boundaries (2) and (3) have two principal angles of incidence, and that the materials whose index of refraction falls within the region considered, including the axis of abscissa, have three principal angles of incidence. The two points of intersection of the curves  $\theta_0 = \text{constant}$  with the axis of abscissa have a physical interpretation. The point on the right-hand side represents Brewster's law for which  $R_2 = 0$ . For the other point we have total reflection, but the two amplitudes of  $R_1$  and  $R_2$  have a difference in phase of  $90^\circ$ .

With application of the approximation given by Eq. (66), the curves would degenerate into circles and show only fair agreement within the area of large indices, requiring the further restriction  $n \sim k$  to obtain accurate results. It follows from Eq. (68) that the points of intersection with the axes are

$$n = 0 \quad k = \sin \theta_0 \tan \theta_0$$

$$k = 0 \quad \begin{cases} n_1 = \tan \theta_0 \\ n_2 = \tan \theta_0 \sqrt{\cos 2\theta_0} \end{cases}$$

### 3.9.4. Angle of Incidence $\theta_0$ for Unpolarized Radiation $R_{\min}$ and $N$

This case was discussed briefly in Section 3.3 and illustrated in Fig. 64 from the available tables and graphs. This particular graph serves as an illustration only and does not claim to be as accurate as the other figures. It will be noted that there is an area for which the minimum reflection occurs at normal incidence, with a small surrounding belt in which the angle of incidence increases very fast. Only the curves for  $\theta_0 = 60^\circ$ ,  $70^\circ$ , and  $80^\circ$  are represented.

### 3.9.5. Angle of Incidence $\theta_0 = 45^\circ$

There exists a remarkable relation between the reflection formulas for  $R_1$  and  $R_2$  for the angle of incidence  $\theta_0 = 45^\circ$ . This can be shown by Eqs. (32) and (33), which we note here again:

$$R_1 = \frac{\left(\frac{q}{\alpha_2} - \cos \theta_0\right)^2 + \left(\frac{p}{\alpha_2}\right)^2}{\left(\frac{q}{\alpha_2} + \cos \theta_0\right)^2 + \left(\frac{p}{\alpha_2}\right)^2} \quad (70)$$

$$R_2 = \frac{\left(\frac{q}{\alpha_2} - \cos \theta_0\right)^2 + \left(\frac{p}{\alpha_2}\right)^2}{\left(\frac{q}{\alpha_2} + \cos \theta_0\right)^2 + \left(\frac{p}{\alpha_2}\right)^2} \cdot \frac{\left(\frac{q}{\alpha_2} - \sin \theta_0 \tan \theta_0\right)^2 + \left(\frac{p}{\alpha_2}\right)^2}{\left(\frac{q}{\alpha_2} + \sin \theta_0 \tan \theta_0\right)^2 + \left(\frac{p}{\alpha_2}\right)^2} \quad (71)$$

The first factor on the right-hand side of Eq. (71) is identical with the right-hand side of Eq. (70), and the only difference between the two factors of Eq. (71) is that the second contains  $\sin \theta_0 \tan \theta_0$  instead of the  $\cos \theta_0$  of the first factor. Both factors become equal if

$$\cos \theta_0 = \sin \theta_0 \tan \theta_0.$$

This implies that if  $\theta_0 = 45^\circ$  the Eqs. (70) and (71) yield:

$$\left. \begin{array}{l} \text{or} \\ \\ \text{and} \end{array} \right\} \begin{array}{l} R_1^2 = R_2 \\ \\ R_1 = \frac{R_2}{R_1} \\ \\ P = \frac{1 - R_1}{1 + R_1} \end{array} \quad \begin{array}{l} \text{For} \\ \theta_0 = 45^\circ \\ \text{only} \end{array} \quad (72)$$

Therefore, the curves for  $R_1$  and for the ratio  $R_2/R_1$  (but not for  $P$ ), if plotted versus the angle of incidence, have a common point. In Fig. 65, for  $N = 0.6 - 0.6i$ , the curves  $R_1$ ,  $R_2$ , and  $R_2/R_1$  are represented simultaneously. The relation expressed by Eq. (72) is a valuable tool in experimental work for (1) checking the influence of matter located between a radiating source and a reflecting surface, (2) determining properties of the matter itself, or (3) if  $R_1^2 = R_2$  is observed, use as an aid in locating a transmitter, the radiation from which hits the reflecting surface at an angle of incidence  $\theta_0 = 45^\circ$ .

### 3.9.6. Linear Eccentricity of the Polarization Ellipse

Associated with the reflection is a phase shift between the two components of electrical field vector  $E$ , which vector describes a conic section (as a special case of Lissajous-Curves), expressed by the equation

$$\left(\frac{E_x}{a_1}\right)^2 - \frac{2E_x E_y}{a_1 a_2} \cos \delta + \left(\frac{E_y}{a_2}\right)^2 = \sin^2 \delta \quad (73)$$

Figure 66 illustrates this case using a harmonic wave with the amplitudes.

$$E_x = a_1 \sin \omega t$$

$$E_y = a_2 \sin (\omega t + \delta) \quad (74)$$

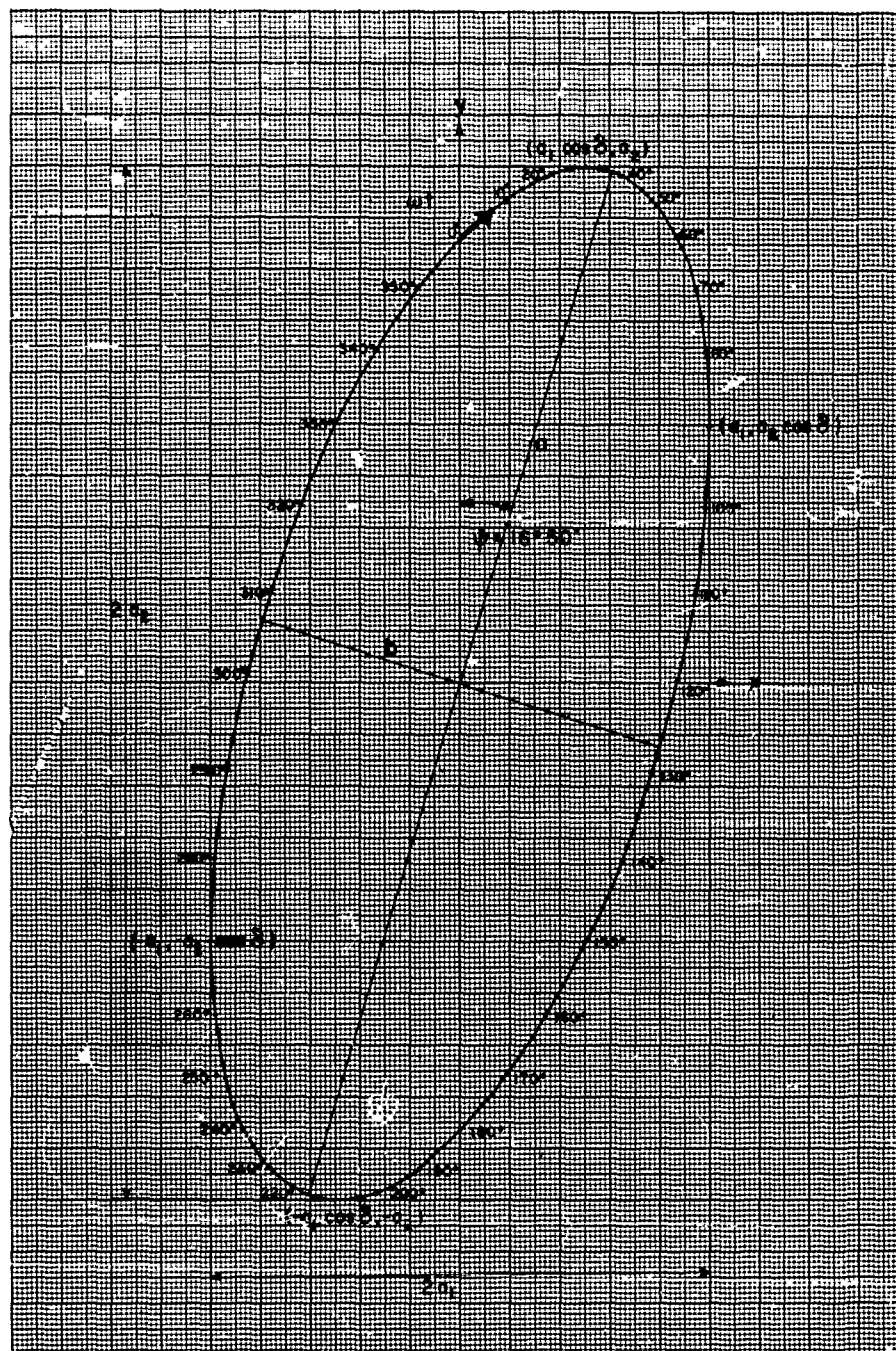


Fig. 66. VIBRATION ELLIPSE OF A HARMONIC WAVE ( $\delta = 60^\circ$ )

where

$$a_1 = 0.5$$

$$b_1 = 1.0$$

$$\delta = 60^\circ$$

This example describes all instances in which  $R_1 : R_2 = 4 : 1$  and the phase shift  $\delta = 60^\circ$ . The linear eccentricity  $e$  is defined by

$$a^2 - b^2 = e^2 \quad (75)$$

where  $a$  and  $b$  are the two semiaxes of the ellipse. It is known from geometry that the following equations hold (Ref. 14):

$$\frac{ab}{a^2 + b^2} = \frac{a_1 a_2}{a_1^2 + a_2^2} \sin \delta \quad (76)$$

$$a^2 + b^2 = a_1^2 + a_2^2 \quad (77)$$

From these we obtain

$$e^2 = a^2 - b^2 = \sqrt{(a_1^2 + a_2^2)^2 - 4a_1^2 a_2^2 \sin^2 \delta} \quad (78)$$

Let us consider the linear eccentricity of the polarization ellipse of a reflected radiation as a function of the angle of incidence  $\theta_0$  and the index of refraction  $N$ . Replacing  $a_1$  and  $a_2$  with the reflection coefficients  $R_1$  and  $R_2$ , we obtain for the square of the eccentricity

$$e^2 = a^2 - b^2 = \sqrt{(R_1 + R_2)^2 - 4R_1 R_2 \sin^2 \delta} \quad (79)$$

For a particular  $N$ , we read the  $R_1$  and  $R_2$  values from the tables and determine  $\delta$  using the equation

$$\tan \delta = \frac{2 \frac{p(\theta_0)}{\alpha_2} \sin \theta_0 \tan \theta_0}{\sin^2 \theta_0 \tan^2 \theta_0 - \left( \frac{q^2(\theta_0)}{\alpha_2^2} + \frac{p^2(\theta_0)}{\alpha_2^2} \right)} \quad (80)$$

A numerical example for  $N = 0.6 - 0.6i$  is illustrated in Fig. 67 which represents the curves  $e^2$ ,  $R_1$ ,  $R_2$ , and  $R_1 - R_2$ .

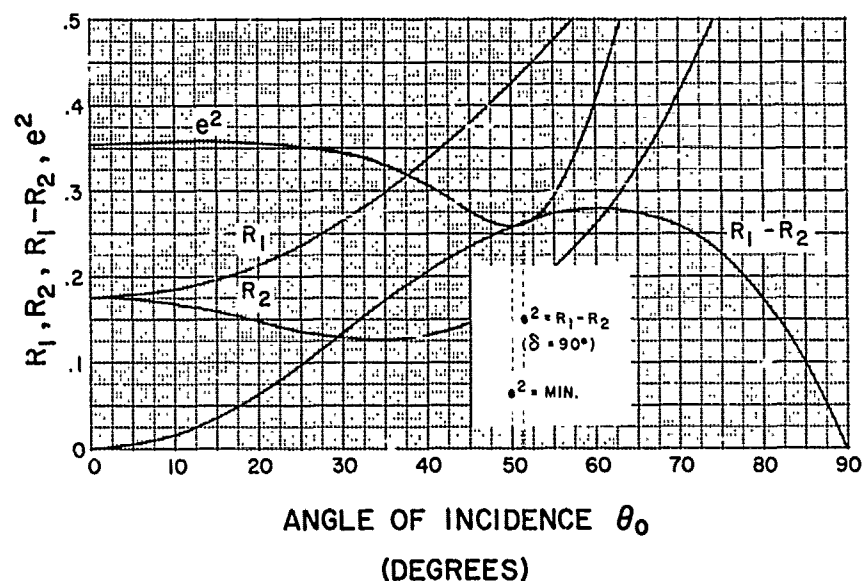


Fig. 67. REFLECTANCE CURVES  $R_1$ ,  $R_2$ , AND  $R_1 - R_2$ , AND THE SQUARE OF THE LINEAR ECCENTRICITY OF THE POLARIZATION ELLIPSE  $e^2$  FOR  $N = 0.6 - 0.61$

At the Third Brewster angle, the phase shift is  $\delta = 90^\circ$  and the two axes  $a_1$  and  $b_1$  of the ellipse are symmetrical to the electric field components. The following relations hold:

$$a^2 = a_1^2 = R_1$$

$$b^2 = a_2^2 = R_2$$

$$e^2 = a^2 - b^2 = R_1 - R_2$$

and the curves for  $e^2$  and  $R_1 - R_2$  have a point of contact. This ellipse has the least linear eccentricity of all the ellipses which can be drawn in the rectangle with the sides  $2a_1$  and  $2b_1$  (if  $a = a_1$  and  $b = b_1$ ). However, there is no basis for believing that the minimum of  $e$  at the phase shift  $\delta = 90^\circ$  is also the minimum of the curve  $e$  if  $e$  is considered to be a function of  $\theta_0$ . The angle of incidence  $\theta_0$  for which  $e = \text{minimum}$  is a characteristic angle of incidence, distinct from these Brewster angles. But it is worth mentioning that the function  $e = e(\theta_0, n, k)$  has application in experimental work.

In our example  $N = 0.6 - 0.6i$ , the minimum of  $e^2$  occurs approximately at  $\theta_0 = 50^\circ$ , while  $\delta = 90^\circ$  occurs at  $\theta_0 = 51.2^\circ$ . From the study of other values of  $N$ , it was observed that there are cases where the difference between these angles is even larger.

### 3.10. Summary

The principal results of these studies can be summarized as follows:

Material	Angle of Incidence $\theta_0$	Reflection Characteristics
Dielectrics and Conductors	$0^\circ$	$R_1 = R_2 < 1$
	$45^\circ$	$R_1 = \frac{R_2}{R_1}$
	$90^\circ$	$R_1 = R_2 = 1$
Dielectrics	Brewster Angle	$R_2 = 0, P = 1$
Conductors	First Brewster Angle	$R_2 = \text{Minimum}$
	Second Brewster Angle	$\frac{R_2}{R_1} = \text{Minimum}$
	Third Brewster Angle	$P = \text{Maximum}$ $\delta = 90^\circ$

Careful inspection of the material presented shows that, where  $N$  is complex, the following relation holds, without exception, for the three Brewster angles for conductors (denoted by  $\theta_1^*$ ,  $\theta_2^*$ , and  $\theta_3^*$ , in numerical order):

$$\theta_1^* < \theta_2^* < \theta_3^*.$$

## Chapter 4

### PROPOSED APPLICATIONS

There are several applications for the tables and graphs containing the numerical results of the Fresnel equations. In general, the problems in which they would be useful fall into two types: (1) extracting the numerical values of the reflectance directly from the tables if the index of refraction of the material and the angle of incidence of the radiation are known (Section 4.1); (2) determining the index of refraction from a combination of the published information and experimental data (Section 4.2).

#### 4.1. Use of the Data

The numerical values for the Fresnel equations are provided in tabular form in the Appendix (Volume II). These numerical values are based on calculations where both the components  $E_1 = E_1^i$  and  $E_2 = E_2^i$  of the electric field vector  $E$  of the incoming radiation were taken as unity, and, consequently, their absolute squares  $I_1 = I_1^i$ , and  $I_2 = I_2^i$ , which represent the power intensities, also become unity. Since the data presented in the tables and graphs are based on the standardization factor 2, the reader is reminded that all the numerical values have to be divided by 2 if the total incoming radiation has components in both planes -- perpendicular and parallel to the plane of incidence.

The selected ranges of the index of refraction  $N = n - ki$ ,  $n = 0.1 (0.1) 4.0$ ,  $k = 0.0 (0.1) 6.0$ , and the angles of incidence  $\theta_0 = 0^\circ (5^\circ) 85^\circ$  cover the area of the index of refraction around the origin of the complex plane for  $N$  to provide a basis for a more detailed survey of the very complex problems of reflection phenomena; the chosen density of the data should be sufficient for interpolation. Using Tables A and C, the numerical values for the unpolarized radiation  $R = 1/2 (R_1 + R_2)$  and the degree of polarization  $P = (R_1 - R_2) / (R_1 + R_2)$  can easily be calculated, while in Tables B and D the reflectance  $R_1$ ,  $R_2$ , and  $R$  are identical. Tables E, F, and G were prepared to cover the special cases, such as  $(R_2)_{\min}$ ,  $P_{\max}$ , or

$(R_2/R_1)_{\min}$ , and  $\delta = 90^\circ$ . The accuracy of Tables A - G is  $\pm 1$  of the last communicated decimal. The second decimal of the index of refraction can easily be determined by interpolation.

Various authors give the components of the index of refraction  $N = n - ki$  in the form  $n^2 - k^2$  and  $2nk$ . Data in this form lead easily to  $n$  and  $k$  if we write

$$n^2 - k^2 = x$$

$$2nk = y$$

and use

$$n = +\sqrt{\frac{x}{2} + \frac{1}{2}\sqrt{x^2 + y^2}} \quad (81)$$

#### 4.2. Determination of N from Reflection Measurements

The Fresnel equations now constitute a solid foundation in physics; much of the experimental work performed in this area during the last century showed good agreement between experiment and theory. Since all the quantities  $R_1$  and  $R_2$  are functions of  $\theta_0$ ,  $n$ , and  $k$ , the numerical values of  $n$  and  $k$  in general can be determined if the values of the other three are known.

The index of refraction can be determined experimentally by measuring either the transparency or the reflectance of radiation. However, massive pieces of conducting materials are opaque for a very small thickness; therefore, the experimental determination which applies the transmitted radiation is relatively limited and has to take into account the internal reflection also. A number of such experimental methods are known, and their appropriateness depends on which region of the electromagnetic spectrum is being considered. A frequently applied method uses the reflectance at the principal angle of incidence.

It is beyond the scope of this study to discuss the numerous experimental methods which can be used. For our purpose we will assume that the experimental results are available, and will consider how we can use them for an economical determination of the unknown material.

#### 4.2.1. Specular Reflection Under Ideal Test Conditions\*

A number of combinations can be selected from the plotted data. We can distinguish the following two major groups:

Group 1: Experimental data of the reflectance for any angle of incidence.

Group 2: Experimental data of the reflectance for characteristic angles of incidence.

As mentioned previously, we denote as characteristic angles the three Brewster angles, the angle  $\theta_0 = 45^\circ$ , and the incidence angle for which the unpolarized radiation has its minimum.

The following combinations of the data may be obtained from experiments.

Group 1:

- a.  $R_1$ ,  $R_2$ , or  $R$  for two different angles  $\theta_0$ .
- b.  $R_1$  and  $R_2$  for the same angle  $\theta_0$ .
- c.  $R_2/R_1$  or  $P$  for two different angles.

Group 2:

- d.  $(R_2)_{\min}$  and  $\theta_0$  of the occurrence.
- e.  $(R_2/R_1)_{\min}$  or  $P_{\max}$ , and  $\theta_0$  of the occurrence.
- f.  $R_1$ ,  $R_2$ ,  $R$  or  $R_2/R_1$  at the principal angle of incidence  $\theta_0$ .
- g.  $R_{\min}$  and  $\theta_0$  of the occurrence, limited to larger angle of incidence where  $\theta_0 > 50^\circ$ .

---

\* Other studies in this area are described in Refs. 12 and 15-18.

The following examples use data which can be taken directly from the tables and graphs.

Example: Group 1

By utilization of monochromatic plane-polarized radiation of the wavelength  $\lambda$ , of two equal amplitudes, the following data were obtained:

Angle of Incidence $\theta_0$	$R_1$	$R_2$	$R_2/R_1$	$P$
$40^\circ$	0.753	0.616	0.818	0.10
(Fig. 23)	23	33		53)
$75^\circ$	0.910	0.387	0.425	0.40
(Fig. 27)	27	37		57)

It follows from the measured data that the index of refraction of the test object at  $\theta_0 = 40^\circ$  will be a point on the isorefractance curve  $R_1 = 0.753$  (Fig. 23), on the curve  $R_2 = 0.616$  (Fig. 33), and on the curve  $P = 0.10$  (Fig. 53). By the same procedure we obtain the results for  $\theta_0 = 75^\circ$ . We now have six curves we can consider, and if all were plotted on one graph, they would have only one intersection point as long as the measured data are of good accuracy.

In this manner, Fig. 68 illustrates examples of a, b, and c of the first group. For clarity, only two curves of this example were plotted together, and only that portion of the curves near the cross point. It will be seen that the three pairs of graphs bisect each other at the same point in the complex plane. The numerical values of the coordinates give the components of the index of refraction of the material. In this particular case, the result is

$$N = n - ki \cong 1.90 - 4.00 i.$$

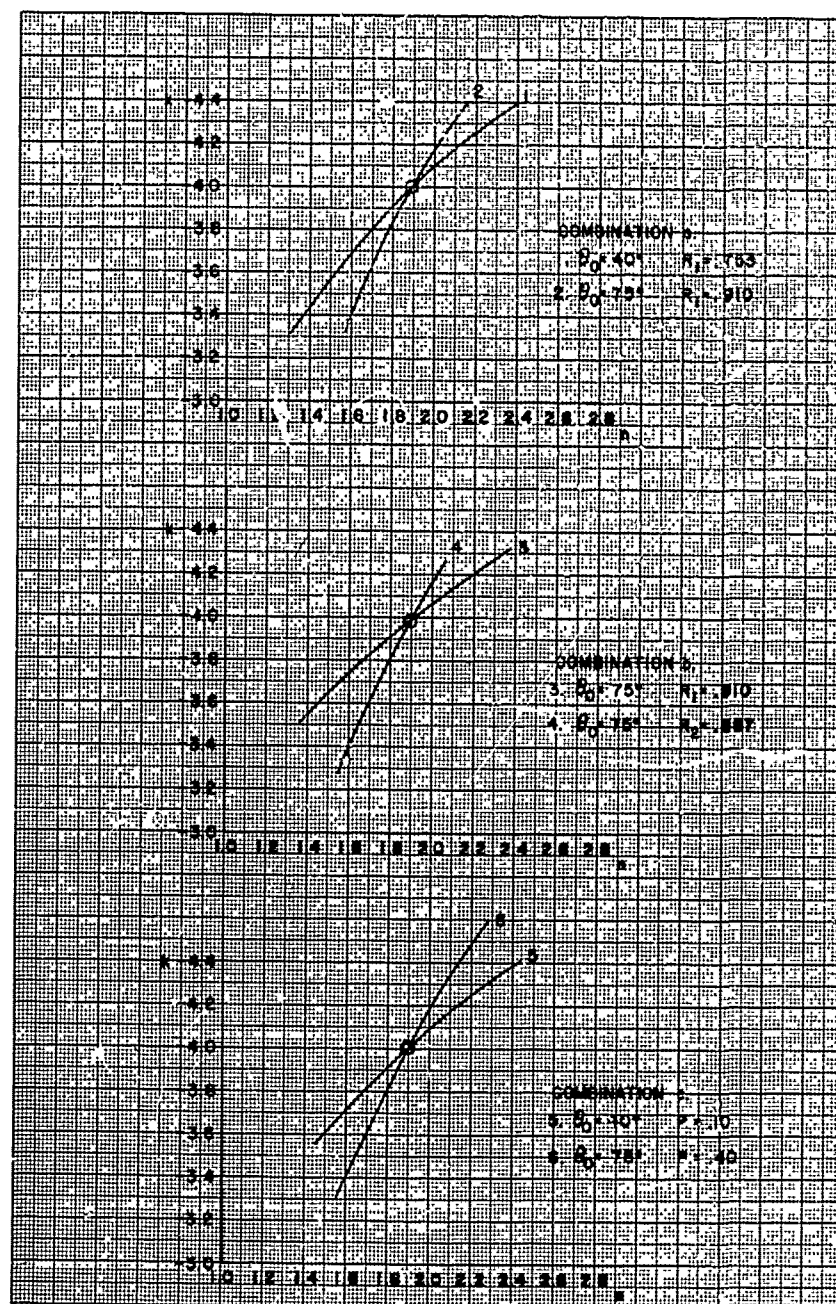


Fig. 68. THE DETERMINATION OF N FROM REFLECTION MEASUREMENTS  
(EXAMPLE OF GROUP 1)

From Fig. 1, which illustrates the index of refraction as a function of the wavelength, and from handbooks such as Ref. 5, we can look for elements with similar refraction indices, e.g.

$$\text{Ni: } N = 1.91 - 3.93i \text{ for } \lambda_1 = 6500 \text{ \AA}.$$

$$\text{Cr: } N = 1.895 - 4.038i \text{ for } \lambda_2 = 4150 \text{ \AA}.$$

If the applied wavelength is identical to one of those above, then the material has been identified. Provided that the experiment was done with a wavelength radiation  $\lambda_3$  which is different from  $\lambda_1$  and  $\lambda_2$ , the name of the material is still unknown (if not known from other information). Once the index of refraction is known, the tables and graphs enable us to study special cases, such as the variation of the reflectance with angle of incidence and the occurrence of reflection phenomena, in more detail and in a relatively short time. However, the equality in index of refraction does indicate that: (1) the three materials have the same reflectance curve with respect to angle of incidence, and (2) in absorption, transparency, and emission, the test material for  $\lambda_3$  will be comparable to nickel at  $\lambda_1$  and chromium at  $\lambda_2$ .

Determining  $N$  by means of the illustration in the Argand diagram is not always the most economical method. The plots of  $R_1$  and  $R_2$  in the Argand diagram were prepared from two graphs on which  $k$  was plotted as a function of  $n$  and  $R_1$ , and  $n$  and  $R_2$ , respectively. Figures 69a and b are examples of such plots for the angle of incidence  $\theta_0 = 40^\circ$ . Let us assume the following experimental results:

$$\theta_0 = 40^\circ \quad R_1 = 0.753$$

$$R_2 = 0.616$$

and draw in Fig. 69a the straight line  $R_1 = 0.753$  and in Fig. 69b the straight line  $R_2 = 0.616$ . The index of refraction is read from the points where these straight lines separately intersect the curve for the same  $k$  at the same values of  $n$ . Again the result for  $N$  becomes  $N = 1.90 - 4.00i$ .

A recommended method for making a quick but precise determination of the index of refraction is to first estimate the value of  $N$  by using the illustration in the Argand diagram, and then refining this value by preparing plots like Fig. 69 from information presented in the tables. For the last, only the area around  $N$  has to be plotted. If these plots are

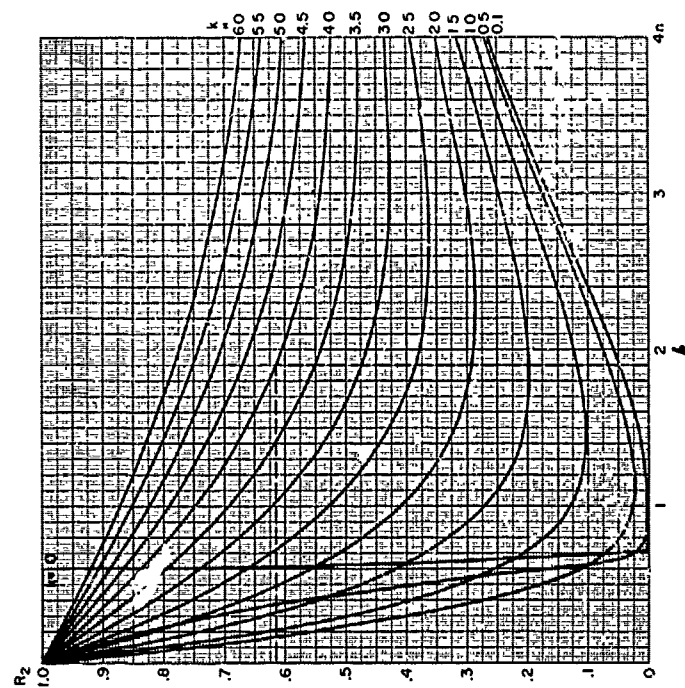
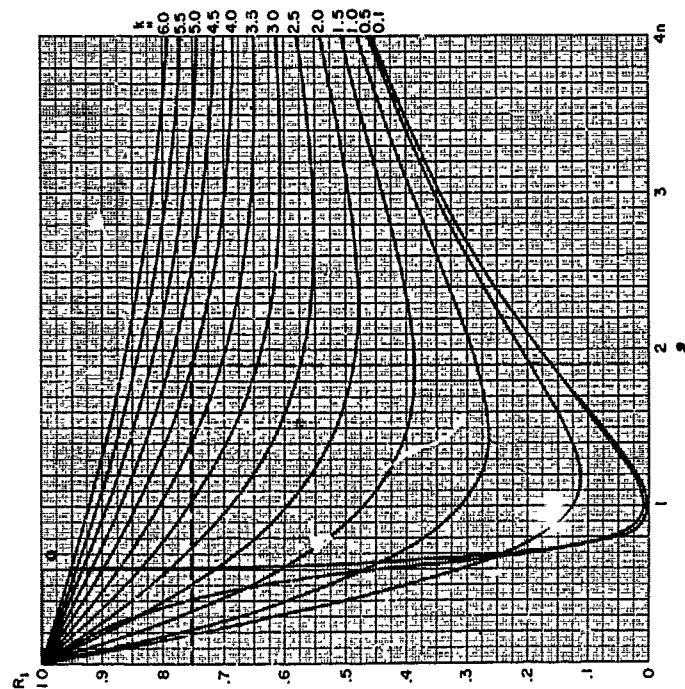


Fig. 69. REFLECTANCE CURVES  $R_1$  AND  $R_2$  ( $\theta_0 = 90^\circ$ )

prepared on transparent paper, we can match the straight lines  $R = R_1$  and  $R = R_2$  on the two graphs and can more easily determine  $n$  and  $k$ .

### Example: Group 2

Reflectance values for the characteristic angles of incidence may be available from experiments. Examples of such data are:

Characteristic Angle for	$\theta_0$	$R_1$	$R_2$	$R_2/R_1$	$P_{\max}$
$(R_2)_{\min}$	$\theta_1^* = 45^\circ.18$	----	0.4535	----	---
$(R_2/R_1)_{\min}$	$\theta_2^* = 56^\circ.76$	----	----	0.6375	0.221
$\delta = 90^\circ$	$\theta_3^* = 60^\circ$	0.7675	0.4916	0.6405	0.219

The various combinations applicable to this group can be derived from Fig. 60 to 64. We can combine any characteristic angle of incidence with a set of curves representing the numerical values of (1)  $R_1$ , (2)  $R_2$ , (3)  $R_1/R_2$ , or (4)  $R$  at this angle. Figures 70 to 72 were prepared by this method.

The sample experimental results identify a material with the index of refraction  $N = n - ki = 0.4 - 1.2i$ , as illustrated in Fig. 73. The following indices of refraction, which approximate this value were obtained from (Ref. 5):

Cesium:  $N = 0.321 - 1.2 i$  for  $\lambda = 5890 \text{ \AA}$

Zinc:  $N = 0.46 - 1.17 i$  for  $\lambda = 2749 \text{ \AA}$

Zinc:  $N = 0.47 - 1.60 i$  for  $\lambda = 2981 \text{ \AA}$

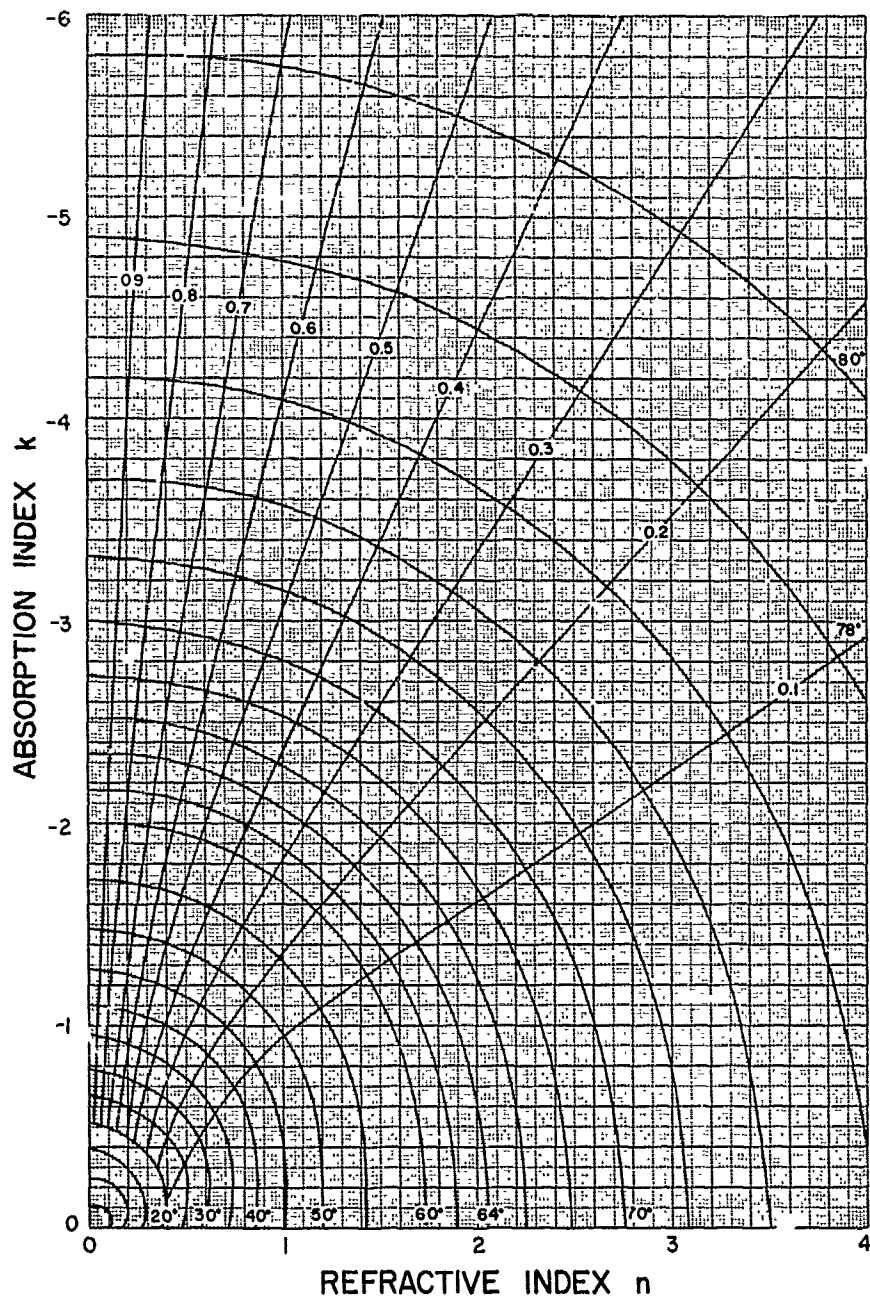


Fig. 70. RELATION AMONG THE FIRST BREWSTER ANGLE OF INCIDENCE (WHERE  $R_2$  IS A MINIMUM), THE REFLECTANCE  $(R_2)_{\min}$ , AND THE COMPLEX INDEX OF REFRACTION  $N = n - ki$

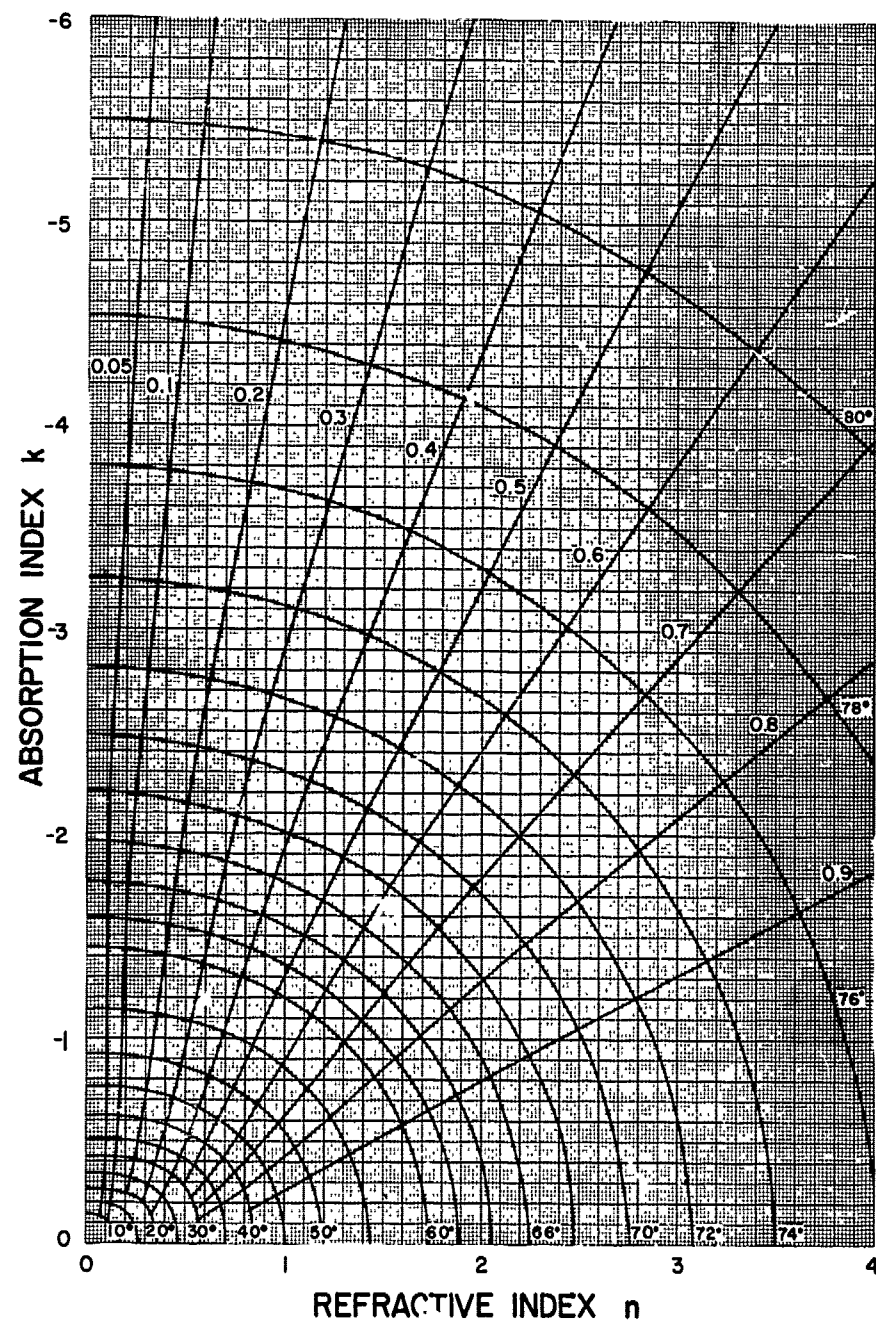


Fig. 71. RELATION AMONG THE SECOND BREWSTER ANGLE OF INCIDENCE (WHERE  $P$  IS A MAXIMUM), THE DEGREE OF POLARIZATION  $P_{max}$ , AND THE COMPLEX INDEX OF REFRACTION  $N = n - ki$

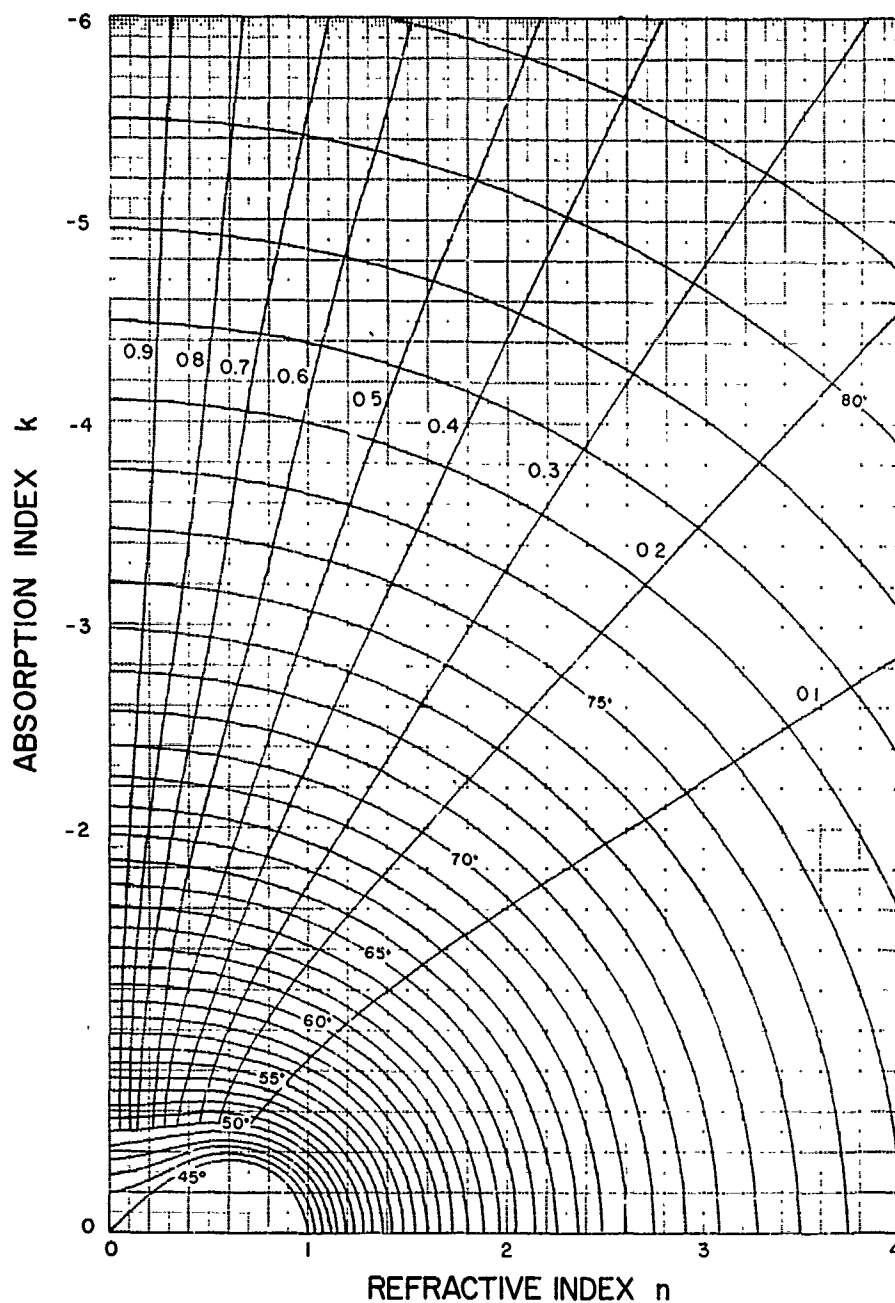


Fig. 72. RELATION AMONG THE THIRD BREWSTER ANGLE OF INCIDENCE = PRINCIPAL ANGLE OF INCIDENCE (WHERE THE PHASE DIFFERENCE  $\delta$  IS  $90^\circ$ ), THE REFLECTANCE  $R_2$ , AND THE COMPLEX INDEX OF REFRACTION  $N = n - ki$

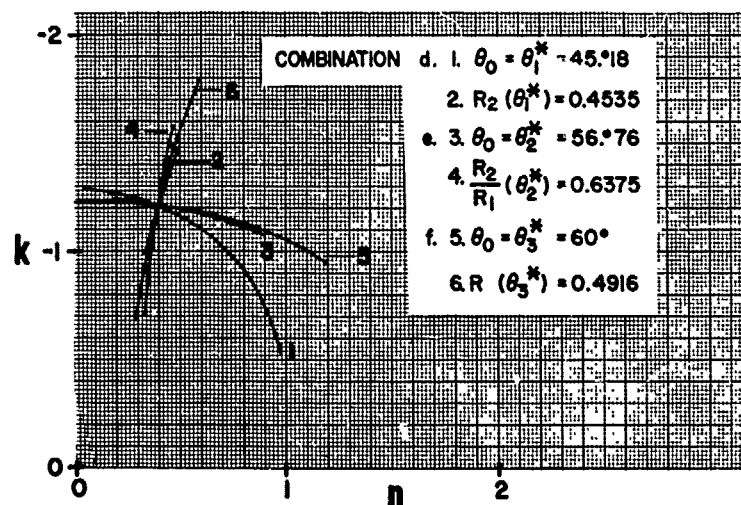


Fig. 73. DETERMINATION OF N FROM REFLECTION VALUES OBTAINED AT CHARACTERISTIC ANGLES OF INCIDENCE (EXAMPLE OF GROUP 2)

#### 4.2.2. Adulterated Experimental Data\*

It is evident that in experimental determination of N all the reflected radiation has to reach the receiver. If attenuation occurs, for instance by absorption on the path from the transmitter (antenna, light source) via the reflecting surface to the receiver (antenna, photo cell, etc.), the experimental data will not give the true value for the index of refraction. Power could also be lost if stops such as diaphragms are used in the instrumentation or if the source illuminates an area larger than the examiner considered. Unless we are concerned with the path through an ionic medium, the effect of these exterior influences will generally be of the same proportion on both amplitudes, which we consider perpendicular and parallel to the plane of incidence. As an example, let us evaluate experimental data which are incorrect due to unknown influences before and after the reflection

\* Other studies in this area are described in Refs. 19-20.

Example: The index of refraction  $N$  of the reflecting material for the employed wavelength is  $N_1 = n_1 - k_1i = 2.00 - 4.40i$ . The  $R_1$  and  $R_2$  values for the angles of incidence considered,  $\theta_0 = 70^\circ$  and  $\theta_0 = 80^\circ$ , were obtained from Tables A to D in (Volume II):

Theoretical Data

$\theta_0$	$R_1$	$R_2$	$R_2/R_1$	$P$
$70^\circ$	0.89431	0.44943	0.50254	0.33108
$80^\circ$	0.94494	0.40836	0.43215	0.39650

Due to exterior influences, the measured intensities may be only 90% of the theoretical values:

Experimental Data (Influenced)

$\theta_0$	$R_1$	$R_2$	$R_2/R_1$	$P$
$70^\circ$	0.80488	0.40449	0.50254	0.33108
$80^\circ$	0.85045	0.36752	0.43215	0.39650

We prepare graphs in the form of Figs. 74-76, and can then determine  $N$  from the measured data. Figure 74 represents the curves for  $R_1$  and  $R_2$  for  $\theta = 70^\circ$ , Fig. 75 does the same for  $\theta_0 = 80^\circ$ , and Fig. 76 contains the curves for  $P$  at both angles. We see that the adulterated data for  $R_1$  and  $R_2$  produce two different values for  $N$ , designated  $N_2$  and  $N_3$ , both of them different from  $N_1$ , the true index of the material considered. The results are

$$\begin{array}{lcl}
 \text{from } R_1 \text{ and } R_2 & \left\{ \begin{array}{ll} \theta_0 = 70^\circ & N_2 = 0.79 - 1.76i \\ \theta_0 = 80^\circ & N_3 = 1.43 - 1.80i \end{array} \right. & \\
 \text{(Figs. 74-75)} & & \\
 \text{from } R_2/R_1 \text{ or } P & \left\{ \begin{array}{ll} \theta_0 = 70^\circ & \\ \theta_0 = 80^\circ & \end{array} \right\} & N_1 = 2.00 - 4.40i \\
 \text{(Fig. 76)} & & 
 \end{array}$$

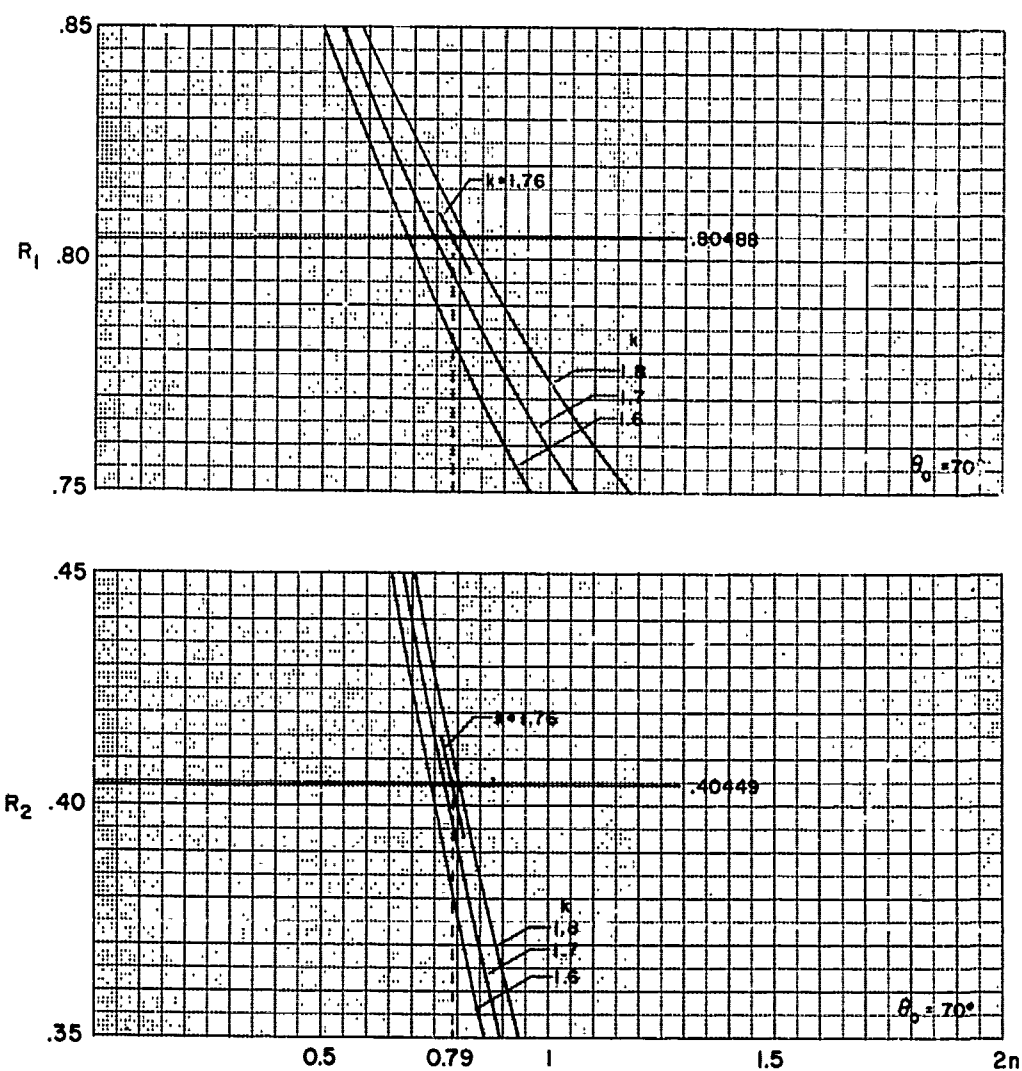


Fig. 74. PARTICULAR EXAMPLE OF THE DETERMINATION OF  $N$  FROM EXPERIMENTAL DATA FOR  $R_1$  AND  $R_2$  ( $\theta_0 = 70^\circ$ )

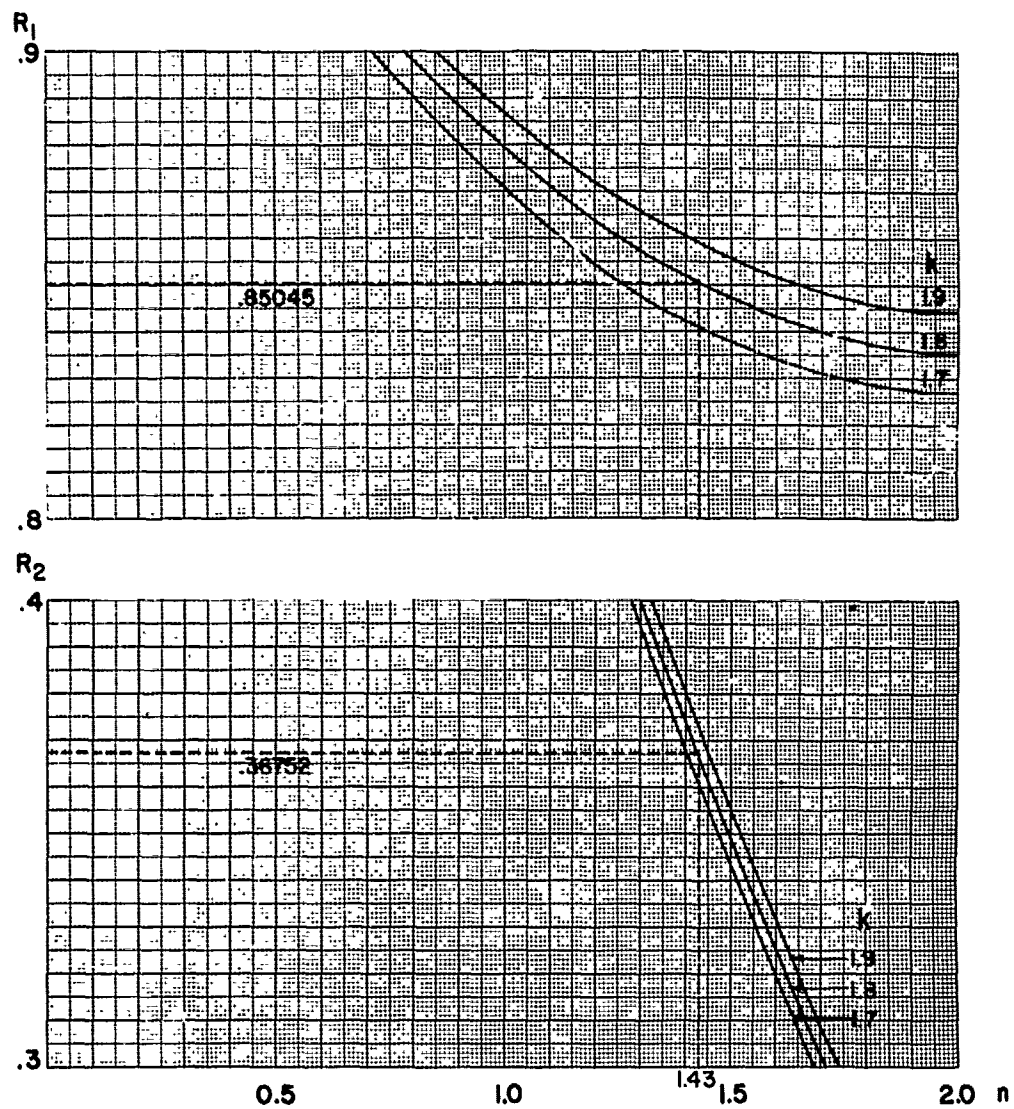


Fig. 75. PARTICULAR EXAMPLE OF THE DETERMINATION OF  $n$  FROM EXPERIMENTAL DATA FOR  $R_1$  AND  $R_2$  ( $\theta_0 = 8n^\circ$ )

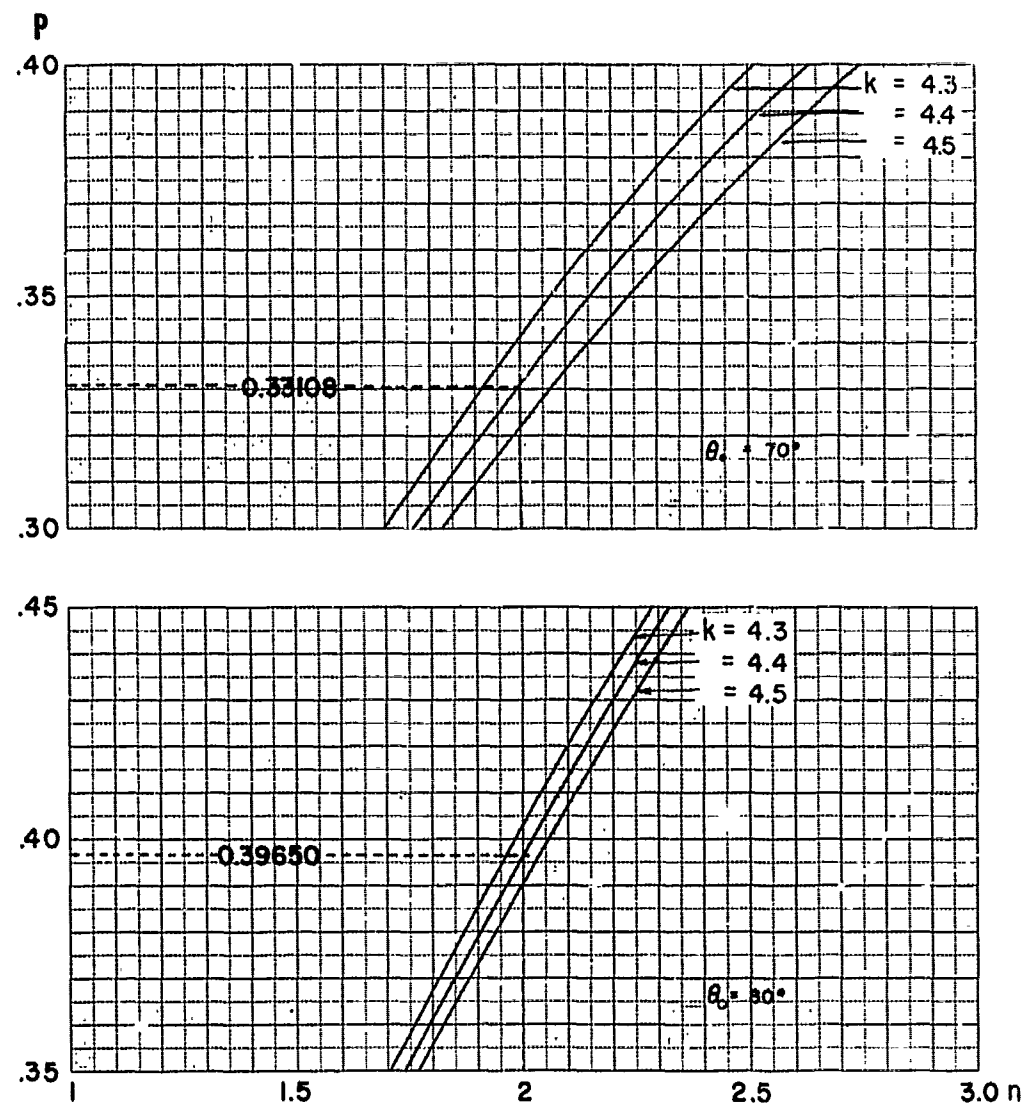


Fig. 76. PARTICULAR EXAMPLE OF THE DETERMINATION OF  $N$  FROM EXPERIMENTAL DATA FOR  $P$

The ratio  $R_2/R_1$ , or the degree of polarization  $P$ , was not influenced by the experimental conditions, and this plot (Fig. 76) gives the true value for  $N$ , which is  $N_1 = 2.00 - 4.40i$ . Figure 77 illustrates all three pairs of curves in the Argand diagram. The reader can easily see that in the cases of adulterated measurements all the indices  $N_2$  for  $\theta = 70^\circ$  will be located on the curve  $P = 0.33108$  which goes through the points of  $N_1$  and  $N_2$ , and for  $\theta = 80^\circ$  on the  $P = 0.39650$  curve which goes through the points of  $N_1$  and  $N_3$ , and that only one curve for  $P = \text{constant}$  is responsible for each angle of incidence. It should be understood that our example was not limited to consideration of the same discrepancy for both angles of incidence, i. e. 90% of the theoretical data in both cases. If, for instance, in an experiment we would receive only 88% of the theoretical values of  $R_1$  and  $R_2$  at  $\theta_0 = 70^\circ$ , and 93% at  $\theta_0 = 80^\circ$ , the corresponding indices would be located in the first case on  $P = 0.33108$  below  $N_2$ , and in the second case on  $P = 0.39650$  between  $N_1$  and  $N_3$ . In order to get a picture of how far the reflection coefficients can depart from the true response, if experimental results are evaluated, an illustration of  $R_1$  and  $R_2$  versus  $\theta_0$  for  $N_1 = 2.00 - 4.40i$ ,  $N_2 = 0.80 - 1.70i$ , and  $N_3 = 1.4 - 1.8i$  is given in Fig. 78. The curves  $0.9 \times R_1$  and  $0.9 \times R_2$  (numbered 10 and 11, respectively) are also drawn in for  $N_1 = 2.00 - 4.40i$ . Such reflection curves no longer follow the Fresnel equation for any index of refraction. This means that if we write the Eq. (32) and (33) in the form

$$\begin{aligned} R_1 &= x_1 \cdot f_1(n, k, \theta_0) \\ R_2 &= x_2 \cdot f_2(n, k, \theta_0), \end{aligned} \quad (82)$$

the functions  $f_1$  and  $f_2$  represent the Fresnel reflection coefficients in the entire interval  $0 \leq \theta_0 \leq 90^\circ$  only if the factors  $x_1$  and  $x_2$  are 1. Reflection coefficients obtained from adulterated experimental data can only be described by indices which vary with the angle of incidence. These indices will not be considered here; however, it should be mentioned that they are not identical to the  $n = n(\theta_0)$  of Eq. 52.

As another example, let us consider the experimental data received when the radiation source illuminated the total reflecting surface at normal incidence but the cross area became smaller with the factor  $\cos \theta_0$  at oblique incidence. The factors  $x_1$  and  $x_2$  of Eq. 82 would be  $\cos \theta_0$  and the reflection curves would be curves (12) and (13) of Fig. 78.

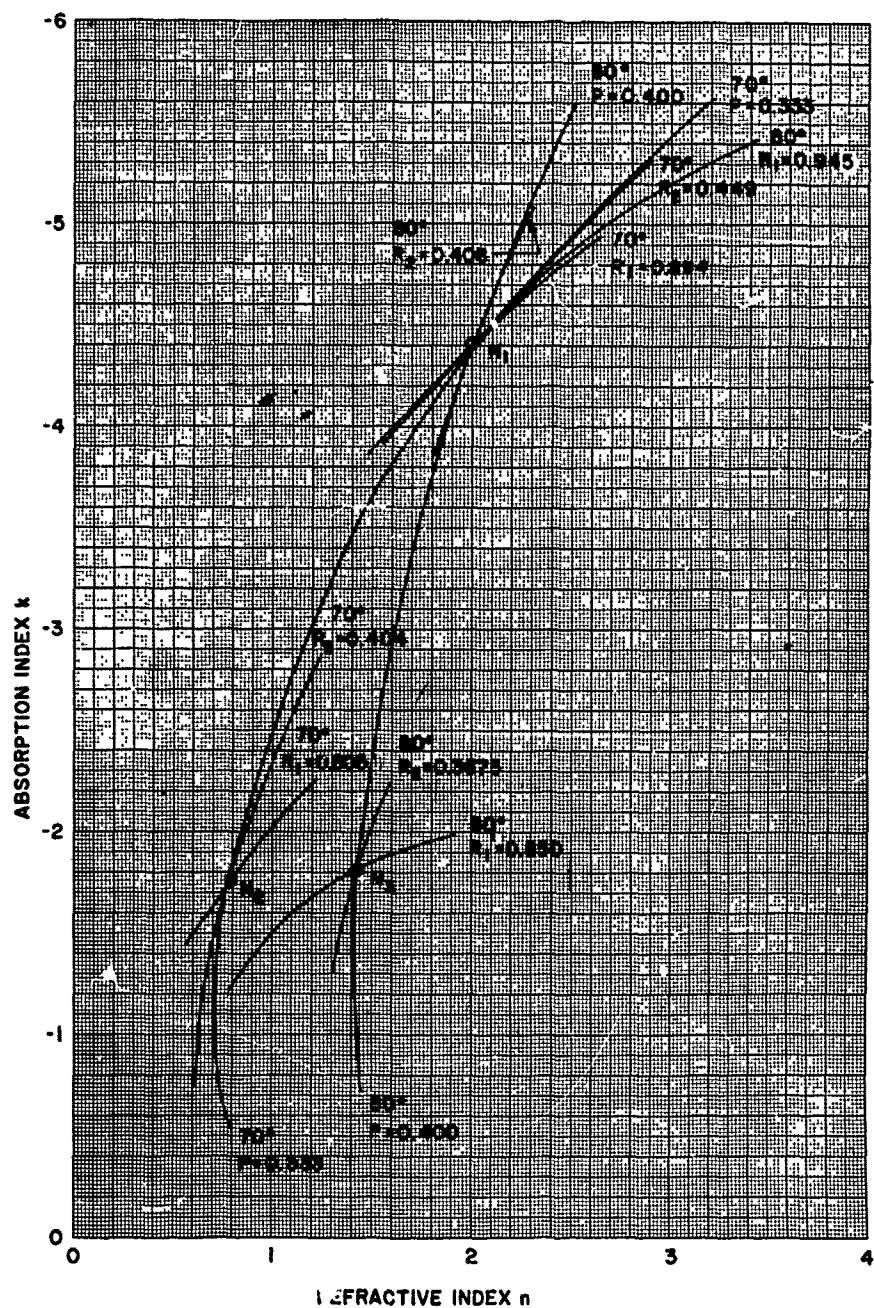


Fig. 77. PARTICULAR EXAMPLE OF THE DETERMINATION OF  $n$  FROM ADULTERATED EXPERIMENTAL DATA

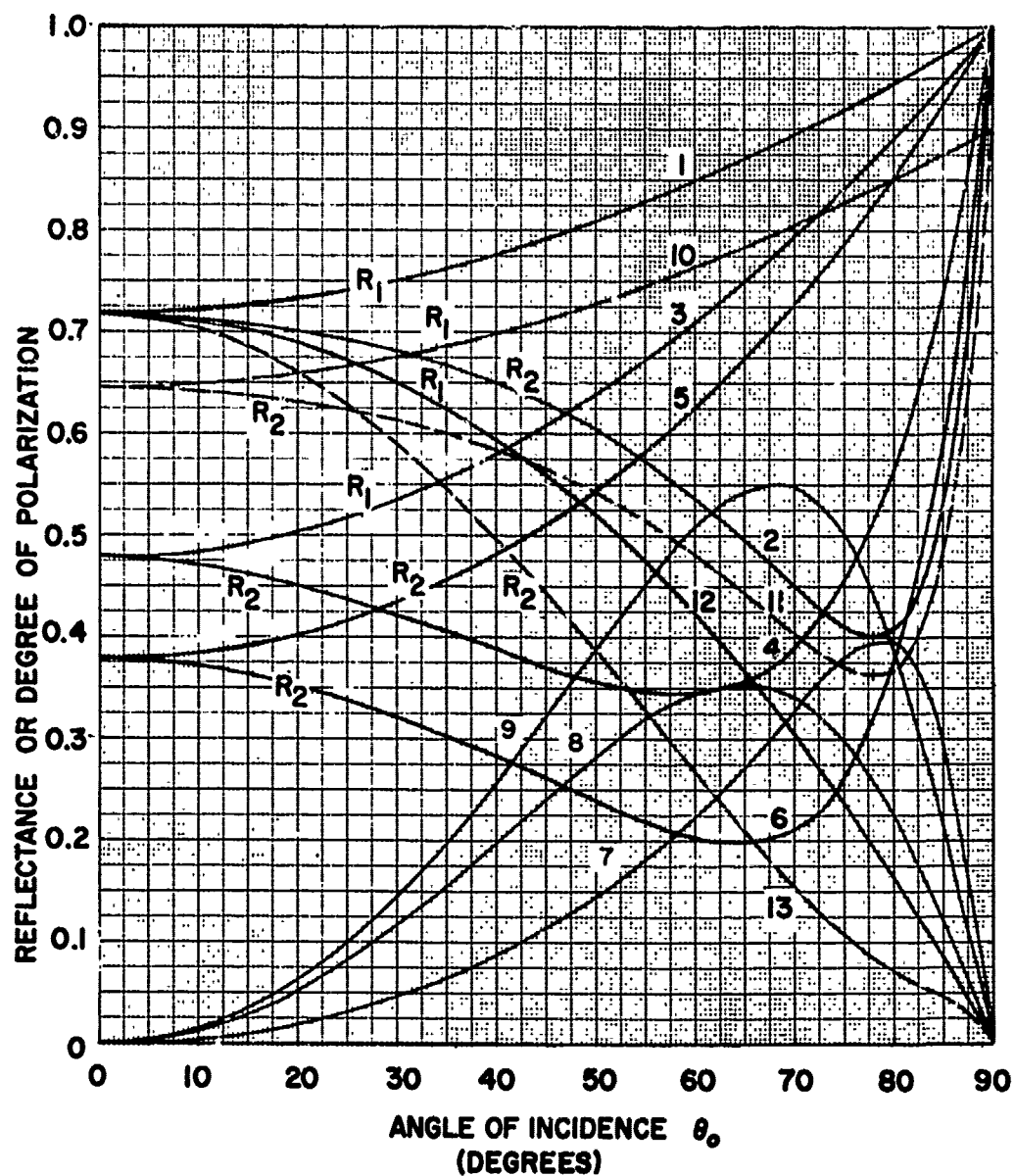


Fig. 78. REFLECTANCE AND DEGREE OF POLARIZATION FOR INDICES OF REFRACTION  $N_1 = 2.00 - 4.40i$ ,  $N_2 = 0.80 - 1.70i$ , AND  $N_3 = 1.40 - 1.80i$

Curves 1 and 2	} $R_1$ and $R_2$ for	{ $N_1$ $N_2$ $N_3$	10	} $0.9 \times$	{ $N_1$	
3 and 4			11			} $R_1$ and $R_2$ for
5 and 6						
7	} ————— P for —————	{ $N_1$ $N_2$ $N_3$	12	} $\cos \theta_0 \times$	{ $N_1$	
8			13			} $R_1$ and $R_2$ for
9						

If the radiation illuminates only a part of the surface at normal incidence and the entire surface at oblique incidence ( $\theta_0 = \theta_n$ ), the measured coefficients for angles of incidence  $\theta_0 > \theta_n$  become

$$R_1 = \cos(\theta_0 - \theta_m) \cdot f_1(n, k, \theta_0)$$

$$R_2 = \cos(\theta_0 - \theta_m) \cdot f_2(n, k, \theta_0) \quad (83)$$

#### 4.2.3. Nonspecular Reflection\*

Nonspecular reflection stems from an imperfect surface which has a certain degree of roughness. Nature does not know a true smooth surface. A material with a surface which reflects radiation in all directions, apparently without preference for any particular direction, is called a diffuse reflector.

All previous discussions were concerned with ideal or specular reflection. The Fresnel equations are derived for a clean and smooth material surface, but are still applicable if the surface has a certain degree of roughness, that is if the wavelength  $\lambda$  considered and the radius of curvature  $\rho$  are not of the same order ( $\lambda \ll \rho$ ). This is true, for instance, in the case of the reflection of radio waves on the surface of the sea.

For the present discussion we assume that the surface has no sophisticated irregularities (such as holes, caves, pits) and is nearly free of sharp edges and peaks, which means that diffraction and multiple reflection do not occur. Such a rough surface can be considered to be formed by numerous small areas, each of which is a plane surface element  $dA$ . The Fresnel equations can be applied to each particular surface element. Figure 79 illustrates a small part of a plane section of a surface parallel to the plane of incidence of the radiation. The surface, of which we considered only a small region of the length of  $dL$ , is illuminated by a radiation source  $S$ . A receiver  $R$  measures the intensity of the reflected radiation. If the receiver is far enough away from the reflecting surface, the radiation forms a plane wavefront. The inclination of the surface elements (all have parallel normals) which contribute to the intensity measured by  $R$  can be determined from the locations of  $S$  and  $R$ . In the example illustrated by Fig. 79, the elements  $dA_1$  and  $dA_2$  are parallel and, therefore,

---

\* Other studies in this area are described in Refs. 21 and 22.

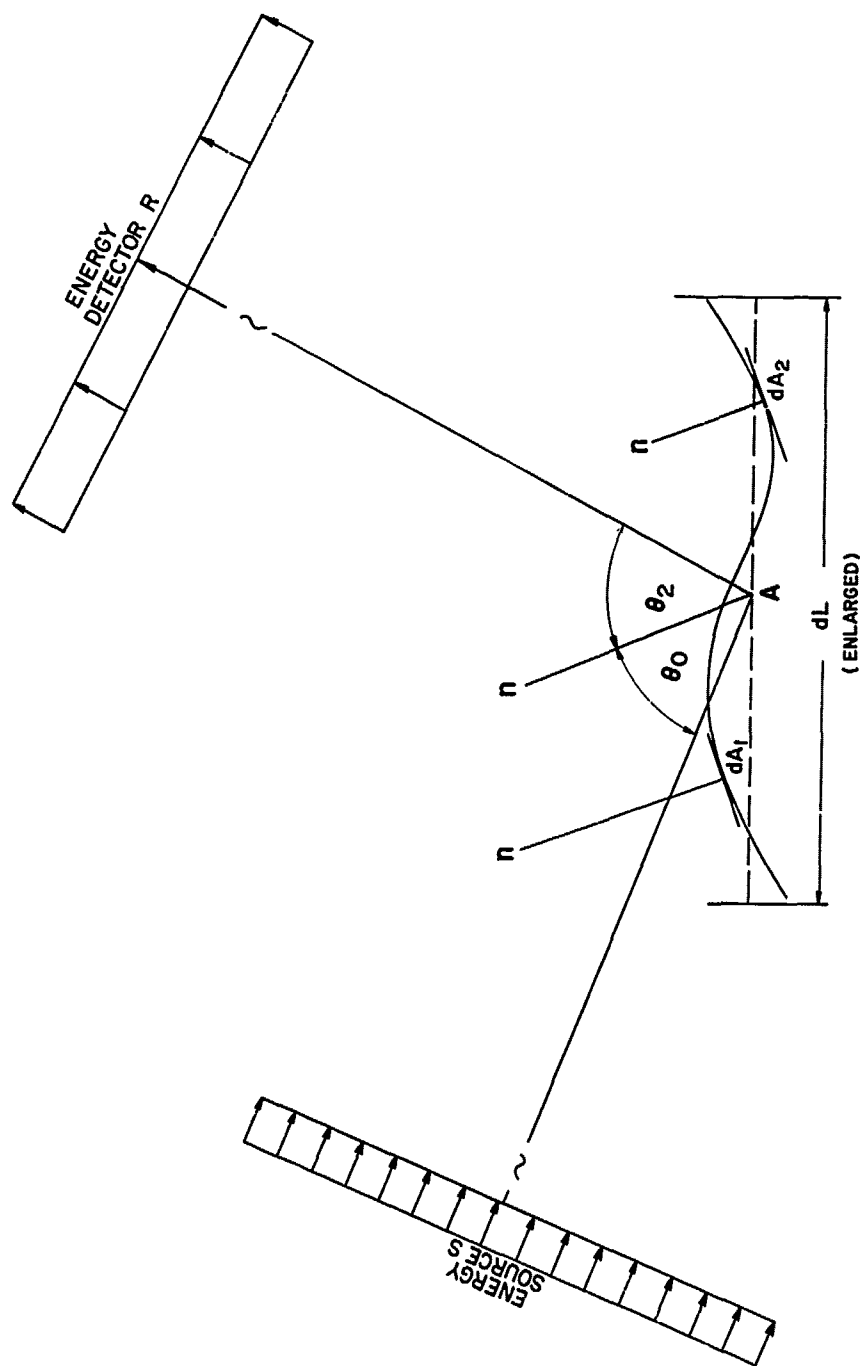


Fig. 79. REFLECTION FROM A NONREGULAR SURFACE (DESCRIPTION IN TEXT)

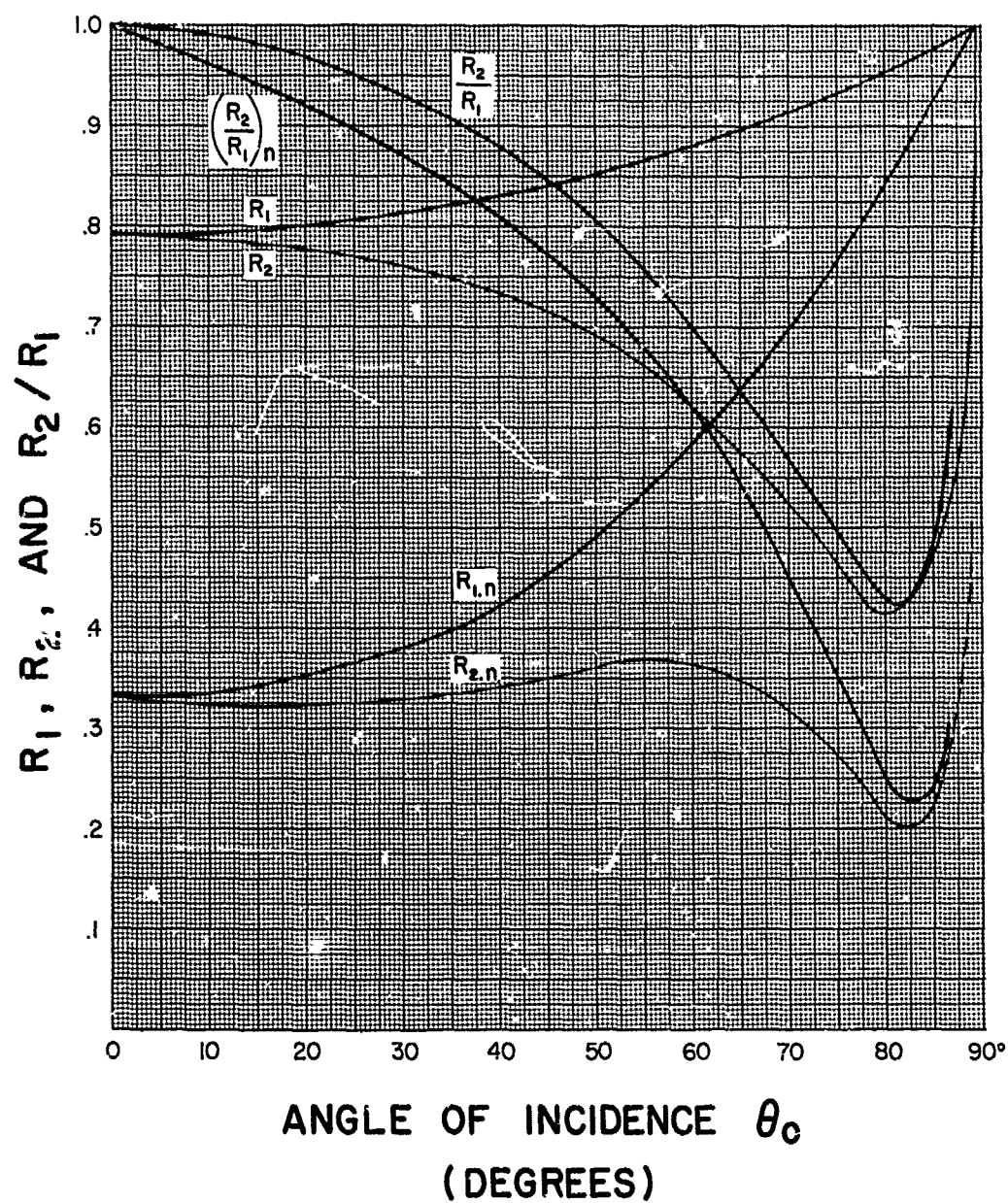


Fig. 80. REFLECTION CURVES FOR NICKEL ( $\lambda \sim 2.5\mu$ )  
( $R_1$  AND  $R_2$ , SMOOTH SURFACE;  $R_{1,n}$  AND  $R_{2,n}$ , ROUGH SURFACE)  
(DESCRIPTION IN TEXT)

their normals are parallel to that of point A. All the surface elements  $\sum dA_v$  together reflect only a small fraction of the incoming radiation directed toward the receiver  $R_2$ , but this contributing area is identical for the intensities  $R_1$  and  $R_2$ . The roughness of a surface can be defined and scaled by this method. The effect of diffraction, if any, could also be determined from such measurements. If we measure the ratio  $R_2/R_1$  for two angles of incidence we can obtain the true index of refraction in the same way as described previously.

If the reflected radiation is a mixture of specular multiple- - reflection rays, this simple concept does not hold. Let us consider an example published recently (Ref. 23). Figure 80 is based on experimental data obtained in this study. Two pairs of reflection curves are given: (1) the curves  $R_1$  and  $R_2$ , which are the reflectance of a smooth metallic surface (Ni, immaculate, ground, and polished); and (2)  $(R_1)_n$  and  $(R_2)_n$ , which represent that portion of the stray light travelling in the direction which follows the reflection law after the material was roughed by coarse-grained corundum. Thus for the second pair of curves the degree of roughness of the material was of the same order as the wavelengths of the radiation source ( $\lambda \sim 2.5\mu$ ). The curves  $R_2/R_1$  and  $R_2/R_1_n$ , given in Fig. 80, also show that purely specular reflection does not occur at any angle of incidence.

## REFERENCES

1. Holl, Herbert B., The Effect of Radiation Force on Satellites of Convex Shape, NASA TN D-604 (May 1961).
2. König, W., Elektromagnetische Lichttheorie, Handbuch der Physik, Vol. XX, Springer (1928).
3. Minkowski, R., Theorie der Reflexion, Brechung und Dispersion, Müller - Pouillet's Lehrbuch der Physik, Friedr. Vieweg und Sohn Akt. Ges., Braunschweig (1929).
4. Stratton, Julius A., Electromagnetic Theory, McGraw-Hill Book Company, Inc., New York (1941).
5. D'Ans, J. and Lax, E., Taschenbuch für Chemiker und Physiker, Vieweg und Sohn, Berlin (1943).
6. Cole, T. T. and Oppenheimer, F., Polarization by Reflection and Some Optical Constants in the Extreme Ultraviolet, Applied Optics, 1.6 (Nov. 1962) 709-710.
7. Goldberg, Philip A., Electrical Properties of High-Altitude Ionized Shock Waves, Chapter 9 of: Drummond, James, E., Plasma Physics, McGraw-Hill Book Company, Inc., New York (1961).
8. Jentzsch, F., Verh. d. D. Phys. Ges., 21 (1919) 361.
9. Schaefer, Clemens, Einführung in die theoretische Physik, Dritter Band. Elektrodynamik und Optik, Walter De Gruyter & Co., Berlin and Leipzig (1932).
10. Moss, T. S., Optical Properties of Semi-Conductors, Butterworths Scientific Publications, London (1959).
11. Häfele, H. G., Die optischen Konstanten von Quarz im Infrarot und ihre Temperatureabhängigkeit I, Zeitschr. für Physik, 168 (1962) 530-541.

# REFERENCES (Concluded)

2. Boeckner, C., A Method of Obtaining the Optical Constants of Metallically Reflecting Substances in the Infrared, J.O.S.A. & R.S.T., 19 (1929) 7-16.
13. Drude, Paul, The Theory of Optics, Dover Book of Science (1959) 363.
14. Born, Max, and Wolf, Emil, Principles of Optics, Pergamon Press, New York (1959).
15. Pfestorf, Gerhard, Bestimmung der optischen Konstanten von Metallen im sichtbaren und ultravioletten Teil des Spektrums, Ann. d. Physik, 81 (1926) 906.
16. Tousey, Richard, On Calculating the Optical Constants from Reflection Coefficients, J.O.S.A. 29 (1939) 235-239.
17. Collins, J. R. and Bock, R. O., Determination of Optical Constants of Metals by Reflectivity Measurements, The Review of Scientific Instruments, Vol. 14, No. 5 (May 1943) 135-141.
18. Simon, Ivan, Spectroscopy in Infrared by Reflection and Its Use for Highly Absorbing Substances, J.O.S.A. 41.5 (1951) 336-345.
19. Heilmann, Gerhard, Die Temperaturabhängigkeit der optischen Konstanten von LiF im Bereich der ultraroten Reststrahlbande Zeitschr. f. Physik, 152 (1958) 368-383.
20. Avery, D. G., An Improved Method for Measurements of Optical Constants by Reflection, Proc. Phys. Soc. 65 (1952) 425-428.
21. Avery, D. G., The Optical Constants of Lead Sulphide, Lead Selenide and Lead Telluride in the 0.5-3 $\mu$  Region of the Spectrum, Proc. Phys. Soc., Lond. B 66 (1953) 133-140.
22. Bennett, H. E. and Porteus, J. O., Relation Between Surface Roughness and Specular Reflectance at Normal Incidence, J.O.S.A. 51.2 (1961) 123-129.
23. Klein, Heinz, Über die thermische Emission der Metalle in den Halbraum, Zeitschr f. Angew. Physik, XIV.6 (1962) 358-362.

AD Accession No. Army Missile Command, Directorate of Research and Development, Advanced Systems Laboratory, Redstone Arsenal, Alabama THE REFLECTION OF ELECTROMAGNETIC RADIATION (BASED ON CLASSICAL ELECTRODYNAMICS) - VOLUME I - Herbert B. Holl. Army Msl Cmd RF-TR-63-4, Vol I, 15 Mar 63, 128 pp. Unclassified Report Numerical values of the Fresnel intensity reflection coefficients in tables and graphs are presented. Reflection coefficients are given for normal and oblique incidence for approximately 2500 indices of refraction. Graphs illustrate the solutions of the Fresnel equations. This volume 1 of the 2 volume report contains all the narrative, discussion, and graphs.	UNCLASSIFIED 1. Electrodynamics--Applications 2. Electromagnetic radiation--Reflection 3. Electromagnetic wave reflections--Mathematical analysis 4. Fresnel integrals I. Holl, Herbert B. DISTRIBUTION: Copies obtainable from DDC, Arlington Hall Station, Arlington 12, Virginia.	AD Accession No. Army Missile Command, Directorate of Research and Development, Advanced Systems Laboratory, Redstone Arsenal, Alabama THE REFLECTION OF ELECTROMAGNETIC RADIATION (BASED ON CLASSICAL ELECTRODYNAMICS) - VOLUME I - Herbert B. Holl. Army Msl Cmd RF-TR-63-4, Vol I, 15 Mar 63, 128 pp. Unclassified Report Numerical values of the Fresnel intensity reflection coefficients in tables and graphs are presented. Reflection coefficients are given for normal and oblique incidence for approximately 2500 indices of refraction. Graphs illustrate the solutions of the Fresnel equations. This volume 1 of the 2 volume report contains all the narrative, discussion, and graphs.	UNCLASSIFIED 1. Electrodynamics--Applications 2. Electromagnetic radiation--Reflection 3. Electromagnetic wave reflections--Mathematical analysis 4. Fresnel integrals I. Holl, Herbert B. DISTRIBUTION: Copies obtainable from DDC, Arlington Hall Station, Arlington 12, Virginia.
AD Accession No. Army Missile Command, Directorate of Research and Development, Advanced Systems Laboratory, Redstone Arsenal, Alabama THE REFLECTION OF ELECTROMAGNETIC RADIATION (BASED ON CLASSICAL ELECTRODYNAMICS) - VOLUME I - Herbert B. Holl. Army Msl Cmd RF-TR-63-4, Vol I, 15 Mar 63, 128 pp. Unclassified Report Numerical values of the Fresnel intensity reflection coefficients in tables and graphs are presented. Reflection coefficients are given for normal and oblique incidence for approximately 2500 indices of refraction. Graphs illustrate the solutions of the Fresnel equations. This volume 1 of the 2 volume report contains all the narrative, discussion, and graphs.	UNCLASSIFIED 1. Electrodynamics--Applications 2. Electromagnetic radiation--Reflection 3. Electromagnetic wave reflections--Mathematical analysis 4. Fresnel integrals I. Holl, Herbert B. DISTRIBUTION: Copies obtainable from DDC, Arlington Hall Station, Arlington 12, Virginia.	AD Accession No. Army Missile Command, Directorate of Research and Development, Advanced Systems Laboratory, Redstone Arsenal, Alabama THE REFLECTION OF ELECTROMAGNETIC RADIATION (BASED ON CLASSICAL ELECTRODYNAMICS) - VOLUME I - Herbert B. Holl. Army Msl Cmd RF-TR-63-4, Vol I, 15 Mar 63, 128 pp. Unclassified Report Numerical values of the Fresnel intensity reflection coefficients in tables and graphs are presented. Reflection coefficients are given for normal and oblique incidence for approximately 2500 indices of refraction. Graphs illustrate the solutions of the Fresnel equations. This volume 1 of the 2 volume report contains all the narrative, discussion, and graphs.	UNCLASSIFIED 1. Electrodynamics--Applications 2. Electromagnetic radiation--Reflection 3. Electromagnetic wave reflections--Mathematical analysis 4. Fresnel integrals I. Holl, Herbert B. DISTRIBUTION: Copies obtainable from DDC, Arlington Hall Station, Arlington 12, Virginia.